

1 Responses to reviews of ‘Effective radiative forcing from emissions of reactive gases and  
2 aerosols – a multi-model comparison’ by G. Thornhill et al

3  
4 We would like to thank the two referees for their helpful comments and suggestions.  
5 Our responses to the reviewers comments are below – reviewer comments in black, our  
6 responses in blue.

7  
8 **Changes and edits to the text are noted in blue.**  
9

#### 10 **Anonymous Referee #1**

11  
12 This paper examines the effective radiative forcing (ERF) of reactive gases (e.g., CH<sub>4</sub>,  
13 NO<sub>x</sub>, VOC, O<sub>3</sub>, N<sub>2</sub>O, HC, NH<sub>3</sub>) and aerosols (e.g., BC, OC, SO<sub>2</sub>) to the climate system  
14 using multi-model output from the AerChemMIP experiments of the CMIP6 project. The  
15 contribution of each species to the total ERF is decomposed, and the differences of  
16 the calculated ERFs by various models are discussed. The paper is overall well written  
17 and easy to follow. I have some minor comments for the authors to consider before  
18 publication:

19  
20 1. It is not clear how many ensemble members are used for each model. Can you  
21 please clarify this?

22 **We have clarified that only one ensemble member was used in these experiments in Section 2.2**  
23

24 2. Fixed SST and sea ice are used in the ERF simulations. Is it the climatological SST  
25 of the 1850s?

26 **These were the fixed SSTs from the Pre-Industrial run – mentioned in L. 185.**  
27

28 3. The description of Eq. 5 is a bit vague. You may want to add “ERFaci” to line 240  
29 after “The effect of the aerosol on cloud radiative forcing”.

30 **We have re-written this section and changed the nomenclature to be consistent with other work in**  
31 **this field, so that the descriptions of each term is clear.**  
32

33  
34 4. “A\_trop” is used in text while “RA Trop” is used in Fig. 1. It’s better to be consistent.

35 **We have changed the nomenclature and definitions in the text so that we use A<sub>total</sub> in the text and**  
36 **the Fig.1 for this quantity.**  
37

38  
39 5. Line 373, “Fig. 6”! “Fig. 5”. And can you explain a bit more about how the total  
40 AOD is used to calculate the sum of the scaled ERFs?

41 **We have corrected the figure number and have added additional explanation on how the AOD is**  
42 **used in this scaling. There is also more detailed discussion in the Supplementary material.**  
43

44 6. Table 6, second row, “Nox”! “NOx”

45 **The typo has been corrected.**

46 7. Line 465, please remove the brackets around “O’Connorl F. M. 2019”

47 **The reference has been fixed.**  
48

49 8. Error bars are used in Fig. 9-10 to quantify the uncertainties due to interannual  
50 variability of model diagnostics. Is it possible to apply similar approach (error bars) to  
51 other figures where data are available?

52 We have added error bars to Fig. 1 and Fig. 6 to show the S.E. for the ERF individual models (for the  
53 inter-annual variability) and the S.D. for the multi-model means.

54

55 9. Line 507, "RFs"! "ERFs"

56 This has been corrected.

57

58 10. Line 525, "+/-"! "\_", please also add explanation about the numbers follow the  
59 sign, for instance, is it a standard deviation of multi-model output?

60 We have clarified where the numbers are standard error or standard deviation throughout the  
61 manuscript.

62

63 11. Lines 541-542, the overall aerosol ERFari from AR5 (-1.5 \_ 0.4 Wm-2) is much  
64 larger than values reported here (-0.16 \_ 0.03 Wm-2). Can you add some discussion  
65 about the differences?

66 In fact the comparison here was incorrect – the AR5 number quoted is the total ERF, not the IRFari  
67 (in the original manuscript this was referred to as the ERFari), so this has been corrected.

68

69 12. Lines 546-550, redundant

70 The redundant lines have been removed.

71

72

73 -----

## 74 **Anonymous Referee #2**

75

76 Thornhill et al. "Effective Radiative forcing from emissions 1 of reactive gases and aerosols – a  
77 multimodel comparison"

78 This paper is a very important contribution to climate and atmospheric chemistry studies. It is  
79 critical for the current IPCC AR6 assessment. My apologies to the authors for the delay in my  
80 review – surprisingly, these isolation times do not make it easier to review. I am rushing to get  
81 this out and so there may be typos in this review.

82 AerChemMIP is a very important project that is trying to make sense of a complex, nonlinear  
83 system of chemistry and clouds. The design has some serious flaws, and we all knew that as it  
84 was being developed since there were obvious limitations in the number and complexity of  
85 experiments. First, there is the nonlinearity, which comes out clearly in these results:  $\text{Exp}(A)$  plus  
86  $\text{Exp}(B)$  does not equal  $\text{Exp}(A+B)$ . Further, and because of the nonlinear nature, the choice of  
87 reference atmosphere (1850) will produce quite different results than another (2014). Personally I  
88 would have much preferred to use the 2014 atmosphere as the reference atmosphere (at least we  
89 can compare the models to measurements) and then subtract the emission or concentration  
90 changes from 1850 to 2014. So, we live with AerChemMIP and use it. The analysis here is very  
91 good, but needs to develop more of an "assessment" view when reporting final numbers. They  
92 should reflect some (subjective) adjustment of values (for non-linearity) or bias (from 1850  
93 atmosphere). Simply reporting the model average for  $\text{Exp}(A)$  and then  $\text{Exp}(B)$  will lead anyone  
94 who uses this paper to assume that the combined effect is the sum. That would not be good for  
95 either policy or attribution work. If the sum is the best answer (I would think that so), then the  
96 contributions of components may need to be expressed in % of total rather than in W/m<sup>2</sup>. I do not  
97 recommend a substantial rewrite, but rather a self-assessment by the author team of how to use  
98 these results.

99 We have added discussion of the non-linearity and where that would affect a simplistic  
100 interpretation of combined results in the relevant sections, and we have added comments on the  
101 limitations of the experimental design.

102  
103  
104  
105  
106  
107  
108  
109  
110  
111  
112  
113  
114  
115  
116  
117  
118  
119  
120  
121  
122  
123  
124  
125  
126  
127  
128  
129  
130  
131  
132  
133  
134  
135  
136  
137  
138  
139  
140  
141  
142  
143  
144  
145  
146  
147  
148  
149  
150  
151  
152  
153

The abstract starts off being very careful and clear, but then I get lost between emissions and composition change. For example, SO<sub>2</sub> is clearly an emission-based ERF, while CH<sub>4</sub> is an abundance-based ERF. VOCs & NO<sub>x</sub> are obviously emissions (having direct RF) but O<sub>3</sub> is not emitted. The HC (L40: halocarbons? as opposed to NMHC?) are negative presumably from the ozone depletion, but this is an odd way to list the CFCs. Methane is singled out at the end of the abstract as increasing ozone, but ozone is listed separately. Is the methane based only on the change in CH<sub>4</sub> concentration? Further, I suspect that the methane includes stratospheric water vapor which is indirect as is ozone, so why the separate listings. This is just inconsistent and you really need to present the framework and rules for partitioning and assigning ERF. Basically, AerChemMIP is a complicated set of overlapping experiments and thus the abstract with simple results is very difficult to write correctly. Try to keep it clear and simple.

We have added text to the abstract to include a better description of the relationship between the ozone pre-cursors and the ERFs calculated.

L53- aerosols are chemically reactive. try again – aerosols and gases that ...

We have re-worded this as chemically reactive gases to make the distinction clearer.

L56- climate feedbacks on natural emissions is a tough one for the non-CO<sub>2</sub> species. I do not think AerChemMIP did anything on that.

The discussion of natural emissions has been removed. These are covered in Thornhill et al. 2020.

L68- "conditions" do you mean SST, I doubt you prescribed different chlorophyll or DMS?

We have clarified which conditions are meant here (SSTs and sea-ice).

L69- why aerosols here? It seems more like and ie than and eg, why not just say aerosols and gases.

This has been reworded.

L71- again the contrast of 'aerosols and chemistry' is really a poor description of AerChemMIP.

Aerosols are a chemically reactive species (most of them are, they were created by gas phase chemistry). This Intro really must have a better inclusive discussion of greenhouse gases (including ozone), of indirect greenhouse gases (CO) and of aerosol (primary and secondary). This is at odds with the content of AerChemMIP.

This section has been expanded to clarify the indirect roles of precursor species as recommended by the reviewer.

L90- again, every time I read this, it sounds odd and misleading: " aerosols and reactive chemistry" are not opposites.

This has been reworded as “aerosols and reactive gases”.

L93- again, this phrasing sounds wrong: " anthropogenic and reactive species" is this two separate species or is it 'both'

This has been reworded as “aerosols and reactive gases”

L103- what does 'down to' mean? from 0.001 to 560 hPa?.

This has been reworded to clarify the levels of the atmosphere.

L107- typo 'is includes'

154 Typo has been corrected.

155

156 L102-L165 This information should really be in a table somewhere, not in the text. Focus on the  
157 results. In fact, most of this is already in Table 1.

158 The summary of different model aerosol and chemistry modules has been retained in the text, and  
159 the details moved to Supplementary Table S1.

160

161

162 L172-173- You should say 'emissions' with the NTCFs, also you should note that methane is an  
163 SLCF, which your statement seems to preclude. Also, I thought that SLCF was new preferred,  
164 but...

165 The use of NTCF was retained because the experiment was called piClim-NTCF, so this  
166 nomenclature was kept to aid in understanding which experiment was referred to. We state that  
167 the point that this nomenclature has changed and that SLCF is now preferred. In the piClim-  
168 NTCF experiment in AerChemMIP methane is deliberately excluded as part of the experimental  
169 design.

170

171 L174- There is a serious problem with the AerChemMIP as defined and we realized this at the  
172 time, but did not address it: viz. because of the large changes in atmospheric chemistry and  
173 oxidants between 1850 and 2014 (including the ozone depletion), it is not clear that the effect of  
174 today's NTCF emissions in today's atmosphere are anywhere close to those calculated here for the  
175 PI atmosphere. This needs to be addressed when compiling results and clearly adds to the  
176 uncertainty. The reason why it is dangerous is that it could totally misrepresent the magnitude of  
177 the response if we were to cut NTCF today.

178 The reviewer has a good point here. We have added discussion of the issue likely differences  
179 between perturbing emissions in a pre-industrial and present day atmosphere, and commented in  
180 places where this would influence the results.

181

182

183 L200- "ocean state" implies much more than SSTs – do you really mean that.

184 This has been corrected.

185

186 L235- I am confused here, it seems like the direct forcing would include, not ignore, the  
187 absorption and scattering by aerosols. Is this a typo.

188 This was a typo, and the section has been re-written in order to explain the method more clearly.

189

190 L239- this section is very confusing as written. I am sure it is simpler than it seems but some of  
191 the writing seems incorrect. In this line surely you mean the aerosol direct radiative effect, since  
192 "radiative effects due only to aerosols" would imply both ari and aci. The notation for ERFcs,af is  
193 inconsistent between eqn and text (comma or not). Eqns 4 & 5 sum to give not ERF, so where is  
194 this missing 'surface albedo' term (ERF-ERFcsaf) and does it matter? It must certainly be counted  
195 as an aerosol ERF. [OK, I see this in Table 3 later, is the cs,af just noise?]

196 This section has been re-written and clarified, with additional discussion and explanation of the  
197 terms and their meanings.

198

199 L254ff- This is odd, you said just above the SARF is calculated from  $ERF - A_{trop}$ , so of course  
200 this should give 0% difference. Are you just checking the math? Also, with SARF calculated as a  
201 residual term, and the ability to denote and sum all the  $A_{trop}$  being highly uncertain, SARF  
202 would not appear to be very certain. In fact the SARF term would depend on the models' ability  
203 to diagnose  $A_{trop}$  correctly.

204 This has been explained more clearly in Section 4.1.2, and the reason for the difference in the  
205 calculations clarified as due to the way the IRF is calculated in the kernel method. We have now  
206 used the IRF instead of the SARF in this section, as it is more consistent with previous work.  
207

208 L260- With BC, the long-standing problem is that some models get far too much in the  
209 stratosphere and that would cause a very large SARF.  
210 We have added more discussion of the BC results, and the reasons for model differences.  
211

212 L285- in this figure and some others, please define carefully what the shorthand for the terms  
213 means.  
214 We have clarified the terms and included the definitions in the figure captions.  
215

216 L296ff- This is a very good discussion of the aerosol components!  
217 Thank you, nice to hear what is good about the paper!  
218

219 L321- This would be a much better lead off to the aerosol section and analysis, begin with the big  
220 picture before the weeds.  
221 We have moved this to the top of the results section.  
222

223 L343 – just put this table into the figure, it is just a summary of the bars anyway.  
224 We have revised the plot, added error bars for both inter-annual variability and the multi-model  
225 mean, and moved the relevant tables to the supplementary material.  
226  
227

228 L354- Please, stop wasting space, Table 5 and Fig 4 has the same information. If you want to  
229 show AOD, then add it to the figure..  
230 We have removed this plot and added the information to Table 4.  
231

232 L370ff & Fig 5- I do not understand the purpose of this AOD scaling, it really does little to help.  
233 The figure shows the key data: ERF from parts vs ERF from all. The ERF-parts consistently over  
234 accounts for the combined ERF. This is as expected wince the cloud effects are largest in a pi  
235 atmosphere with little background aerosols. So herein lies one of the fundamental problems with  
236 the AerChemMIP that must be acknowledged and accounted for. I am not sure that scaling by  
237 AOD is any more justified than just scaling the indirect to match – An interesting question is  
238 whether the ERF-ari sum of the parts equals the whole? Keep this fudge factor simple since there  
239 is no correct way to do this.  
240 I have moved the discussion on scaling to the Supplementary material, and removed the  
241 unnecessary figure. I have added appropriate caveats on the non-linearity and the effect of using  
242 the PI atmosphere, and the effect on these results.  
243  
244

245 L393- Again, this title jars a bit, SO<sub>2</sub> and NH<sub>3</sub> are reactive gases.  
246 This has been renamed to reactive greenhouse gases.  
247

248 L406- How big is the error in GHGas ERF if one ignores clouds? I would think large.  
249 We have added a discussion of the expected size of the cloud masking effect.  
250

251 Fig 6 & Table 6, can easily combine and understand the Std Dev better.  
252 This has been done, as for the previous ERF plots. The Fig. now contains the error bars and the  
253 multi-model means, with a Table of values in the Supplemental material.  
254

255 L419- Here is a case where some assessment is due as to how well these model simulations are  
256 accurate in the sense of including all the effects. As noted the N2O-O3 link is important and  
257 missing in some, and the other key link between N2O and tropospheric OH and methane (and  
258 maybe aerosols) is established but missing here.

259 [We have added more discussion on this. For the relevant impacts on stratospheric/tropospheric](#)  
260 [ozone, and methane lifetime, only the models with appropriate chemical processes are](#)  
261 [considered.](#)

262

263 L431-441- This is a very interesting and important discussion about the additivity of the  
264 components. I suspect that the CH4 result is similarly affected.

265 BTW, where is the effect of stratospheric H2O from CH4 noted or counted?

266 [We have added plots of the water vapour changes from the CH4 experiment in the Supplementary](#)  
267 [Materials.](#)

268

269 L480- Yes halocarbons, but also N2O, and N2O may be more important since it depletes ozone in  
270 the tropics (there are papers on this). I do not see what difference stratospheric Cl will make on  
271 the total lifetime – hopefully the Stevenson paper becomes referencable. Also, you need to be  
272 careful here since the methane feedback factors ff, apply to the PI atmosphere, and that is  
273 different from the present, particularly lower CO and NOx.... . The feedback factor used for  
274 GWPs etc, is the current one, not the PI one, so these results should NOT be used to change any  
275 previous assessments.

276 [We have mentioned the change due to N2O as well, and clarified that the f factors are starting](#)  
277 [from a pre-industrial atmosphere.](#)

278

279 Fig 11 is really hard to understand or see clearly, it will need a cleanup.

280 [This figure has been revised to make it cleaner and easier to read.](#)

281

282 L525- Here is a very important statement and I am not sure that you have put together all the  
283 reasonable uncertainties or non-linear scaling. The individual components here must be adjusted  
284 to recognize that the total ERF (with all simultaneously) is much less than the sum of the  
285 components. Thus you cannot recommend the individual results without scaling and without  
286 increasing the uncertainty.

287 [We have revised the discussion to explain the differences between the individual components and](#)  
288 [the total, and the implications for uncertainty.](#)

289

290 L561- Same as above. The individual values will not sum correctly and so these do NOT reflect  
291 the ERF of NOx emissions as we progress from 1850 to 2014. Thus they should not be used as  
292 part of an assessment until they are more critically evaluated and put in context.

293 These are all very important AerChemMIP results, and the analysis here is highly valuable, but  
294 their use in attribution and related studies should reflect the bias and uncertainties in combining  
295 nonlinear parts that were calculated separately, and in basing these all on a pi-atmosphere.

296 [This discussion has been revised to explain the differences between the sum of NOx and VOC](#)  
297 [and the total. The ERFs are typically defined starting from a pre-industrial atmosphere, there is](#)  
298 [no unique way to reflect the ERF of NOx emissions as we progress from 1850 to 2014](#)  
299 [\(subtracting components from a present atmosphere would overestimate the ERF\).](#)

300

301

302

303



# Effective radiative forcing from emissions of reactive gases and aerosols – a multi-model comparison

Gillian D. Thornhill<sup>1</sup>, William J. Collins<sup>1</sup>, Ryan J. Kramer<sup>2</sup>, Dirk Olivie<sup>3</sup>, Ragnhild B. Skeie<sup>4</sup>,  
Fiona O'Connor<sup>5</sup>, Nathan L. Abraham<sup>6</sup>, Ramiro Checa Garcia<sup>7</sup>, Susanne E. Bauer<sup>8</sup>, Makoto  
Deushi<sup>9</sup>, Louisa K. Emmons<sup>10</sup>, Piers Forster<sup>11</sup>, Larry W. Horowitz<sup>12</sup>, Ben Johnson<sup>5</sup>, James  
Keeble<sup>6</sup>, Jean-Francois Lamarque<sup>10</sup>, Martine Michou<sup>13</sup>, Mike Mills<sup>10</sup>, Jane P. Mulcahy<sup>5</sup>,  
Gunnar Myhre<sup>4</sup>, Pierre Nabat<sup>13</sup>, Vaishali Naik<sup>12</sup>, Naga Oshima<sup>9</sup>, Michael Schulz<sup>3</sup>, Christopher  
J. Smith<sup>11</sup>, Toshihiko Takemura<sup>14</sup>, Simone Tilmes<sup>10</sup>, Tongwen Wu<sup>15</sup>, Guang Zeng<sup>16</sup>, Jie  
Zhang<sup>15</sup>.

<sup>1</sup>Department of Meteorology, University of Reading, Reading, RG6 6BB, UK

<sup>2</sup>Climate and Radiation Laboratory, NASA Goddard Space Flight Center, Greenbelt, MD 20771, USA, and  
Universities Space Research Association, 7178 Columbia Gateway Drive, Columbia, MD 21046, USA

<sup>3</sup>Norwegian Meteorological Institute, Oslo, Norway

<sup>4</sup>CICERO – Centre for International Climate and Environmental Research Oslo, Oslo, Norway

<sup>5</sup>Met Office, Exeter, UK

<sup>6</sup>Department of Chemistry, University of Cambridge, Lensfield Road, Cambridge, CB2 1EW, U.K., National  
Centre for Atmospheric Science, U.K

<sup>7</sup>IPSL/LSCE CEA-CNRS-UVSQ-UPSaclay UMR Gif sur Yvette, FRANCE

<sup>8</sup>NASA Goddard Institute for Space Studies, USA

<sup>9</sup>Meteorological Research Institute, Tsukuba, Japan

<sup>10</sup>National Center for Atmospheric Research, Boulder, CO, USA

<sup>11</sup>University of Leeds, Leeds, UK and International Institute for Applied Systems Analysis (IIASA), Laxenburg,  
Austria

<sup>12</sup>NOAA, Geophysical Fluid Dynamics Laboratory (GFDL), Princeton, NJ 08540-6649

<sup>13</sup>Centre National de Recherches Météorologiques, Meteo-France, Toulouse Cedex, France

<sup>14</sup>Research Institute for Applied Mechanics, Kyushu University, Japan

<sup>15</sup>Climate System Modeling Division, Beijing Climate Center, Beijing, China

<sup>16</sup>NIWA, Wellington, New Zealand

*Correspondence to:* Gillian D. Thornhill (g.thornhill@reading.ac.uk)

## Abstract

This paper quantifies effective radiative forcing (ERF) of the present-day anthropogenic emissions of NO<sub>x</sub>, VOCs  
(including CO), SO<sub>2</sub>, NH<sub>3</sub>, black carbon and organic carbon. Effective radiative forcings from pre-industrial to  
present-day changes in the concentrations of methane, N<sub>2</sub>O and ozone-depleting halocarbons are quantified.  
Concentration and emission changes of reactive species can cause multiple changes in the composition of  
radiatively active species: tropospheric ozone, stratospheric ozone, stratospheric water vapour, secondary

339 inorganic and organic aerosol and methane. Where possible we break down the ERFs from each emitted species  
340 into the contributions from the composition changes.

341 The ERFs are calculated using models that participated in the AerChemMIP experiments as part of the CMIP6  
342 project.

343 The 1850 to 2014 multi-model mean ERFs ( $\pm$  standard deviations) are  $-1.03 \pm 0.37 \text{ Wm}^{-2}$  for  $\text{SO}_2$  emissions, -  
344  $0.25 \pm 0.09 \text{ Wm}^{-2}$  for organic carbon (OC),  $0.15 \pm 0.17 \text{ Wm}^{-2}$  for black carbon (BC), for  $\text{NH}_3$  it is  $-0.07 \pm 0.01 \text{ Wm}^{-2}$   
345 and for the aerosols combined it is  $-1.01 \pm 0.25 \text{ Wm}^{-2}$ . The multi-model means for the reactive well-mixed  
346 greenhouse gases (including any effects on ozone and aerosol chemistry) are  $0.67 \pm 0.17 \text{ Wm}^{-2}$  for methane ( $\text{CH}_4$ ),  
347  $0.26 \pm 0.07 \text{ Wm}^{-2}$  for nitrous oxide ( $\text{N}_2\text{O}$ ) and  $0.12 \pm 0.2 \text{ Wm}^{-2}$  for ozone-depleting halocarbons (HC), Emissions  
348 of the ozone precursors nitrogen oxides ( $\text{NO}_x$ ), volatile organic compounds (VOC) and both together ( $\text{O}_3$ ) lead  
349 to ERFs of  $0.14 \pm 0.13 \text{ Wm}^{-2}$ ,  $0.09 \pm 0.14 \text{ Wm}^{-2}$  and  $0.20 \pm 0.07 \text{ Wm}^{-2}$  respectively. The differences in ERFs  
350 calculated for the different models reflect differences in the complexity of their aerosol and chemistry schemes,  
351 especially in the case of methane where tropospheric chemistry captures increased forcing from ozone production.

352

### 353 1. Introduction

354 The characterisation of the responses of the atmosphere, climate, and earth systems to various forcing agents is  
355 essential for understanding, and countering, the impacts of climate change. As part of this effort there have been  
356 several projects directed at using climate models from different groups around the world to produce a systematic  
357 comparison of the simulations from these models, via the Coupled Model Intercomparison Project (CMIP), which  
358 is now in its 6<sup>th</sup> iteration (Eyring et al., 2016). This CMIP work has been subdivided into different areas of interest  
359 for addressing specific questions about climate change, such as the impact of aerosols and reactive greenhouse  
360 gases, and the AerChemMIP (Collins et al., 2017) project is designed to examine the specific effects of these  
361 factors on the climate. The aerosol and aerosol precursor species considered are sulphur dioxide ( $\text{SO}_2$ ), black  
362 carbon (BC), organic carbon (OC). The reactive greenhouse gases and ozone precursors are methane ( $\text{CH}_4$ ),  
363 nitrogen oxide ( $\text{NO}_x$ ), volatile organic compounds (VOCs – including carbon monoxide), nitrous oxide ( $\text{N}_2\text{O}$ )  
364 and ozone-depleting halocarbons (HC).

365 The focus of this work is to characterise the effect of the change from pre-industrial (1850) to present day (2014)  
366 in aerosols and their precursors, and chemically-reactive greenhouse gases (including species that affect ozone)  
367 on the radiation budget of the planet, referred to as radiative forcing, as an initial step to understanding the  
368 response of the atmosphere and earth system to changes in these components. In previous reports of the  
369 Intergovernmental Panel on Climate Change (IPCC) the effect of the various forcing agents on the radiation  
370 balance has been investigated in terms of the radiative forcing, (RF), which is a measure of how the radiative  
371 fluxes at the top of atmosphere (TOA) change in response to changes in, e.g., concentrations or emissions of  
372 greenhouse gases and aerosols. There have been several definitions of radiative forcing, (Forster et al.,  
373 2016;Sherwood et al., 2015), which generally considered the instantaneous radiative forcing (IRF), or a  
374 combination of the IRF including the adjustment of the stratospheric temperature to the driver, generally termed  
375 the stratospheric-temperature adjusted radiative forcing. More recently (Boucher, 2013;Chung and Soden, 2015)  
376 there has been a move towards using the effective radiative forcing (ERF) as the preferred metric, as this includes  
377 the rapid adjustments of the atmosphere to the perturbation, e.g. changes in cloud cover or type, water vapour,



378 tropospheric temperature, which may affect the overall radiative balance of the atmosphere. In this work, ERF is  
379 calculated using two atmospheric model simulations both with the same prescribed sea-surface temperatures  
380 (SSTs) and sea ice, but one having the perturbation we are interested in investigating, e.g. a change in emissions  
381 or concentrations of aerosols or reactive gases. The difference in the net TOA flux between these two simulations  
382 is then defined as the ERF for that perturbation.

383 Previous efforts to understand the radiative forcing due to aerosols and reactive gases in CMIP simulations have  
384 resulted in a wide spread of values from the different climate models, in part due to a lack of suitable model  
385 simulations for extracting the ERF from, e.g., a specific change to an aerosol species. The experiments in the  
386 AerChemMIP project have been designed to address this in part, by defining consistent model set-ups to be used  
387 to calculate the ERFs, although the individual models will still have their own aerosol and chemistry modules,  
388 with varying levels of complexity and different approaches.

389 There are complexities in assessing how a particular forcing agent affects the climate system due to the  
390 interactions between some of the reactive gases; for example methane and ozone are linked in complex ways, and  
391 this increases the problem of understanding the specific contribution of each to the overall ERF when one of them  
392 is perturbed. An attempt to understand some of these interactions is discussed in Section 4.2 below.

393 The experimental set-up and models used are described in Section 2, the methods for calculating the ERFs for the  
394 aerosol and chemistry experiments are described in Section 3, and the results are discussed in section 4. Final  
395 conclusions are drawn in Section 5.

## 396 **2. Experimental Setup**

### 397 **2.1 Models**

398 This analysis is based on models participating in the Coupled Model Intercomparison Project (CMIP6) (Eyring et  
399 al., 2016), which oversees climate modelling efforts from a number of centres with a view to facilitating  
400 comparisons of the model results in a systematic framework. The overall CMIP6 project has a number of sub-  
401 projects, where those with interests in specific aspects of the climate can design and request specific experiments  
402 to be undertaken by the modelling groups. To understand the effects of aerosols and reactive gases on the climate,  
403 a set of experiments was devised under the auspices of AerChemMIP (Collins et al., 2017), described in Section  
404 2.2.

405 The anthropogenic emissions of the aerosols, aerosol precursors and ozone precursors (excluding methane) for  
406 use in the models are given by Hoesly et al. (2018) and van Marle et al. (2017) Models use their own natural  
407 emissions (Eyring et al., 2016). The well-mixed greenhouse gases (WMOGHG), CO<sub>2</sub>, CH<sub>4</sub>, N<sub>2</sub>O and halocarbons  
408 are specified as concentrations either at the surface or in the troposphere. Not all of the models include interactive  
409 aerosols, tropospheric chemistry and stratospheric chemistry, which is the ideal for the AerChemMIP  
410 experiments, but those models which do not include all these processes provide results for a subset of the  
411 experiments described in Section 2.2.

412 The models included in this analysis are summarised below, and in Table 1 with an overview of the model set-up,  
413 aerosol scheme and type of chemistry models used included. A more detailed description of each model and the  
414 aerosol and chemistry schemes used in each is available in the supplementary materials, Table S1.

415 The CNRM-ESM2-1 model (Séférian et al., 2019; Michou et al., 2020) includes an interactive tropospheric aerosol  
416 scheme, and an interactive gaseous chemistry scheme only above the level of 560 hPa. The sulfate precursors

417 evolve to SO<sub>4</sub> using a simple dependence on latitude. The cloud droplet number concentration (CDNC) depends  
418 on SO<sub>4</sub>, organic matter and sea-salt concentrations, so the aerosol cloud-albedo effect is represented, although  
419 other aerosol-cloud interactions are not.

420 The UKESM1 model (Sellar et al., 2020) includes an interactive stratosphere-troposphere gas-phase chemistry  
421 scheme (Archibald et al., 2020) using the UK Chemistry and Aerosol (UKCA); (Morgenstern et al.,  
422 2009;O'Connor et al., 2014) model. The UKCA aerosol scheme, called GLOMAP-mode is two-moment  
423 simulation of tropospheric black carbon, organic carbon, SO<sub>4</sub> and sea salt. Dust is modelled independently using  
424 the bin scheme of Woodward (2001). A full description and evaluation of the chemistry and aerosol schemes in  
425 UKESM1 can be found in Archibald et al. (2020) and Mulcahy et al. (2020) respectively.

426 The MIROC6 model includes the Spectral Radiation-Transport Model for Aerosol Species (SPRINTARS) aerosol  
427 model which predicts mass mixing ratios of the main tropospheric aerosols and models aerosol-cloud interactions  
428 in which aerosols alter cloud microphysical properties and affect the radiation budget by acting as cloud  
429 condensation and ice nuclei (Takemura et al., 2005;Watanabe et al., 2010;Takemura and Suzuki, 2019;Takemura,  
430 2018;Tatebe et al., 2019).

431 The MRI-ESM2 model (Yukimoto et al., 2019) has the Model of Aerosol Species in the Global Atmosphere mark-  
432 2 revision 4-climate (MASINGAR mk-2r4c) aerosol model, and a chemistry model, MRI-CCM2 (Deushi and  
433 Shibata, 2011) which models chemistry processes for ozone and other trace gases from the surface to middle  
434 atmosphere. The model includes aerosol-chemistry interactions, and aerosol-cloud interactions (Kawai et al.,  
435 2019). The ERFs of anthropogenic gases and aerosols under present-day conditions relative to preindustrial  
436 conditions estimated by MRI-ESM2 as part of the Radiative Forcing Model Intercomparison Project (RFMIP)  
437 (Pincus et al., 2016) and AerChemMIP are summarized in Oshima et al. (2020).

438 The BCC-ESM1 model (Wu et al., 2019;Wu et al., 2020) models major aerosol species including gas-phase  
439 chemical reactions, secondary aerosol formation, and aerosol-cloud interactions including indirect effects are  
440 represented. It does not include stratospheric chemistry, so concentrations of ozone, CH<sub>4</sub>, and N<sub>2</sub>O at the top two  
441 model levels are the zonally and monthly values derived from the CMIP6 data package.

442 The NorESM2 model contains interactive aerosols and uses the OsloAero6 aerosol module ((Seland et al., 2020),  
443 Olivié et al., in prep.) describes the formation and evolution of BC, OC, SO<sub>4</sub>, dust, sea-salt and SOA. There is a  
444 limited gas-phase chemistry describing the oxidation of the aerosol precursors DMS, SO<sub>2</sub>, isoprene, and  
445 monoterpenes and oxidant fields of OH, HO<sub>2</sub>, NO<sub>3</sub> and ozone are prescribed climatological fields, and there is no  
446 ozone chemistry in the model.

447 The GFDL-ESM4 model consists of the GFDL AM4.1 atmosphere component, (Dunne et al., 2020;Horowitz et  
448 al., 2020) which includes an interactive tropospheric and stratospheric gas-phase and aerosol chemistry scheme.  
449 Nitrate aerosols are explicitly treated in this model.

450 The CESM2-WACCM model includes interactive chemistry and aerosols for the troposphere, stratosphere and  
451 lower thermosphere (Emmons et al., 2010); (Gettelman et al., 2019). The representation of secondary organic  
452 aerosols follows the Volatility Basis Set approached (Tilmes et al., 2019).

453 The IPSLCM6A-LR-INCA (referred to subsequently as IPSL-INCA) model used for this analysis has interactive  
454 aerosols but a limited gas-phase model. The aerosol scheme is based on a sectional approach with to represent the  
455 size distribution of dust, sea- salt (which has an additional super-coarse mode to model largest emission of spray-  
456 salt aerosols), BC, NH<sub>4</sub>, NO<sub>3</sub>, SO<sub>4</sub>, SO<sub>2</sub> and OA with a combination of accumulation and coarse log-normal modes

457 with both soluble and insoluble treated as independent modes. DMS emissions are prescribed and not interactively  
 458 calculated. BC is modelled as internally mixed with sulphate (Wang et al. (2016), where the refractive index is  
 459 relies on Garnet-Maxwell method. Its emissions are derived from inventories. A new dust refractive index is  
 460 implemented (Di Biagio et al., 2019). Well mixed trace gases concentrations/emissions are forced with  
 461 AMIP/CMIP6 datasets (Lurton et al., 2020) ozone using Checa-Garcia et al. (2018) and solar forcing from Matthes  
 462 et al. (2017).

463 The GISS-E2-1 model aerosol scheme (One-Moment Aerosol (OMA)) module, which includes sulfate, nitrate,  
 464 ammonium, carbonaceous aerosols (BC and OC), is coupled to both the tropospheric and stratospheric chemistry  
 465 scheme. For the results reported here, the physics version 3 of this model configuration was used, which includes  
 466 the aerosol impacts on clouds. For details of the model, see Bauer et al. (2020).

467

468 **Table 1 Components used in the Earth system models (detailed Table is in Supplementary material, Table S1)**

	<u>Aerosols</u>	<u>Tropospheric chemistry</u>	<u>Stratospheric chemistry</u>
<u>IPSL-CM6A-LR- INCA</u>	<u>Interactive</u>	<u>No</u>	<u>No</u>
<u>NorESM2-LM</u>	<u>Interactive</u>	<u>SOA and sulfate precursor chemistry</u>	<u>No</u>
<u>UKESM1-LL</u>	<u>Interactive Tropospheric. Prescribed stratospheric</u>	<u>Interactive</u>	<u>Interactive</u>
<u>CNRM-ESM2-1</u>	<u>Interactive</u>	<u>Chemical reactions down to 560 hPa</u>	<u>Interactive</u>
<u>MRI-ESM2</u>	<u>Interactive</u>	<u>Interactive</u>	<u>Interactive</u>
<u>MIROC6</u>	<u>Interactive</u>	<u>SOA and sulfate precursor chemistry</u>	<u>No</u>
<u>BCC-ESM1</u>	<u>Interactive</u>	<u>Interactive</u>	<u>No</u>
<u>GFDL-ESM4</u>	<u>Interactive</u>	<u>Interactive</u>	<u>Interactive</u>
<u>CESM2-WACCM</u>	<u>Interactive</u>	<u>Interactive</u>	<u>Interactive</u>
<u>GISS-E2-1</u>	<u>Interactive</u>	<u>Interactive</u>	<u>Interactive</u>

469 **2.2 Experiments**

470 The AerChemMIP timeslice experiments (Table 2) are used to determine the present-day (2014) ERFs for the  
 471 changes in emissions or concentrations of reactive gases, and aerosols or their precursors (Collins et al., 2017).

472 The ERFs are calculated by comparing the change in net TOA radiation fluxes between two runs with the same  
 473 prescribed sea surface temperatures (SSTs) and sea ice, but with near-term climate forcers (NTCFs - also referred  
 474 to as short-lived climate forcers - SLCFs), reactive gas and aerosol emissions, and well-mixed greenhouse gases

475 (WMOGHG - methane, nitrous oxide, halocarbon) concentrations perturbed. It should be noted that in  
476 AerChemMIP the NTCF experiment excludes CH<sub>4</sub> the experimental design. The control run uses set 1850 pre-  
477 industrial values for the aerosol and aerosol precursors, CH<sub>4</sub> N<sub>2</sub>O, ozone precursors and halocarbons, either as  
478 emissions or concentrations (Hoesly et al., 2018;van Marle et al., 2017;Meinshausen et al., 2017). Monthly  
479 varying prescribed SSTs and sea-ice are taken from the CMIP6 DECK coupled pre-industrial (1850) control  
480 simulation. Each experiment then perturbs the pre-industrial value by changing one (or more) of the species  
481 (emissions or concentrations) to the 2014 value, while keeping SSTs and sea-ice prescribed as in the pre-industrial  
482 control. Note adding individual species to a pre-industrial control will likely give different results to a setup where  
483 species were individually subtracted from a present-day control. The NTCFs are perturbed individually or in  
484 groups. This provides ERFs for the specific emission or concentration change, but also for all aerosol precursor  
485 or NTCFs combined (Collins et al., 2017). For models without interactive tropospheric chemistry “NTCF” and  
486 “aer” experiments are the same; in the case of NorESM2 for the NTCF experiments the model attempts to mimic  
487 the full chemistry by setting the oxidants and ozone to 2014 values. The WMOGHG experiments include the effects  
488 on aerosol oxidation, tropospheric and stratospheric ozone, and stratospheric water vapour depending on the  
489 model complexity.  
490 Thirty years of simulation are required to minimise internal variability (mainly from clouds) (Forster et al, 2016.),  
491 and one ensemble member was used for each experiment (almost all models provided only a single ensemble  
492 member).

493  
494 **Table 2** List of fixed SST ERF simulations. (NTCF in (Collins et al., 2017) is also referred to as 'SLCF' - short-lived  
495 climate forcers - in other publications) and for the purposes of this study excludes methane.

<u>Experiment ID</u>	<u>CH<sub>4</sub></u>	<u>N<sub>2</sub>O</u>	<u>Aerosol Precursors</u>	<u>Ozone Precursors</u>	<u>CFC/ HCFC</u>	<u>Number of models</u>
<u><i>piClim-control</i></u>	<u>1850</u>	<u>1850</u>	<u>1850</u>	<u>1850</u>	<u>1850</u>	<u>11</u>
<u><i>piClim-NTCF</i></u>	<u>1850</u>	<u>1850</u>	<u>2014</u>	<u>2014</u>	<u>1850</u>	<u>8</u>
<u><i>piClim-aer</i></u>	<u>1850</u>	<u>1850</u>	<u>2014</u>	<u>1850</u>	<u>1850</u>	<u>9</u>
<u><i>piClim-BC</i></u>	<u>1850</u>	<u>1850</u>	<u>1850 (non BC) 2014 (BC)</u>	<u>1850</u>	<u>1850</u>	<u>7</u>
<u><i>piClim-O3</i></u>	<u>1850</u>	<u>1850</u>	<u>1850</u>	<u>2014</u>	<u>1850</u>	<u>4</u>
<u><i>piClim-CH4</i></u>	<u>2014</u>	<u>1850</u>	<u>1850</u>	<u>1850</u>	<u>1850</u>	<u>8</u>
<u><i>piClim-N2O</i></u>	<u>1850</u>	<u>2014</u>	<u>1850</u>	<u>1850</u>	<u>1850</u>	<u>5</u>
<u><i>piClim-HC</i></u>	<u>1850</u>	<u>1850</u>	<u>1850</u>	<u>1850</u>	<u>2014</u>	<u>6</u>
<u><i>piClim-NOX</i></u>	<u>1850</u>	<u>1850</u>	<u>1850</u>	<u>1850 (non NO<sub>x</sub>) 2014 (NO<sub>x</sub>)</u>	<u>1850</u>	<u>5</u>
<u><i>piClim-VOC</i></u>	<u>1850</u>	<u>1850</u>	<u>1850</u>	<u>1850 (non CO/VOC) 2014 (CO/VOC)</u>	<u>1850</u>	<u>5</u>
<u><i>piClim-SO2</i></u>	<u>1850</u>	<u>1850</u>	<u>1850 (non SO<sub>2</sub>) 2014 (SO<sub>2</sub>)</u>	<u>1850</u>	<u>1850</u>	<u>6</u>
<u><i>piClim-OC</i></u>	<u>1850</u>	<u>1850</u>	<u>1850 (non OC) 2014 (OC)</u>	<u>1850</u>	<u>1850</u>	<u>6</u>

<u>piClim-NH3</u>	<u>1850</u>	<u>1850</u>	<u>1850 (non NH<sub>3</sub>)</u> <u>2014 (NH<sub>3</sub>)</u>	<u>1850</u>	<u>1850</u>	<u>2</u>
-------------------	-------------	-------------	--	-------------	-------------	----------

496 **3. Methods**

497 In the following analysis we use several methods to analyse the ERF and the relative contributions from different  
498 aerosols, chemistry and processes to the overall ERF for the models and experiments described above, where the  
499 appropriate model diagnostics were available.

500 **3.1 Calculation of ERF using fixed SSTs**

501 The ERF is calculated from the experiments described above, where the sea surface temperatures and sea-ice are  
502 fixed to climatological values. Here the ERF is defined as the difference in the net TOA flux between the perturbed  
503 experiments and the piClim-control experiment (Sherwood et al., 2015), calculated as the global mean for the 30  
504 years of the experimental run (where the models were run longer than 30 years, only the last 30 years was used).  
505 This allows us to calculate the ERF for the individual species based on the changes to the emission or  
506 concentrations between the control and perturbed runs of the models. The assumption is that there is minimal  
507 contribution from the climate feedback when the SSTs are fixed, but the resultant ERF includes rapid adjustments  
508 to the forcing agent in the atmosphere (Forster et al., 2016).

509 The ERF calculated using this method includes any contributions to the ERF resulting from changes in the land  
510 surface temperature ( $T_s$ ), which ideally should be removed (Shine et al., 2003; Hansen et al., 2005; Vial et al.,  
511 2013) (as the ocean temperature changes are removed by using fixed SSTs). However, there is no simple way to  
512 prescribe land surface temperatures in the models considered here analogous to the fixing the SSTs, so we make  
513 the land surface temperature correction by calculating the surface temperature adjustment from the radiative  
514 kernel (see Section 3.2) and subtracting it from the standard ERF as calculated above (see also Smith et al.  
515 (2020a);(Tang et al., 2019)). This is designated the ERF<sub>ts</sub> to differentiate it from the standard ERF as described  
516 above.

518 **3.2 Kernel Analysis**

519 Where the relevant data are available, we use the radiative kernel method (Smith et al., 2018; Soden et al.,  
520 2008; Chung and Soden, 2015) to break down the ERF into the instantaneous radiative forcing (IRF) and individual  
521 rapid adjustments (designated by  $A$ ) which are radiative responses to changes in atmospheric state variables that  
522 are not coupled to surface warming. In this approach, ERF is defined as:

$$523 \text{ERF} = \text{IRF} + A_T + A_{Ts} + A_q + A_a + A_c + e \quad (1)$$

524 where  $A_T$  = atmospheric temperature,  $A_{Ts}$  = surface temperature,  $A_q$  = water vapour,  $A_a$  = albedo,  $A_c$  = clouds,  $e$   
525 = radiative kernel error. Individual rapid adjustments ( $A_x$ ) are computed as:

$$526 A_x = \frac{\delta R}{\delta x} dx \quad (2)$$

528 where  $\frac{\delta R}{\delta x}$  is the radiative kernel, a diagnostic tool typically computed with an offline version of a GCM radiative  
529 transfer model that is initialized with climatological base state data and  $dx$  is the climate response of atmospheric  
530 state variable  $x$ , diagnosed directly from each model. Cloud rapid adjustments ( $A_c$ ) are estimated by diagnosing  
531 cloud radiative forcing from model flux diagnostics and correcting for cloud masking using the kernel-derived  
532 non-cloud adjustments and IRF, following common practice (e.g. (Soden et al., 2008; Smith et al., 2018)),  
533 whereby:

$$534 A_c = (ERF - ERF^{clr}) - (IRF - IRF^{clr}) - \sum_{x=[T,ts,q,a]} (A_x - A_x^{clr}) \quad (3)$$

535 For the calculation of the IRF (for aerosols this is the direct effect) here, the clear-sky IRF ( $IRF^{clr}$ ) is estimated  
536 as the difference between clear-sky ERF ( $ERF^{clr}$ ) and the sum of kernel-derived clear-sky rapid adjustments  
537 ( $A_x^{clr}$ ). Since estimates of  $A_c$  are dependent on IRF, the same differencing method cannot be used to estimate IRF  
538 under all-sky conditions without special diagnostics (in particular the International Satellite Cloud Climatology  
539 Project diagnostics (ISCCP) diagnostics) not widely available in the AerChemMIP archive. Instead, for the  
540 calculations presented here all-sky IRF is computed by scaling  $IRF^{clr}$  by a species-specific factor to account for  
541 cloud masking (Soden, Held et al. 2008).

542 Kernels are available from several sources, and for this analysis we used kernels from CESM, (Pendergrass et al.,  
543 2018), GFDL (Soden et al., 2008), HadGEM3, (Smith et al., 2020b), and ECHAM6 (Block and Mauritsen, 2013)  
544 and took the mean from the four kernels for each model. Overall the individual kernels produced very similar  
545 results for each model, as reported in Smith et al. (2018).

### 546 **3.3 Calculation of ERF using aerosol-free radiative fluxes**

547 To understand the contributions of various processes to the overall ERF we can attempt to separate the ERF that  
548 is due to direct radiative forcing from that due to the effects of clouds. Greenhouse gases and aerosols can alter  
549 the thermal structure of the atmosphere and hence cloud thermodynamics (the semi-direct effect, (Ackerman et  
550 al., 2000)), and aerosols can act via microphysical effects (e.g. increasing the number of condensation nuclei and  
551 decreasing the effective radii of cloud droplets, referred to as the aerosol cloud albedo effect and the cloud lifetime  
552 effect (Twomey, 1974; Albrecht, 1989; Pincus and Baker, 1994). Following the method of Ghan (2013) the  
553 contribution of the aerosol-radiation interactions to the ERF can be distinguished from that of the aerosol-cloud  
554 interactions by using a ‘double-call’ method. This means that the model radiative flux diagnostics are calculated  
555 a second time but ignoring the scattering and absorption by the aerosol – referred to in the equations below with  
556 the subscript ‘af’. The other effects of the aerosol on the atmosphere (i.e. cloud changes, stability changes,  
557 dynamics changes) will still be present, however. The IRF<sub>af</sub> as defined here is the direct radiative forcing from  
558 the aerosol, due to scattering and absorption of radiation. The cloud radiative forcing (ERF<sub>af</sub>) due to the aerosol-  
559 cloud interactions is then obtained by using the difference between the aerosol-free all-sky fluxes and the aerosol-  
560 free clear-sky fluxes, which isolates the cloud effects (see eqns 4-6, where equation 6 is included for  
561 completeness). The ERF<sub>af</sub> may include non-cloud rapid adjustments in cloudy regions of the atmosphere. The  
562 final term is the ERF as calculated from fluxes with neither clouds nor aerosols (ERF<sub>cs,af</sub>).

563 The ERFs are calculated in the same way as for the all-sky ERF described in Section 3.1, except that the all-sky  
564 radiative flux diagnostics are replaced by the relevant aerosol-free fluxes for both the clear-sky and all-sky cases.

565



566  $IRF_{ari} = (ERF - ERF_{af})$  \_\_\_\_\_ (4)

567  $ERF_{aci} = ERF_{af} - ERF_{cs,af}$  \_\_\_\_\_ (5)

568  $ERF_{cs,af} = ERF_{cs,af}$  \_\_\_\_\_

569 (6)

570 Separating the IRF in equation 1 into aerosols and greenhouse gas contributions,  $IRF = IRF_{aer} + IRF_{GHG}$ , we can re-  
 571 write equations 4-6.

572  $IRF_{ari} = IRF_{aer}$  \_\_\_\_\_ (7)

573  $ERF_{aci} = A_c + \sum_{x=[T,ts,q,a]} (A_x - A_x^{clr}) + (IRF_{GHG} - IRF_{GHG}^{clr})$  \_\_\_\_\_ (8)

574  $ERF_{cs,af} = \sum_{x=[T,ts,q,a]} A_x^{clr} + IRF_{GHG}^{clr}$  \_\_\_\_\_ (9)

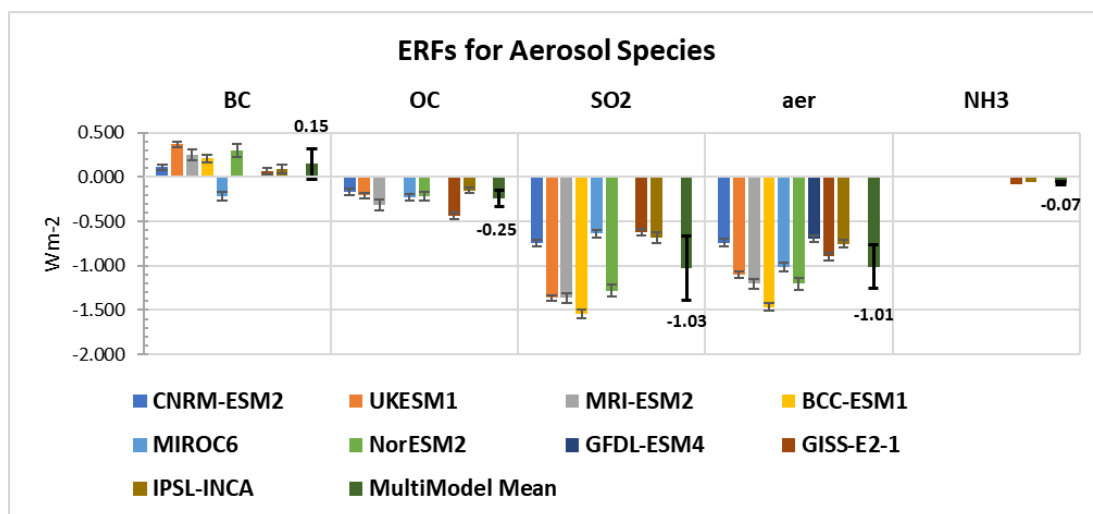
575 So  $ERF_{aci}$  is equivalent to  $A_c$  in equation 3 with extra terms to account for the all-sky - clear-sky difference in  
 576 the non-cloud adjustments and all-sky - clear-sky difference in any greenhouse gas IRF. With no greenhouse gas  
 577 changes  $ERF_{cs,af}$  is the total clear-sky non-cloud adjustment. Ghan (2013) attributes this mostly to the surface  
 578 albedo change  $A_{\alpha}^{clr}$ , however the kernel analysis shows other non-cloud adjustments are larger (table S4). For  
 579 greenhouse gases  $ERF_{cs,af}$  is the total clear-sky ERF. Assuming the non-cloud adjustments are small apart from  
 580  $T_{strat}$  (table S4),  $ERF_{cs,af}$  is approximately  $SARF_{GHG}^{clr}$ . The  $SARF_{GHG}^{clr}$  is expected to be an overestimate of  
 581  $SARF_{GHG}$  by 10-40% due to cloud masking (Myhre and Stordal 1997). Thus for greenhouse gases the  $ERF_{aci}$   
 582 will be a combination of the cloud adjustment and cloud-masking.

583 **4. Results**

584 **4.1 Aerosols and precursors**

585 **4.1.1 Inter-model Variability**

586 The ERFs are calculated as described in Section 3.1, and the summary chart of the ERFs is shown in Fig. 1 for  
 587 those models with available results – it should be noted that not all models ran all the experiments. The multimodel  
 588 mean is shown as a separate bar in Fig. 1, with the value given and the standard error indicated with error bars. A  
 589 table of the individual values for each model and the multimodel mean are included Table S2 in the supplementary  
 590 materials.



592

593 Fig. 1 Aerosol ERFs for the models with the available diagnostics for the aerosol species experiments, with interannual  
594 variability represented by error bars showing the standard error. The multimodel mean is shown with the mean value  
595 and error bars indicating the standard deviation.

596 For the piClim-BC results, the range of values is from  $-0.21 \text{ Wm}^{-2}$  to  $0.37 \text{ Wm}^{-2}$ , while the MIROC6 model has a  
597 negative ERF for BC, contrasting with the positive values from the other models - see further discussion on this  
598 in Section 4.1.2.

599 The experiments for the OC (organic carbon) have a range from  $-0.44 \text{ Wm}^{-2}$  to  $-0.15 \text{ Wm}^{-2}$ , and the variability  
600 between the models is much less than for the other experiments. The calculated ERFs for the SO<sub>2</sub> experiment  
601 show a variation from  $-1.54 \text{ Wm}^{-2}$  to  $-0.62 \text{ Wm}^{-2}$ , with CNRM-ESM2-1, MIROC6, IPSL-INCA and GISS-E2-1  
602 at the lower end of the range. These models show a smaller rapid adjustment to clouds which would account for  
603 this (see fig S1); also note that CNRM-ESM2-1 does not include aerosol effects apart from the cloud-albedo  
604 effect. The two models with results for the NH<sub>3</sub> (GISS-E2-1 and IPSL-INCA) experiment have ERFs of  $-0.08$  and  
605  $-0.06 \text{ Wm}^{-2}$  respectively.

606 The piClim-aer experiment which uses the 2014 values of aerosol precursors and PI (pre-industrial) values for  
607 CH<sub>4</sub>, N<sub>2</sub>O and ozone precursors shows a range from  $-1.47 \text{ Wm}^{-2}$  to  $-0.7 \text{ Wm}^{-2}$  among the models, making it  
608 difficult to narrow the range of uncertainty of aerosols from global models. However, the range in the CMIP6  
609 models is consistent with that reported in Bellouin et al. (2019), who suggest a probable range of  $-1.60$  to  $-0.65$   
610  $\text{Wm}^{-2}$  for the total aerosol ERF, and compares well with the range of  $-1.37$  to  $-0.63 \text{ Wm}^{-2}$  for the set of piClim-  
611 aer experiments considered in (Smith et al., 2020a) as part of the RFMIP project. In general, the sum of the ERFs  
612 from the individual BC, OC and SO<sub>2</sub> experiments does not equal the piClim-aer experiment, due to non-linearity  
613 in the aerosol-cloud interactions, particularly since the aerosol perturbation is added to the relatively pristine pre-  
614 industrial atmosphere.

615 The issue of the effect of perturbing the pre-industrial atmosphere with the aerosol changes is examined in more  
616 detail in the Supplementary material (see section S6) for NorESM2, where a sensitivity analysis was carried out.  
617 This analysis does not repeat the AerChemMIP experiments with the perturbation in a present-day atmosphere  
618 but examines the effect of adding the SO<sub>2</sub> and combined aerosol perturbation to an already polluted present day  
619 atmosphere. In this simplified sensitivity study the differences are 13% for the SO<sub>2</sub> experiment, and 20% for the  
620 combined aerosol experiment. However, it should be borne in mind that this is for a specific model, and the  
621 perturbed experiment still has the 1850 climate conditions.

622 The ERF<sub>ts</sub> is a simplified method for corrections of land surface warming in fixed sea surface temperature  
623 simulations which in addition to land surface changes leads to changes in land surface albedo changes,  
624 tropospheric temperature, water vapor and cloud changes (Smith et al., 2020a;Tang et al., 2019).

625 The ERF<sub>ts</sub> for the models where the land surface temperature adjustment is removed are also included in  
626 Supplemental Tables S2 and S3, for comparison with the standard ERF. In general, the difference between the  
627 two values is small, of the order of 5 -10%.

628

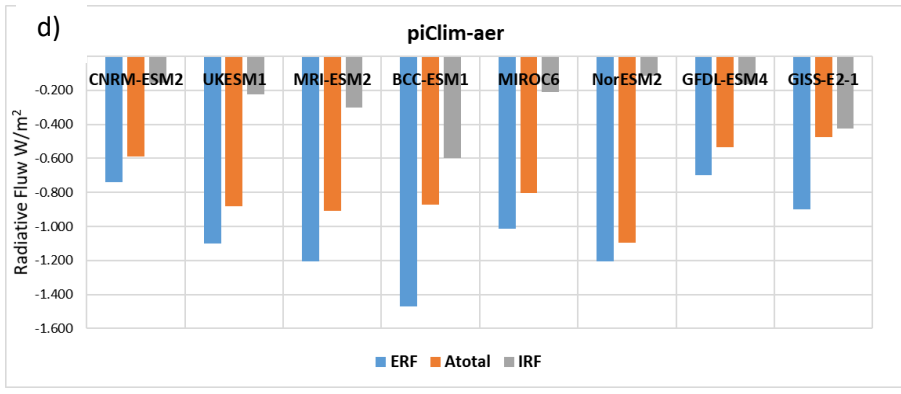
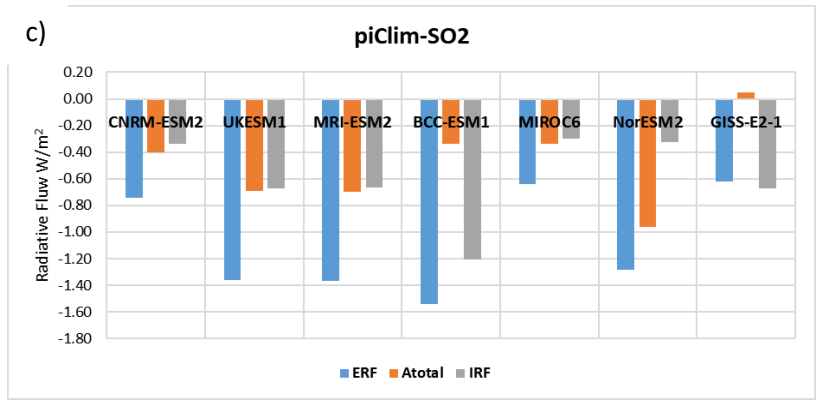
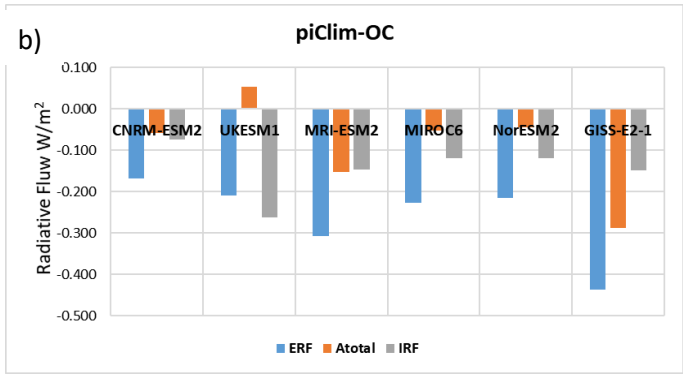
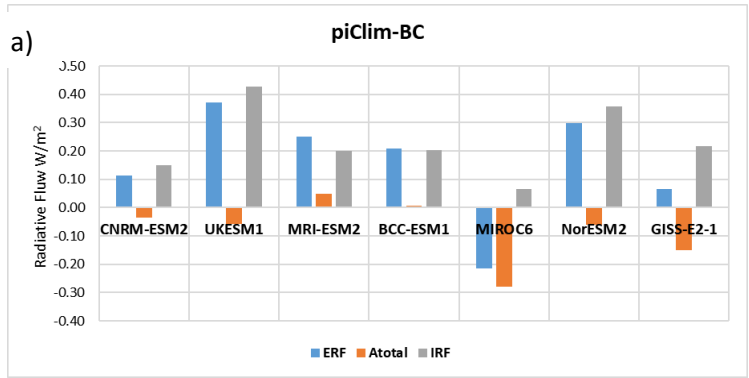


Figure 2 Breakdown of the ERFs into the atmospheric rapid adjustments (Atotal) and IRF (instantaneous radiative forcing) for the aerosols. (a) piClim-BC experiment, (b) piClim-SO2 experiment, (c) piClim-OC experiment, (d) piClim-aer experiment

629  
630

4.1.2 Breakdown of the ERF into atmospheric adjustments and IRF

631 The results in Fig. 2 show the ERF as calculated from the radiative fluxes in the fixed SST experiments (Section  
632 3.1), the total of the atmospheric adjustments,  $A_{total}$ , described in Section 3.2 (where  $A_{total} = A_T + A_{ts} + A_q + A_a +$   
633  $A_c$  c.f. eqn. 1), and the instantaneous radiative forcing (IRF).  
634 The sum of the IRF and the atmospheric adjustments should equal the overall ERF, however as the calculation of  
635 the IRF depends upon an empirical factor for cloud masking to find the all-sky IRF from the clear-sky IRF (see  
636 Section 3.2) the sum of the IRF and the  $A_{total}$  will not necessarily equal the ERF as calculated directly from the  
637 model radiative flux diagnostics. However, in general the difference is less than 3%, suggesting that the  
638 approximation used in the calculation of the IRF is reasonable. Using the kernel method described above it is  
639 important to note that the IRF calculated here accounts for the presence of the clouds but does not include cloud  
640 changes such as the cloud albedo effect.  
641 The models show a variability in the IRF for  $SO_2$  (Fig. 2c) with a range of  $-0.3 \text{ Wm}^{-2}$  to  $-1.2 \text{ Wm}^{-2}$  with the BCC-  
642 ESM1 model being the outlier, having the largest overall ERF. The OC experiments (Fig. 2b) range from  $-0.08$   
643  $\text{Wm}^{-2}$  to  $-0.26 \text{ Wm}^{-2}$ , with a range for BC of  $0.07 \text{ Wm}^{-2}$  to  $0.43 \text{ Wm}^{-2}$  (Fig. 2a). In MIROC6 the treatment of BC  
644 (Takemura & Suzuki 2019; Suzuki & Takemura 2019) leads to faster wet removal of BC and hence a lower IRF.  
645 For the combined aerosols (Fig 2d) the range is from  $-0.1 \text{ Wm}^{-2}$  to  $-0.6 \text{ Wm}^{-2}$ .  
646 There are significant differences between the models in the  $A_{total}$  for  $SO_2$ ; these range from  $0.05 \text{ Wm}^{-2}$  to  $-1.0$   
647  $\text{Wm}^{-2}$ , where the differences are dominated by the cloud adjustments which here include the cloud albedo effect  
648 as part of the adjustment (see Fig S3 for breakdowns of the atmospheric adjustments for all models). The  
649 adjustments to BC are vary in sign and magnitude, with the MRI-ESM2 and BCC-ESM1 models having a slight  
650 positive adjustment. The overall model mean has a weaker negative adjustment to that reported by (Stjern et al.,  
651 2017; Samset et al., 2016; Smith et al., 2018). The MIROC6 model has a large negative adjustment which is large

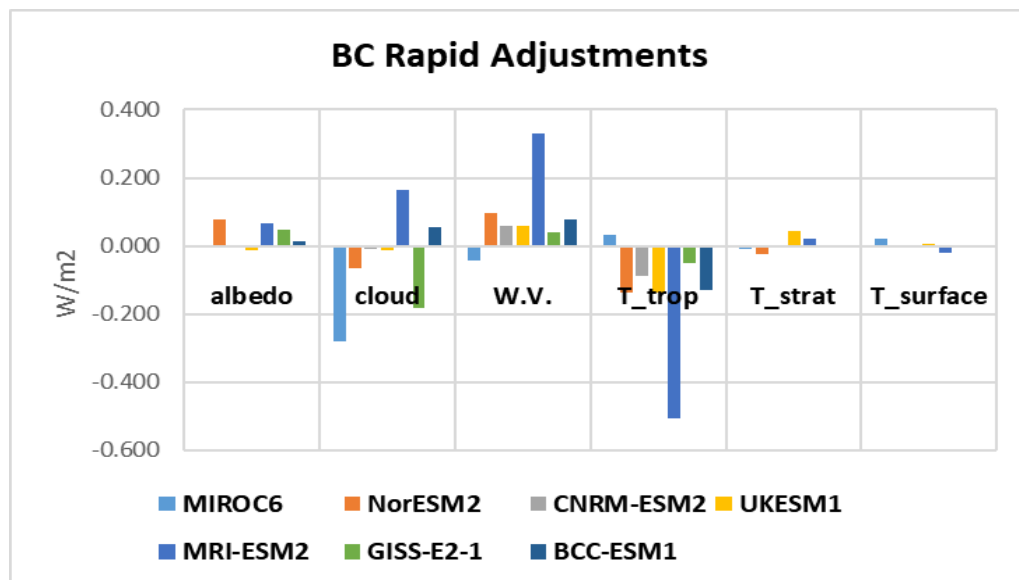


Figure 3 Breakdown of the atmospheric adjustments (albedo, cloud, water vapour, troposphere temperature, stratosphere temperature and surface temperature) for the piClim-BC experiments, showing the variability between models.

652 enough to lead to an overall negative ERF. We explore the contribution of the individual adjustments to BC in  
653 more detail in Fig. 3.

654 Examining the breakdown of the rapid adjustments for the piClim-BC experiments (Fig. 3) we see considerable  
655 variability in the relative importance of the rapid adjustments; the cloud adjustment dominates in MIROC6,  
656 consistent with the increase in low clouds reported for this model, and the treatment of BC as ice nuclei causes  
657 the large negative cloud adjustment here (Takemura and Suzuki, 2019;Suzuki and Takemura, 2019). The GISS-  
658 E2-1 model also has a strong cloud rapid adjustment, but the larger positive value of the IRF leads to an overall  
659 positive ERF for this model. With the exception of MIROC6 the negative tropospheric temperature adjustment is  
660 balanced by the water vapour (specific humidity) adjustment, although the magnitude of these adjustments for  
661 MRI-ESM2 is at least twice that for the other two models. The interaction of BC with clouds in the MRI-ESM2  
662 model is discussed in detail in Oshima et al. (2020), in particular the impact of BC on ice nucleation in high  
663 clouds. The larger surface albedo adjustment for both NorESM2 and MRI-ESM2 is most likely due to the  
664 representation of deposition of BC on snow and ice in these models (Oshima et al., 2020).

665 The piClim-aer experiments (Fig. 1d) show all models have a negative  $A_{total}$ , covering a range from -0.47 to -1.1  
666  $Wm^{-2}$ . Overall, the cloud rapid adjustments dominate for the piClim-aer experiments, with a contribution ranging  
667 from -0.45 to -1.1  $Wm^{-2}$  (See fig S1). Smith et al. (2020) also recently diagnosed forcing and adjustments in a  
668 similar subset of CMIP6 models for the piClim-aer experiment as part of the Radiative Forcing Model  
669 Intercomparison Project (RFMIP) efforts. While they also diagnosed IRF as a residual calculation between ERF  
670 and the sum of rapid adjustments, they estimated cloud adjustments using a modified version of the APRP method  
671 instead of radiative kernels. In their approach, the cloud albedo effect (i.e. Twomey Effect) is considered part of  
672 the IRF, whereas in the traditional kernel decomposition, it is considered a cloud adjustment. Table S5 compares  
673 the two sets of estimates, highlighting the IRF and total cloud adjustment exhibit a near equal absolute difference  
674 between the two studies and the sum of IRF and total cloud adjustment are in close agreement (Mean % difference  
675  $\sim 1.0\%$  for this subset of models). This indicates the classification of the first indirect effect is the only noticeable  
676 difference between the two approaches.

677 The breakdown of the rapid adjustments for all the models are included in supplementary Figure S1, showing the  
678 contributions from each type of rapid adjustment for all the experiments for which we have the relevant  
679 diagnostics.

680

### 681 **4.1.3 Radiation and Cloud interactions**

682 The second method of breaking down the ERF to constituents is described in Section 3.3, (the Ghan method), the  
683 results from which are shown in Table 3. The detailed ERF results for MRI-ESM2 are summarized in Oshima et  
684 al. (2020), and for UKESM1 in O'Connor et al. (2020a) . Only four of the models under consideration have so far  
685 produced the necessary diagnostics for this calculation , and the results are presented in Table 3. For the  
686 experiments on aerosols (aer, BC,  $SO_2$ , OC) the ERF<sub>cs,af</sub> (non-cloud adjustments) contribution is small, and the  
687 ERF is largely a combination of the direct radiative effect IRF<sub>ari</sub>, and the cloud radiative effect, ERF<sub>aci</sub>. The  
688 IRF<sub>ari</sub> is the direct effect of the aerosol due to scattering and absorption, while the ERF<sub>aci</sub> is the contribution  
689 from the aerosol-cloud interactions and is approximately equal to the rapid adjustments due to clouds ( $A_c$  see  
690 Section 3.2).

691  
692  
693  
694

**Table 3 Results for IRFari, ERFaci and ERFcs,af for aerosol experiments from several models**

	<u>UKESM1</u>			<u>CNRM-ESM2</u>			<u>NorESM2</u>			<u>MRI-ESM2</u>		
	<u>IRFari</u>	<u>cs,af</u>	<u>ERFaci</u>	<u>IRFari</u>	<u>cs,af</u>	<u>ERFaci</u>	<u>IRFari</u>	<u>cs,af</u>	<u>ERFaci</u>	<u>IRFari</u>	<u>cs,af</u>	<u>ERFaci</u>
<u>aer</u>	<u>-0.15</u>	<u>0.05</u>	<u>-1.00</u>	<u>-0.21</u>	<u>0.08</u>	<u>-0.61</u>	<u>0.03</u>	<u>-0.03</u>	<u>-1.21</u>	<u>-0.32</u>	<u>0.09</u>	<u>-0.98</u>
<u>BC</u>	<u>0.37</u>	<u>0.001</u>	<u>-0.005</u>	<u>0.13</u>	<u>0.01</u>	<u>-0.03</u>	<u>0.35</u>	<u>0.07</u>	<u>-0.12</u>	<u>0.26</u>	<u>0.08</u>	<u>-0.09</u>
<u>OC</u>	<u>-0.15</u>	<u>-0.01</u>	<u>-0.07</u>	<u>-0.07</u>	<u>0.04</u>	<u>-0.14</u>	<u>-0.07</u>	<u>0.02</u>	<u>-0.16</u>	<u>-0.07</u>	<u>-0.05</u>	<u>-0.21</u>
<u>SO2</u>	<u>-0.49</u>	<u>0.03</u>	<u>-0.91</u>	<u>-0.29</u>	<u>0.08</u>	<u>-0.53</u>	<u>-0.19</u>	<u>-0.09</u>	<u>-1.01</u>	<u>-0.48</u>	<u>0.05</u>	<u>-0.93</u>

695

696 For the BC experiment the contribution of the aerosol-cloud interaction has a strong contribution to the overall  
697 ERF, except in the case of UKESM1 where it is much weaker; this may be due to the strong SW and LW cloud  
698 adjustments in this model cancelling out (O'Connor et al., 2020;Johnson et al., 2019). The SO<sub>2</sub> experiment shows  
699 a large cloud radiative effect, in fact the ERFaci is mostly double the IRFari in all the models, due to the large  
700 effect on clouds of SO<sub>2</sub> and sulfates through the indirect effects. For the OC experiments the ERFaci to IRFari  
701 comparison is mixed, with the ERFaci general half or less the IRFari, except in the case of UKESM1, where this  
702 ratio is reversed.

703 The IRFari are compared with the IRF calculated via the kernel analysis (Section 3.2) where the relevant model  
704 results are available. These are shown in fig S2(a), the agreement is generally good giving confidence in the kernel  
705 analysis. Similarly ERFaci compares well with the cloud adjustment Ac (fig S2(b)).

706

#### 707 **4.1.4 AOD Forcing Efficiencies**

708 In order to break down the contributions of the constituent aerosol species to the overall aerosol ERF, we use the  
709 AOD (aerosol optical depth) as a forcing efficiency metric for each of the species, and use this to assess their  
710 contributions to the overall ERF. Not all models had diagnostics available for the AOD for the individual species,  
711 so the analysis uses a subset of the models.

712 By looking at the single species piClim-BC, piClim-OC and piClim-SO<sub>2</sub> experiments we can find the change in  
713 the AOD for the individual species (e.g. ΔAOD for BC for the piClim-BC experiment), and use this to scale the  
714 the piClim-BC ERF by the AOD change. This assumes that the ERF in the single-species experiment is wholly  
715 due to the change in that species as indicated by the AOD, an assumption which is explored in the Supplementary  
716 material in Section S4. Table 5 shows the AOD forcing efficiency for the piClim-BC, piClim-SO<sub>2</sub> and piClim-  
717 OC experiments for each of the five models which had the relevant optical depth diagnostics available.

718



719 Table 4 Values of ERF,  $\Delta$ AOD and ERF/AOD, and IRFari/AOD change for aerosol experiments for CNRM-ESM2-,  
 720 MIROC6, Nor-ESM2, GISS-E2-1 and MRI-ESM2 models.

<u>BC Exp</u>	<u>BC ERF</u>	<u>Change in BC</u>	<u>ERF/AOD</u>
		<u>AOD</u>	
<u>CNRM-ESM2</u>	<u>0.114</u>	<u>0.0015</u>	<u>77.64</u>
<u>MIROC6</u>	<u>-0.214</u>	<u>0.0006</u>	<u>-339.38</u>
<u>NorESM2</u>	<u>0.300</u>	<u>0.0019</u>	<u>159.75</u>
<u>GISS-E2-1</u>	<u>0.065</u>	<u>0.002</u>	<u>31.65</u>
<u>MRI-ESM2</u>	<u>0.251</u>	<u>0.0073</u>	<u>34.22</u>
<u>OC Exp</u>	<u>OC ERF</u>	<u>Change in OA</u>	<u>ERF/AOD</u>
		<u>AOD</u>	
<u>CNRM-ESM2</u>	<u>-0.169</u>	<u>0.0030</u>	<u>-57.20</u>
<u>MIROC6</u>	<u>-0.227</u>	<u>0.0065</u>	<u>-35.05</u>
<u>NorESM2</u>	<u>-0.215</u>	<u>0.0053</u>	<u>-40.57</u>
<u>GISS-E2-1</u>	<u>-0.438</u>	<u>0.0041</u>	<u>-107.16</u>
<u>MRI-ESM2</u>	<u>-0.317</u>	<u>0.0034</u>	<u>-94.39</u>
<u>SO2 Exp</u>	<u>SO2 ERF</u>	<u>Change in SO4</u>	<u>ERF/AOD</u>
		<u>AOD</u>	
<u>CNRM-ESM2</u>	<u>-0.746</u>	<u>0.0118</u>	<u>-63.22</u>
<u>MIROC6</u>	<u>-0.637</u>	<u>0.0152</u>	<u>-41.91</u>
<u>NorESM2</u>	<u>-1.281</u>	<u>0.0099</u>	<u>-129.24</u>
<u>GISS-E2-1</u>	<u>-0.622</u>	<u>0.0308</u>	<u>-20.22</u>
<u>MRI-ESM2</u>	<u>-1.365</u>	<u>0.0279</u>	<u>-49.08</u>

721 The MIROC6 model results in a negative scaling for BC due to the negative ERF for this experiment for this  
 722 model (Takemura & Suzuki 2019; Suzuki & Takemura 2019) (see Section 4.1.1). The change in the BC AOD is  
 723 similar for CNRM-ESM2-1 and Nor-ESM2, and the scale factors reflect the differences in the ERF. The scaling  
 724 for the SO4 in the NorESM2 experiment is twice that of the other models, suggesting a larger impact of the SO4  
 725 AOD on the ERF in this model. These values differ somewhat from those found in Myhre et al. (2013b) where  
 726 they examined the radiative forcing normalised to the AOD using models in the AeroCom Phase II experiments.  
 727 They found values for sulfate ranging from  $-8 \text{ Wm}^{-2}$  to  $-21 \text{ Wm}^{-2}$  per unit AOD, much weaker than those in our  
 728 results. However, it is important to note that in the Aerocom Phase II experiments the cloud and cloud optical  
 729 properties are identical between their control and perturbed runs, so no aerosol indirect effects are included, nor

730 is any rapid adjustments (IRFari in equation 4). For the BC experiment their values range from 84  $\text{Wm}^{-2}$  to 216  
 731  $\text{Wm}^{-2}$  per unit AOD, broadly similar to the results presented here (with the exception of the negative MIROC6  
 732 result). Their results for OA (organic aerosols) which include fossil fuel and biofuel emissions have values ranging  
 733 from  $-10 \text{ Wm}^{-2}$  to  $-26 \text{ Wm}^{-2}$  per unit AOD, weaker than our values for the piClim-OC experiments which range  
 734 from  $-35 \text{ Wm}^{-2}$  to  $-107 \text{ Wm}^{-2}$  per unit AOD but include the cloud indirect effects here.

735 The sum of the individual AODs from BC,  $\text{SO}_4$ , OA, dust and sea salt gives the total aerosol AOD in the piClim-  
 736 aer experiment, where the various aerosols were combined. We can then use the AOD for each aerosol in the  
 737 piClim-aer experiment and the forcing efficiency above to find the contribution of the individual aerosol to the  
 738 overall change in ERF, providing an approximate estimate of the relative contribution of each aerosol to the  
 739 overall ERF. In Fig. 4 the relative contributions to the ERF from black carbon (BC), organic aerosols (OA) and  
 740 sulfate ( $\text{SO}_4$ ) are shown for three of the models. The sum of the ERFs from the individual species is also compared  
 741 to the ERF calculated from the piClim-aer experiment (NB the sea salt and dust contributions to the ERF are less

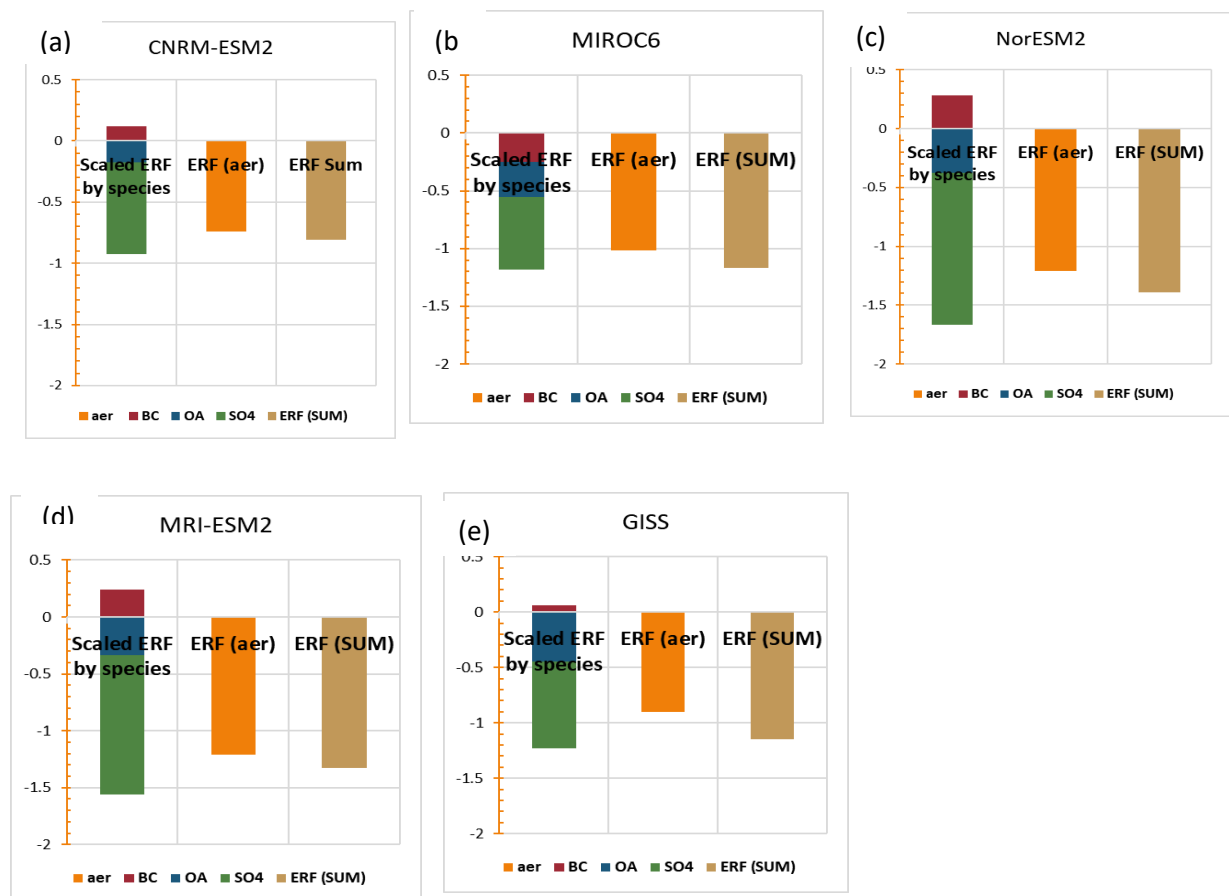


Fig. 5-4 The contributions to the ERF for piClim-aer from the individual species, the sum of the scaled ERFs and the ERF calculated directly from the piClim-aer experiment for five of the models.

742 than 1%, and not shown in this figure for clarity - the ERF/AOD forcing efficiency for these is presented in  
 743 (Thornhill et al., 2020). There is considerable variation in the ERF for the piClim-aer experiments between models  
 744 (see Section 4.1), but from this analysis the  $\text{SO}_4$  is the largest contributor in all cases, although in the case of the  
 745 MIROC6 model its relative importance is reduced. The positive ERF contribution from the BC tends to partly

746 offset the negative ERF from the OA and SO<sub>4</sub>, except in the MIROC6 model, where the BC has a negative  
747 contribution to the ERF.

748 The difference between the calculated ERF from the sum of the scaled ERFs is a result of the non-linearity of the  
749 aerosol-cloud interactions, a factor which is increased because the aerosols are added to the pre-industrial  
750 atmosphere. However, using the IRFari instead of the total ERF to calculate the forcing efficiency and using the  
751 same method also results in a difference between the total IRFari derived from the scaled individual experiments  
752 and the IRFari for the combined aerosol experiment, suggesting that the difference is not simply a result of the  
753 aerosol-cloud interactions.

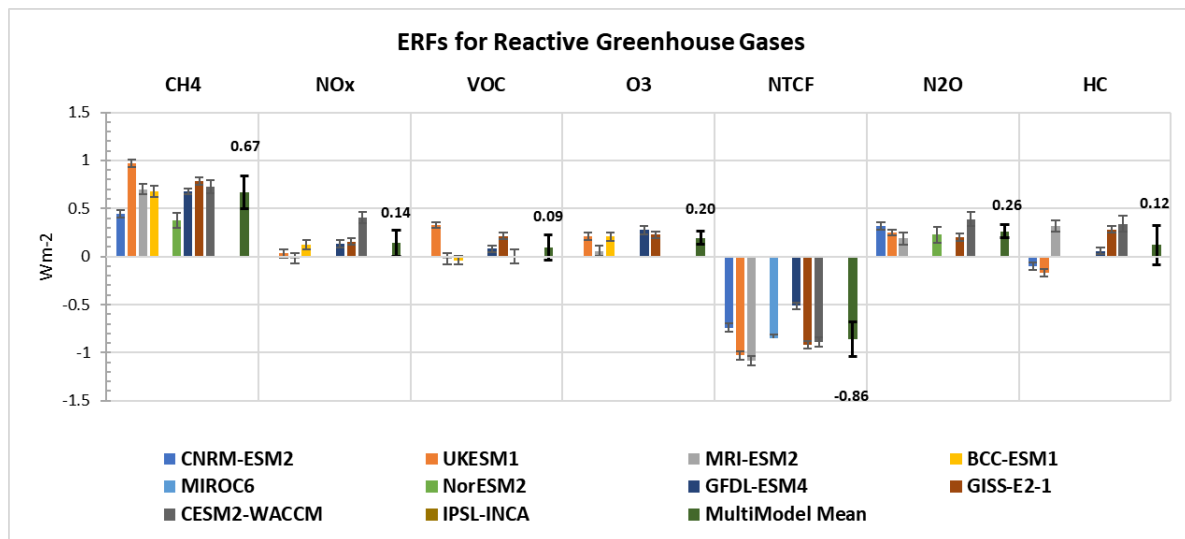
754 Using the burden as a scaling factor following the same analysis as described for the AOD results in a largely  
755 similar result for the scaling factor, although interestingly the burden scaling for SO<sub>2</sub> in the Nor-ESM2 model is  
756 similar to the other models (see Table S6 for the burden forcing efficiency).

#### 758 **4.2 Reactive greenhouse gases**

759 The different Earth system models include different degrees of complexity in their chemistry, so their responses  
760 to changes in reactive gas concentrations or emissions differ. NorESM2 has no atmospheric chemistry, so there  
761 is no change to ozone (tropospheric or stratosphere) or to aerosol oxidation following changes in methane or N<sub>2</sub>O  
762 concentrations. CNRM-ESM2-1 includes stratospheric ozone chemistry, but no non-methane hydrocarbon  
763 chemistry and so ozone is prescribed below 560 hPa. There are no effects of chemistry on aerosol oxidation. BCC-  
764 ESM1 includes tropospheric chemistry, but not stratospheric chemistry. Stratospheric concentrations are relaxed  
765 towards climatological values. UKESM1, GFDL-ESM4, CESM2-WACCM, GISS-E2 and MRI-ESM2 all include  
766 tropospheric and stratospheric ozone chemistry as well as changes to aerosol oxidation rates. The ERFs calculated  
767 for the reactive gases for several models are shown in Fig. 5, with the multi-model means given in Supplementary  
768 Table S3.

769 The contributions from gas-phase and aerosol changes to the ERF can be pulled apart to some extent by using the  
770 clear-sky and aerosol-free radiation diagnostics (Table 5). The direct aerosol forcing (IRFari) is diagnosed as for  
771 the aerosol experiments (section 3.3). The diagnosed changes in aerosol mass are shown in Table S8. GFDL-  
772 ESM4 and GISS-ES-1 include nitrate aerosol and show expected responses from NO<sub>x</sub> emissions (including O<sub>3</sub>  
773 experiment). CESM2-WACCM shows an increase in secondary organic aerosol from VOC emissions. Sulphate  
774 responses are generally inconsistent across the models. There seems little correlation between aerosol mass  
775 changes and diagnosed IRFari.

776 For gas-phase experiments the diagnosed cloud interactions (ERFaf-ERFcs,af) comprise the ERFaci from effects  
777 on aerosol chemistry (as in section 3.3) but also any cloud adjustments and effects of cloud masking on the gas-  
778 phase forcing (equation 8). The clear-sky aerosol-free diagnostic (ERFcs,af) is an indication of the greenhouse  
779 gas forcing however this will be an over-estimate as it neglects cloud masking effects (section 3.3).



781 **Fig. 5** Reactive gas ERFs for the models with the available diagnostics for the reactive gas experiments with interannual  
 782 variability represented by error bars showing the standard error. The multimodel mean is shown with the mean value  
 783 and error bars indicating the standard deviation.

#### 784 4.2.1 ERF vs SARF

785 For methane the ERFs are largest for those models that include tropospheric ozone chemistry reflecting the  
 786 increased forcing from ozone production, see section 4.2.2. The analytic calculation for CH<sub>4</sub>-only based on  
 787 Etminan et al. (2016) gives a SARF of 0.56 Wm<sup>-2</sup>. The tropospheric adjustments are negative for all models except  
 788 UKESM1 (Fig 6). The negative cloud adjustment comes from an increase in the LW emissions, possibly due to  
 789 less high cloud. In UKESM1 (O'Connor et al., 2020b) show that methane decreases sulfate new particle  
 790 formation, thus reducing cloud albedo and hence a positive cloud adjustment in that model.

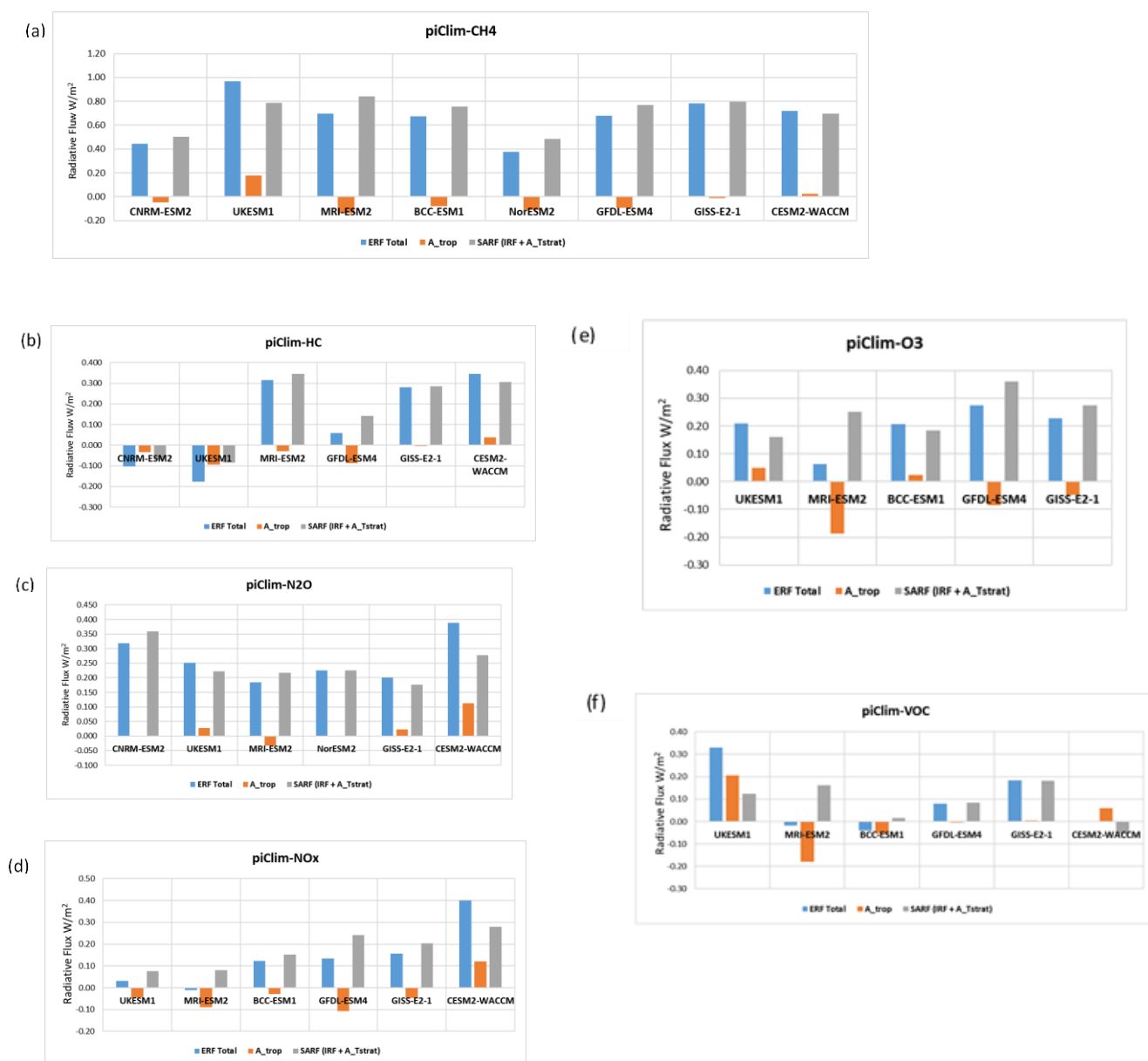


Figure 6 Breakdown of the ERF into SARF and tropospheric rapid adjustments for the chemically reactive species (a) for piClim-CH<sub>4</sub> experiments, (b) for piClim-HC experiments, (c) for piClim-N<sub>2</sub>O experiments, (d) for piClim-NO<sub>x</sub> experiments, (e) for piClim-O<sub>3</sub> experiments, and (f) for piClim-VOC experiments

792 only calculation gives a SARF of 0.17 Wm<sup>-2</sup>). There appears little net rapid adjustment to N<sub>2</sub>O apart from CESM2-  
 793 WACCM. Note that due to the method of calculating the all-sky IRF (section 3.2), the IRF and the adjustment  
 794 terms do not sum to give the ERF.

795 The models respond very differently to changes in halocarbons. The expected halocarbon-only SARF is +0.30  
 796 Wm<sup>-2</sup> depending on exact speciation used in the model (WMO 2018). For CNRM-ESM2, UKESM1 and GFDL-  
 797 ESM4 the ERFs are negative or only slightly positive (see also Morgenstern et al. (2020)), whereas for GISS-E2-1

and MRI-ESM2 the ERFs and SARF are both strongly positive. The differences in stratospheric ozone destruction in these models can partially explain the inter-model differences (section 4.2.2).

**Table 5** Calculations of IRFar<sub>i</sub>, ERF<sub>aci</sub> (cloud) and ERF<sub>cs,af</sub> for the chemically reactive species

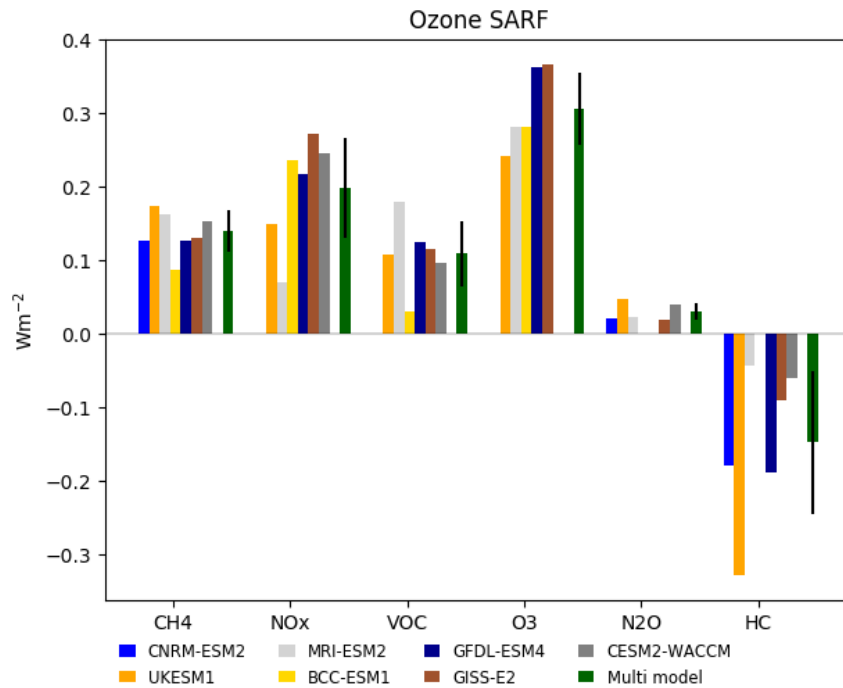
	<u>UKESM</u>			<u>GFDL-ESM4</u>			<u>CNRM-ESM2</u>			<u>NorESM2</u>			<u>MRI-ESM2</u>		
	<u>IRFar<sub>i</sub></u>	<u>cs,af</u>	<u>cloud</u>	<u>IRFar<sub>i</sub></u>	<u>cs,af</u>	<u>cloud</u>	<u>IRFar<sub>i</sub></u>	<u>cs,af</u>	<u>cloud</u>	<u>IRFar<sub>i</sub></u>	<u>cs,af</u>	<u>cloud</u>	<u>IRFar<sub>i</sub></u>	<u>cs,af</u>	<u>cloud</u>
<u>CH4</u>	<u>-0.01</u>	<u>0.86</u>	<u>0.12</u>	<u>-0.01</u>	<u>0.91</u>	<u>-0.22</u>	<u>0.00</u>	<u>0.56</u>	<u>-0.12</u>	<u>-0.01</u>	<u>0.48</u>	<u>-0.10</u>	<u>0.00</u>	<u>0.91</u>	<u>-0.21</u>
<u>HC</u>	<u>-0.02</u>	<u>0.02</u>	<u>-0.18</u>	<u>-0.02</u>	<u>0.22</u>	<u>-0.14</u>	<u>-0.01</u>	<u>-0.02</u>	<u>-0.08</u>				<u>-0.02</u>	<u>0.50</u>	<u>-0.17</u>
<u>N2O</u>	<u>-0.01</u>	<u>0.26</u>	<u>0.01</u>				<u>0.00</u>	<u>0.41</u>	<u>-0.09</u>	<u>-0.01</u>	<u>0.24</u>	<u>-0.00</u>	<u>-0.00</u>	<u>0.23</u>	<u>-0.03</u>
<u>O3</u>	<u>-0.02</u>	<u>0.16</u>	<u>0.07</u>	<u>-0.04</u>	<u>0.49</u>	<u>-0.18</u>							<u>-0.00</u>	<u>0.24</u>	<u>-0.18</u>
<u>NOx</u>	<u>-0.03</u>	<u>0.10</u>	<u>-0.05</u>	<u>-0.02</u>	<u>0.25</u>	<u>-0.09</u>							<u>-0.01</u>	<u>0.03</u>	<u>-0.04</u>
<u>VOC</u>	<u>0.00</u>	<u>0.13</u>	<u>0.20</u>	<u>-0.02</u>	<u>0.18</u>	<u>-0.08</u>							<u>0.004</u>	<u>0.17</u>	<u>-0.2</u>

#### 4.2.2 Ozone changes

The ozone radiative forcing is diagnosed using a kernel to scale the 3D ozone changes based on Skeie et al. (2020). This kernel includes stratospheric temperature adjustment, but not tropospheric adjustments so gives a SARF. These are shown in Fig. 7. Corresponding changes in the tropospheric and stratospheric ozone columns are shown in figure S5. Increased CH<sub>4</sub> concentrations give a SARF for ozone produced by methane of 0.14±0.03 W m<sup>-2</sup>, anthropogenic NO<sub>x</sub> emissions and VOC (including CO) emissions give SARFs of 0.20±0.07 and 0.11±0.04 Wm<sup>-2</sup> respectively. The O<sub>3</sub> experiment comprised both NO<sub>x</sub> and VOC emission changes. The SARF in this experiment (0.31±0.05 Wm<sup>-2</sup>) is close to the sum of the NO<sub>x</sub> and VOC experiments (0.30±0.05 Wm<sup>-2</sup> for the same set of models) showing little non-linearity in the chemistry (Stevenson et al., 2013).

There is a larger variation across models in the stratospheric ozone depletion from halocarbons (-0.15±0.10 Wm<sup>-2</sup>) with UKESM1 having noticeably larger depletion as seen in Keeble et al. (2020) giving a SARF of -0.33 Wm<sup>-2</sup>. N<sub>2</sub>O causes some stratospheric ozone depletion in these models, mainly in the tropical upper stratosphere where depletion causes a positive forcing (Skeie et al., 2020), and increases tropospheric ozone (Fig. S6) giving a small net positive SARF (0.03±0.01 Wm<sup>-2</sup>).





819

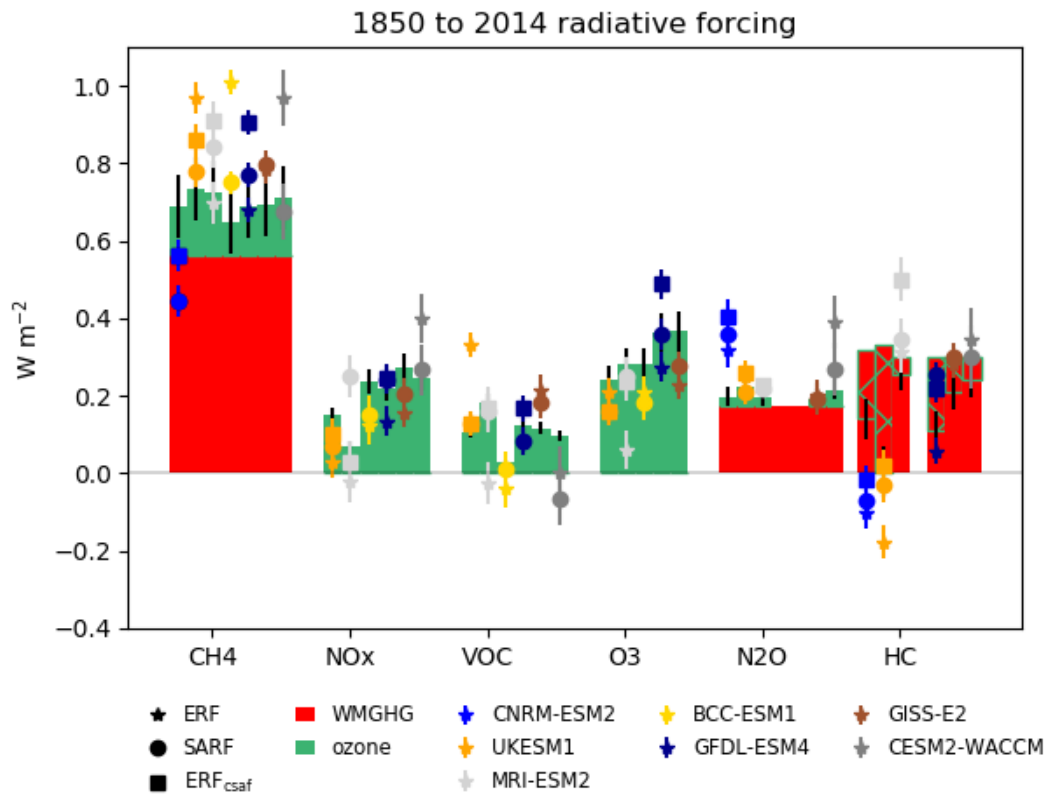
820 **Fig. 7 Changes in ozone stratospheric-temperature adjusted radiative forcing (SARF) for each experiment, diagnosed**  
 821 **using kernels (see text). . Uncertainties for the multi model means are standard deviations across models.**

822 **Methane oxidation also leads to water vapour production. Figure S6 shows increases in the stratosphere for the piClim-**  
 823 **CH4 of up to 20% . The kernel analysis however finds very low radiative forcing associated with this increase**  
 824 **(-0.002±0.003 Wm<sup>-2</sup>).**

825 **4.2.3 Comparison with greenhouse gas forcings**

826 The ERFs, ERFcs,af and SARFs diagnosed for the greenhouse gas changes (Fig. 6, Table 5) are compared with  
 827 the expected greenhouse gas SARFs in Fig. 8. The expected SARFs from the well-mixed gases are given by  
 828 Etminan et al. (2016) for CH<sub>4</sub> and N<sub>2</sub>O, and by WMO (2018) for the halocarbons (the halocarbon changes are  
 829 slightly different in each model). The expected SARFs from ozone changes are from Fig. 7.

830 For methane the ERFs are typically higher than the expected GHG SARF (except for CNRM-ESM2).The  
 831 diagnosed ERFcs,af and SARF agree better with the expected SARF in UKESM1, BCC-ESM1 and CESM2-  
 832 WACCM, but not in other models. For N<sub>2</sub>O the modelled ERF is larger than the expected SARF for CNRM-  
 833 ESM2-1 and CESM2-WACCM, this is explained by the rapid adjustments for CESM2-WACCM, but not for  
 834 CNRM-ESM2. For halocarbons the stratospheric ozone depletion offsets the direct SARF and accounts for much  
 835 of the spread in the model SARF, although the CNRM-ESM2-1 ERF and SARF is lower than expected. The  
 836 modelled HC ERF for UKESM1 is strongly negative due to increased aerosol cloud interactions, (O'Connor et  
 837 al., 2020a;Morgenstern et al., 2020) but removing cloud effects using the SARF or ERFcs,af agrees better with  
 838 the expected value. The estimated ozone SARF from the NO<sub>x</sub>, VOC and O<sub>3</sub> experiments generally agrees with  
 839 the model SARF and ERFcs,af. For CESM2-WACCM the ERF from the VOC experiment is zero, and the SARF  
 840 negative even though the diagnosed ozone SARF is positive. For all experiments and models ERFcs,af is generally  
 841 higher than the expected or diagnosed SARF (see section 3.3).



842

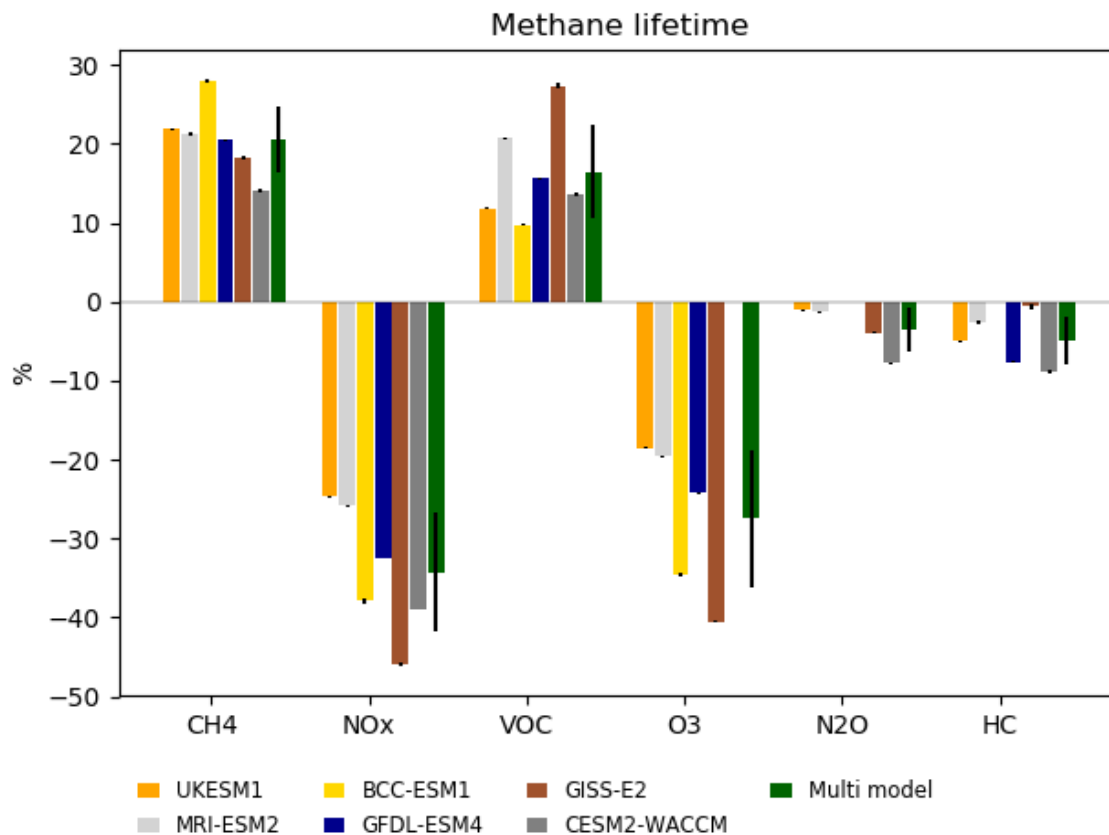
843 Fig. 8 Estimated SARF from the greenhouse gas changes (WMGHGs and ozone), using radiative efficiencies for the  
 844 WMGHGs and kernel calculations for ozone (see text). Hatched bars show decreases in ozone SARF. Symbols show  
 845 the modelled ERF, SARF and ERF<sub>csaf</sub> (estimate of greenhouse gas clear-sky ERF). Uncertainties on the bars are due  
 846 to uncertainties in radiative efficiencies. Uncertainties on the symbols are errors in the mean due to interannual  
 847 variability in the model diagnostic.

#### 848 4.2.4 Methane Lifetime

849 In the CMIP6 setup the modelled methane concentrations do not respond to changes in oxidation rates. The  
 850 methane lifetime is diagnosed (which includes stratospheric loss to OH as parameterised within each model) and  
 851 assuming losses to chlorine oxidation and soil uptake of 11 and 30 Tg yr<sup>-1</sup> ((Saunio et al., 2020)(Myhre et al.,  
 852 2013b) and this can be used to infer the methane changes that would be expected if methane were allowed to vary.  
 853 Fig. 9 shows the methane lifetime response is large and negative for NO<sub>x</sub> emissions, with a smaller positive change  
 854 for VOC emissions. Halocarbon concentration increases decrease the methane lifetime, as ozone depletions leads  
 855 to increased UV in the troposphere and increased methane loss to chlorine in the stratosphere (Stevenson et al.,  
 856 2020). N<sub>2</sub>O also decreases the methane lifetime by depleting ozone in the tropics although the effect is less than  
 857 for halocarbons. The O<sub>3</sub> experiment has a significantly more negative effect (-27±9 %) than the sum of NO<sub>x</sub> and  
 858 VOC (-16±8 %) (uncertainties are multi-model standard deviation). This suggests significant non-additivity. Note  
 859 that a combined CH<sub>4</sub>+NO<sub>x</sub>+VOC experiment is not available to test the additivity further.

860 The lifetime response to changing methane concentrations can be used to diagnose the methane lifetime feedback  
 861 factor  $f$  ((Fiore et al., 2009). The results here give  $f=1.32, 1.31, 1.43, 1.30, 1.26, 1.19$  (mean  $1.30\pm0.07$ ) for  
 862 UKESM1, MRI-ESM2, BCC-ESM1, GFDL-ESM4, GISS-E2-1 and CESM-WACCM. This is in very good  
 863 agreement with AR5, although their values are starting from a year 2000 baseline rather than pre-industrial.

864  
865



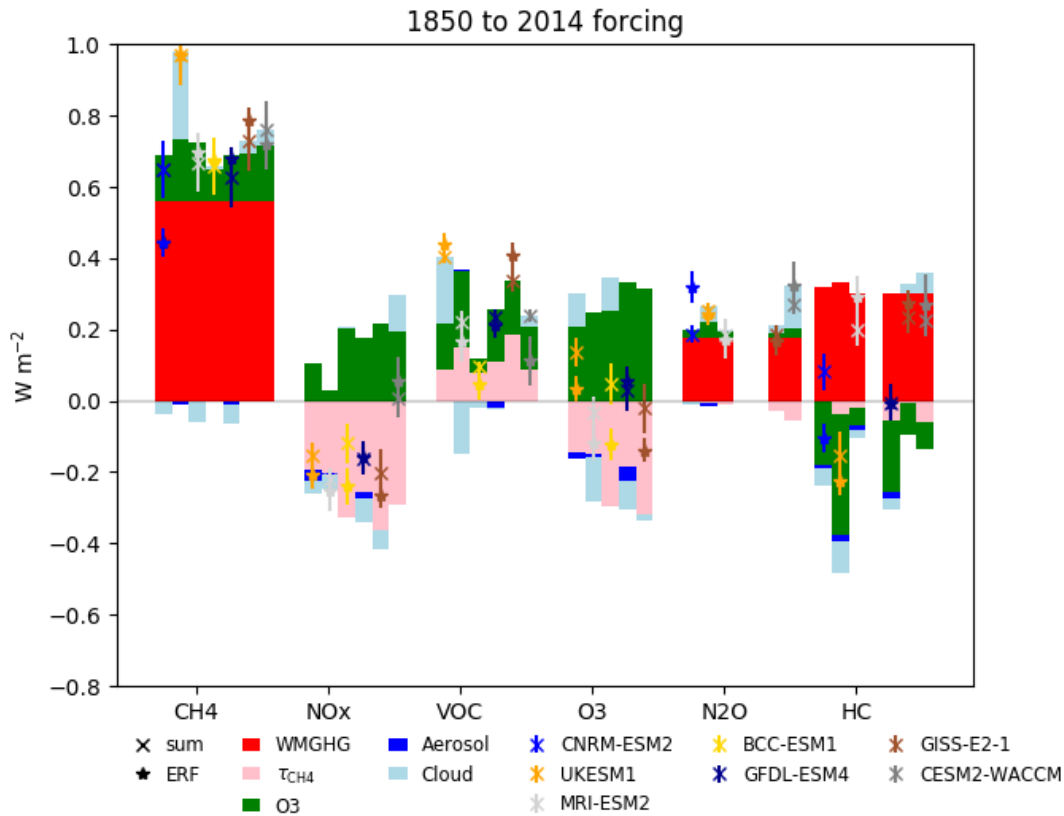
866

867 **Fig. 9 Changes in methane lifetime (%), for each experiment. Uncertainties for individual models are errors on the**  
868 **mean from interannual variability. Uncertainties for the multi model mean are standard deviations across models.**

#### 869 4.2.5 Total ERFs

870 The methane lifetime changes can be converted to expected changes in concentration if methane were allowed to  
871 freely evolve following Fiore et al. (2009), using the *f*-factors appropriate to each model (section 3.3.4). The  
872 inferred radiative forcing is based on radiative efficiency of methane (Etminan et al., 2016). The methane changes  
873 also have implications for ozone production, so we assume an ozone SARF per ppb of CH<sub>4</sub> diagnosed for each  
874 model from section 4.2.

875 The breakdown of the information from the analyses above is shown in Fig. 10, using the SARF calculated for  
876 the gases (WMGHGs and ozone) and kernel-diagnosed cloud adjustments (which include aerosol cloud  
877 interactions). Direct contributions from the aerosols IRF<sub>ari</sub> are shown for models where this is available. The  
878 contributions from methane lifetime changes have also been added to the diagnosed ERF as these aren't accounted  
879 for in the models. Differences between the diagnosed ERF (stars) and the sum of the components (crosses) then  
880 shows to what extent this decomposition into components can account for the modelled ERF. For many of the  
881 species, this breakdown is reasonable, and illustrates that cloud radiative effects can make significant  
882 contributions to the total radiative impacts of WMGHGs and ozone precursors. This analysis cannot distinguish  
883 between cloud effects due to changes in atmospheric temperature profiles or those due to increased cloud  
884 nucleation from aerosols.



885

886 **Fig. 10 SARF for WMGHGs, ozone and diagnosed changes in methane. Model diagnosed direct aerosol RF and cloud**  
 887 **radiative effect. Crosses mark the sum of the five terms for each model. Stars mark the diagnosed ERF with the effect**  
 888 **of methane lifetime (on methane and ozone) added. Differences between stars and crosses shows undiagnosed**  
 889 **contributions. Uncertainties on the sum are mainly due to the uncertainties in the radiative efficiencies. Uncertainties**  
 890 **in the ERF are errors on the mean due to interannual variability. Note for CESM2-WACCM, BCC-ESM1, GISS-E2-1**  
 891 **the direct aerosol effect is unavailable.**

892 **5. Discussion**

893 For all of the species shown we see considerable variation in the calculated ERFs across the models, which is due  
 894 in part to differences in the model aerosol and chemistry schemes; not all models have interactive schemes for all  
 895 of the species, and whether or not chemistry is considered will impact the evolution of some of the aerosol species.  
 896 We can use the differences in model complexity from the multi-model approach together with the separation of  
 897 the effects of the various species in the individual AerChemMIP experiments to understand how the various  
 898 components contribute to the overall ERFs we have calculated.

899

900 **5.1 Aerosols**

901 The 1850-2014 multi-model mean and standard deviation of the ERFs for SO<sub>2</sub>, OC and BC are: -1.03 +/- 0.37  
 902 Wm<sup>-2</sup> for SO<sub>2</sub>, -0.25 +/- 0.09 Wm<sup>-2</sup> for OC, and 0.15 +/- 0.17 Wm<sup>-2</sup> for BC. The total ERF for the aerosols is -  
 903 1.01 +/- 0.25 Wm<sup>-2</sup>, within the range of -1.65 to -0.6 Wm<sup>-2</sup> reported by (Bellouin et al., 2019).

904 The radiative kernels and double-call diagnostics are used to separate the direct and cloud effects of aerosols for  
 905 those models where all the relevant diagnostics are available. These two methods broadly agree on the cloud

906 contribution for the BC, SO<sub>2</sub> and OC experiments. We generally find a weaker total adjustment to black carbon  
907 compared to other studies (Samset and Myhre, 2015;Stjern et al., 2017;Smith et al., 2018). The exceptions are  
908 MIROC6 and GISS-E2-1. These previous studies used much larger changes in black carbon (up to 10 times)  
909 which may cause non-linear effects such as self-lofting.

910 As the ISCCP cloud diagnostics become available for more of the CMIP6 models, it will be possible to do a direct  
911 calculation of the cloud rapid adjustments using the kernels from (Zelinka et al., 2014) and compare those with  
912 the adjustments calculated using the kernel difference method described in (Smith et al., 2018) and used here  
913 (Section 3.2; see also figure 4 and figure S2 from Smith et al. (2020a)).

914 The radiative efficiencies per AOD calculated here are generally larger than those from the AeroCom Phase II  
915 experiments (Myhre et al., 2013b), with the caveat that the models included here did not have fixed clouds, so  
916 that indirect effects would be included.

917 The values diagnosed for the IRFari (for the models we have available diagnostics for) in CMIP6 are similar to  
918 those from CMIP5 (Myhre et al., 2013a) where they reported values for sulfate of -0.4 (-0.6 to -0.2) Wm<sup>-2</sup>  
919 compared to our -0.36 (-0.19 to -0.49) Wm<sup>-2</sup> for the SO<sub>2</sub> experiment, for OC they found -0.09 (-0.16 to -0.03)  
920 Wm<sup>-2</sup> compared to our value of -0.09 (-0.07 to -0.15) Wm<sup>-2</sup> and for BC they had +0.4 (+0.05 to +0.80) compared  
921 to our value of 0.28 (0.13- 0.37) Wm<sup>-2</sup>, so broadly the IRFari for the individual species agree with those found in  
922 the previous set of models used in CMIP5.

923 The overall aerosol ERF from AR5 is reported as in the range -1.5 to 0.4 Wm<sup>-2</sup>, compared to ERF values reported  
924 here for the piClim-aer experiment in the range -0.7 to -1.47 Wm<sup>-2</sup>.

## 926 5.2 Reactive greenhouse gases

927 The diagnosed ERFs from methane, N<sub>2</sub>O, halocarbons and ozone precursors are: 0.75±0.10, 0.26±0.07, 0.12±0.21  
928 and 0.20±0.07 W m<sup>-2</sup> (excluding CNRM-ESM2-1 for methane as it cannot represent the lower tropospheric ozone  
929 changes, and excluding NorESM2 for all as it has no ozone chemistry). These compare with 0.79±0.13, 0.17±0.03,  
930 0.18±0.15 and 0.22±0.14 W m<sup>-2</sup> for 1750-2011 from AR5 (Myhre et al., 2013a) - where the effects on methane  
931 lifetime and CO<sub>2</sub> have been removed from the AR5 calculations, and the halocarbons are for CFCs and HCFCs  
932 only. Section 4.2.5 shows that cloud effects can make a significant contribution to the overall ERF even for  
933 WMGHGs. However, clouds cannot explain all the differences. The ERF for N<sub>2</sub>O is larger than estimated in AR5.  
934 The ozone contribution here is estimated as 0.03±0.01 Wm<sup>-2</sup> whereas it was zero in AR5, but that does not explain  
935 all the difference. The multi-model ERF for halocarbons is smaller than AR5, due to larger ozone depletion  
936 although the models have a wide spread with some showing significantly lower ERFs and some significantly  
937 higher due to varying strengths of ozone depletion in these models.

938 The estimated ozone SARFs from the changes in levels of methane, NO<sub>x</sub> and VOC from 1850 to 2014 are  
939 0.14±0.03, 0.20±0.07, and 0.11±0.04 W m<sup>-2</sup> compared to 0.24±0.13, 0.14±0.09, and 0.11±0.05 W m<sup>-2</sup> in CMIP5  
940 (Myhre et al., 2013a). The ozone from methane contribution is smaller, here only 25% of the direct Etminan et al.  
941 (2016) methane SARF compared to 50% in AR5 (or 39% using the Etminan et al. (2016) formula). The NO<sub>x</sub>  
942 contribution is larger in this study. The CMIP5 results were based on (Stevenson et al., 2013) in which species  
943 were reduced from present day levels rather than being increased from pre-industrial levels. The NO<sub>x</sub> emission

944 changes are also larger for CMIP6 compared to CMIP5 (Hoesly et al. 2018). The sum of the ozone terms  
945 (CH<sub>4</sub>+N<sub>2</sub>O+HC+O<sub>3</sub>) is 0.33±0.11 Wm<sup>-2</sup>, agreeing well with the total 1850-2014 ozone SARF of 0.35 ±0.16 Wm<sup>-2</sup>  
946 (1.s.d) from Skeie et al. (2020) which included a few additional models.

947

948 The overall effect of NTCF emissions (excluding methane and other WMGHGs) on the 1850-2014 ERF  
949 experienced by models that include tropospheric chemistry is strongly negative (-0.89±0.20 W m<sup>-2</sup>) due to the  
950 dominance of the aerosol forcing over that from ozone. There is a large spread in the NTCF forcing due to the  
951 different treatment of atmospheric chemistry within these models. Models without tropospheric and/or  
952 stratospheric chemistry prescribe varying ozone levels which are not included in the NTCF experiment. Hence  
953 the overall forcing experienced by these models due to ozone and aerosols will be different from that diagnosed  
954 here.

## 955 **6. Conclusion**

956 The experimental setup and diagnostics in CMIP6 have allowed us for the first time to calculate the effective  
957 radiative forcing (ERF) for present day reactive gas and aerosol concentrations and emissions in a range of Earth  
958 system models. Quantifying the forcing in these models is an essential step to understanding their climate  
959 responses.

960 This analysis also allows us to quantify the radiative responses to perturbations in individual species or groups of  
961 species. These responses include physical adjustments to the imposed forcing as well as chemical adjustments  
962 and adjustments related to the emissions of natural aerosols. The total adjustment is therefore a complex  
963 combination of individual process, but the diagnosed ERF implicitly includes these and represents the overall  
964 forcing experienced by the models.

965 We find that the ERF from well-mixed greenhouse gases (methane, nitrous oxide and halocarbons) has significant  
966 contributions through their effects on ozone, aerosols and clouds, that vary strongly across Earth system models.  
967 This indicates that Earth system processes need to be taken into account when understanding the contribution  
968 WMGHGs have made to present climate and when projecting the climate effects of different WMGHG scenarios.

## 969 **7. Acknowledgements**

970 GT, WC, MM, FO'C, DO, MS, acknowledge funding received from the European Union's Horizon 2020 research  
971 and innovation programme under grant agreement No 641816 (CRESCENDO).

972 FMO'C, JPM were funded by the Met Office Hadley Centre Climate Programme funded by BEIS and Defra  
973 (GA01101). CS was supported by a NERC-IIASA Collaborative Research Fellowship (no. NE/T009381/1). GZ  
974 was supported by the NZ government's Strategic Science Investment Fund (SSIF) through the NIWA  
975 programme CACV. MD and NO were supported by the Japan Society for the Promotion of Science (grant  
976 numbers: JP18H03363, JP18H05292, and JP20K04070), the Environment Research and Technology  
977 Development Fund (JPMEERF20172003, JPMEERF20202003, and JPMEERF20205001) of the Environmental  
978 Restoration and Conservation Agency of Japan, the Arctic Challenge for Sustainability II (ArCS II), Program  
979 Grant Number JPMXD1420318865, and a grant for the Global Environmental Research Coordination System

980 from the Ministry of the Environment, Japan. T. T. was supported by the supercomputer system of the National  
981 Institute for Environmental Studies, Japan, and JSPS KAKENHI Grant Number JP19H05669.

982 R.B.S. and G.M. were funded through the Norwegian Research Council project KEYCLIM (grant number  
983 295046) and the European Union's Horizon 2020 Research and Innovation Programme under Grant Agreement  
984 820829 (CONSTRAIN).

985 The CESM project is supported primarily by the National Science Foundation. This material is based upon work  
986 supported by the National Center for Atmospheric Research, which is a major facility sponsored by the NSF  
987 under Cooperative Agreement No. 1852977. Computing and data storage resources, including the Cheyenne  
988 supercomputer (doi:10.5065/D6RX99HX), were provided by the Computational and Information Systems  
989 Laboratory (CISL) at NCAR.

990 We acknowledge the World Climate Research Programme, which, through its Working Group on Coupled  
991 Modelling, coordinated and promoted CMIP6. We thank the climate modeling groups for producing and making  
992 available their model output, the Earth System Grid Federation (ESGF) for archiving the data and providing  
993 access, and the multiple funding agencies who support CMIP6 and ESGF.

994

## 995 **8. Author Contributions**

996 Manuscript preparation was done by GDT, WJC, RJK, DO and additional contributions from all co-authors.  
997 Model simulations were set up, reviewed and/or ran by DO, FMO'C, NLA, MD, LE, LH, J-FL, MMichou,  
998 MMills, JM, PN, VN, NO, MS, TT, ST, TW, GZ, JZ. Analysis was carried out by GT, WC, RK, DO.

999

## 1000 **9. Data Availability**

1001 All data from the various earth system models used in this paper are available on the Earth System Grid Federation  
1002 Website, and can be downloaded from there. <https://esgf-index1.ceda.ac.uk/search/cmip6-ceda/>

## 1003 **10. References**

1004 Ackerman, A. S., Toon, O. B., Taylor, J. P., Johnson, D. W., Hobbs, P. V., and Ferek, R. J.: Effects of  
1005 Aerosols on Cloud Albedo: Evaluation of Twomey's Parameterization of Cloud Susceptibility Using  
1006 Measurements of Ship Tracks, Journal of the Atmospheric Sciences, 57, 2684-2695, 10.1175/1520-  
1007 0469(2000)057<2684:eoaoa>2.0.co;2, 2000.

1008 Albrecht, B. A.: Aerosols, cloud microphysics, and fractional cloudiness, Science, 245, 1227-1230,  
1009 1989.

1010 Archibald, A. T., O'Connor, F. M., Abraham, N. L., Archer-Nicholls, S., Chipperfield, M. P., Dalvi,  
1011 M., Folberth, G. A., Dennison, F., Dhomse, S. S., Griffiths, P. T., Hardacre, C., Hewitt, A. J., Hill, R.,  
1012 Johnson, C. E., Keeble, J., Köhler, M. O., Morgenstern, O., Mulchay, J. P., Ordóñez, C., Pope, R. J.,  
1013 Rumbold, S., Russo, M. R., Savage, N., Sellar, A., Stringer, M., Turnock, S., Wild, O., and Zeng, G.:



1014 [Description and evaluation of the UKCA stratosphere-troposphere chemistry scheme \(StratTrop vn 1.0\)](#)  
1015 [implemented in UKESM1, Geosci. Model Dev. Discuss., 2019, 1-82, 10.5194/gmd-2019-246, 2020.](#)

1016 [Bauer, S. E., Tsigaridis, K., Faluvegi, G., Kelley, M., Lo, K. K., Miller, R. L., Nazarenko, L., Schmidt,](#)  
1017 [G. A., and Wu, J.: Historical \(1850–2014\) Aerosol Evolution and Role on Climate Forcing Using the](#)  
1018 [GISS ModelE2.1 Contribution to CMIP6, Journal of Advances in Modeling Earth Systems, 12,](#)  
1019 [e2019MS001978, 10.1029/2019ms001978, 2020.](#)

1020 [Bellouin, N., Quaas, J., Gryspeerdt, E., Kinne, S., Stier, P., Watson-Parris, D., Boucher, O., Carslaw,](#)  
1021 [K. S., Christensen, M., Daniau, A.-L., Dufresne, J.-L., Feingold, G., Fiedler, S., Forster, P., Gettelman,](#)  
1022 [A., Haywood, J. M., Lohmann, U., Malavelle, F., Mauritsen, T., McCoy, D. T., Myhre, G.,](#)  
1023 [Mülmenstädt, J., Neubauer, D., Possner, A., Rugenstein, M., Sato, Y., Schulz, M., Schwartz, S. E.,](#)  
1024 [Sourdeval, O., Storelmo, T., Toll, V., Winker, D., and Stevens, B.: Bounding global aerosol radiative](#)  
1025 [forcing of climate change, Reviews of Geophysics, n/a, 10.1029/2019rg000660, 2019.](#)

1026 [Block, K., and Mauritsen, T.: Forcing and feedback in the MPI-ESM-LR coupled model under abruptly](#)  
1027 [quadrupled CO<sub>2</sub>, Journal of Advances in Modeling Earth Systems, 5, 676-691, 10.1002/jame.20041,](#)  
1028 [2013.](#)

1029 [Boucher, O. e. a.: Clouds and Aerosols, In: Climate Change 2013: The Physical Science Basis.](#)  
1030 [Contribution of Working Group I to the Fifth Assessment Report of the Intergovernmental Panel on](#)  
1031 [Climate Change, in, Cambridge University Press, Cambridge, United Kingdom and New York, NY,](#)  
1032 [USA., 2013.](#)

1033 [Checa-Garcia, R., Hegglin, M. I., Kinnison, D., Plummer, D. A., and Shine, K. P.: Historical](#)  
1034 [Tropospheric and Stratospheric Ozone Radiative Forcing Using the CMIP6 Database, Geophysical](#)  
1035 [Research Letters, 45, 3264-3273, 10.1002/2017gl076770, 2018.](#)

1036 [Chung, E.-S., and Soden, B. J.: An Assessment of Direct Radiative Forcing, Radiative Adjustments,](#)  
1037 [and Radiative Feedbacks in Coupled Ocean–Atmosphere Models, Journal of Climate, 28, 4152-4170,](#)  
1038 [10.1175/jcli-d-14-00436.1, 2015.](#)

1039 [Collins, W. J., Lamarque, J. F., Schulz, M., Boucher, O., Eyring, V., Hegglin, M. I., Maycock, A.,](#)  
1040 [Myhre, G., Prather, M., Shindell, D., and Smith, S. J.: AerChemMIP: quantifying the effects of](#)  
1041 [chemistry and aerosols in CMIP6, Geosci. Model Dev., 10, 585-607, 10.5194/gmd-10-585-2017, 2017.](#)

1042 [Deushi, M., and Shibata, K.: Development of a Meteorological Research Institute Chemistry-Climate](#)  
1043 [Model version 2 for the Study of Tropospheric and Stratospheric Chemistry, Papers in Meteorology](#)  
1044 [and Geophysics, 62, 1-46, 10.2467/mripapers.62.1, 2011.](#)

1045 [Di Biagio, C., Formenti, P., Balkanski, Y., Caponi, L., Cazaunau, M., Pangui, E., Journet, E., Nowak,](#)  
1046 [S., Andreae, M., Kandler, K., Saeed, T., Piketh, S., Seibert, D., Williams, E., and Doussin, J.-F.:](#)  
1047 [Complex refractive indices and single scattering albedo of global dust aerosols in the shortwave](#)  
1048 [spectrum and relationship to iron content and size, Atmospheric Chemistry and Physics Discussions, 1-](#)  
1049 [42, 10.5194/acp-2019-145, 2019.](#)

1050 [Dunne, J. P., Horowitz, L. W., Adcroft, A. J., Ginoux, P., Held, I. M., John, J. G., Krasting, J. P.,](#)  
1051 [Malyshev, S., Naik, V., Paulot, F., Shevliakova, E., Stock, C. A., Zadeh, N., Balaji, V., Blanton, C.,](#)  
1052 [Dunne, K. A., Dupuis, C., Durachta, J., Dussin, R., Gauthier, P. P. G., Griffies, S. M., Guo, H., Hallberg,](#)  
1053 [R. W., Harrison, M., He, J., Hurlin, W., McHugh, C., Menzel, R., Milly, P. C. D., Nikonov, S., Paynter,](#)  
1054 [D. J., Ploshay, J., Radhakrishnan, A., Rand, K., Reichl, B. G., Robinson, T., Schwarzkopf, D. M.,](#)  
1055 [Sentman, L. T., Underwood, S., Vahlenkamp, H., Winton, M., Wittenberg, A. T., Wyman, B., Zeng,](#)  
1056 [Y., and Zhao, M.: The GFDL Earth System Model version 4.1 \(GFDL-ESM 4.1\): Overall coupled](#)  
1057 [model description and simulation characteristics, Journal of Advances in Modeling Earth Systems, n/a,](#)  
1058 [e2019MS002015, 10.1029/2019ms002015, 2020.](#)

1059 [Emmons, L. K., Walters, S., Hess, P. G., Lamarque, J. F., Pfister, G. G., Fillmore, D., Granier, C.,](#)  
1060 [Guenther, A., Kinnison, D., Laepple, T., Orlando, J., Tie, X., Tyndall, G., Wiedinmyer, C., Baughcum,](#)  
1061 [S. L., and Kloster, S.: Description and evaluation of the Model for Ozone and Related chemical Tracers,](#)  
1062 [version 4 \(MOZART-4\), Geosci. Model Dev., 3, 43-67, 10.5194/gmd-3-43-2010, 2010.](#)

1063 [Etmann, M., Myhre, G., Highwood, E. J., and Shine, K. P.: Radiative forcing of carbon dioxide,](#)  
1064 [methane, and nitrous oxide: A significant revision of the methane radiative forcing, Geophysical](#)  
1065 [Research Letters, 43, 12,614-612,623, 10.1002/2016gl071930, 2016.](#)

1066 [Eyring, V., Bony, S., Meehl, G. A., Senior, C. A., Stevens, B., Stouffer, R. J., and Taylor, K. E.:](#)  
1067 [Overview of the Coupled Model Intercomparison Project Phase 6 \(CMIP6\) experimental design and](#)  
1068 [organization, Geosci. Model Dev., 9, 1937-1958, 10.5194/gmd-9-1937-2016, 2016.](#)

1069 [Fiore, A. M., Dentener, F. J., Wild, O., Cuvelier, C., Schultz, M. G., Hess, P., Textor, C., Schulz, M.,](#)  
1070 [Doherty, R. M., Horowitz, L. W., MacKenzie, I. A., Sanderson, M. G., Shindell, D. T., Stevenson, D.](#)  
1071 [S., Szopa, S., Van Dingenen, R., Zeng, G., Atherton, C., Bergmann, D., Bey, I., Carmichael, G., Collins,](#)  
1072 [W. J., Duncan, B. N., Faluvegi, G., Folberth, G., Gauss, M., Gong, S., Hauglustaine, D., Holloway, T.,](#)  
1073 [Isaksen, I. S. A., Jacob, D. J., Jonson, J. E., Kaminski, J. W., Keating, T. J., Lupu, A., Marmer, E.,](#)  
1074 [Montanaro, V., Park, R. J., Pitari, G., Pringle, K. J., Pyle, J. A., Schroeder, S., Vivanco, M. G., Wind,](#)  
1075 [P., Wojcik, G., Wu, S., and Zuber, A.: Multimodel estimates of intercontinental source-receptor](#)  
1076 [relationships for ozone pollution, Journal of Geophysical Research: Atmospheres, 114,](#)  
1077 [10.1029/2008jd010816, 2009.](#)

1078 [Forster, P. M., Richardson, T., Maycock, A. C., Smith, C. J., Samset, B. H., Myhre, G., Andrews, T.,](#)  
1079 [Pincus, R., and Schulz, M.: Recommendations for diagnosing effective radiative forcing from climate](#)  
1080 [models for CMIP6, Journal of Geophysical Research: Atmospheres, 121, 12,460-412,475,](#)  
1081 [doi:10.1002/2016JD025320, 2016.](#)

1082 [Gettelman, A., Mills, M. J., Kinnison, D. E., Garcia, R. R., Smith, A. K., Marsh, D. R., Tilmes, S., Vitt,](#)  
1083 [F., Bardeen, C. G., McInerny, J., Liu, H. L., Solomon, S. C., Polvani, L. M., Emmons, L. K., Lamarque,](#)  
1084 [J. F., Richter, J. H., Glanville, A. S., Bacmeister, J. T., Phillips, A. S., Neale, R. B., Simpson, I. R.,](#)  
1085 [DuVivier, A. K., Hodzic, A., and Randel, W. J.: The Whole Atmosphere Community Climate Model](#)  
1086 [Version 6 \(WACCM6\), Journal of Geophysical Research: Atmospheres, n/a, 10.1029/2019JD030943,](#)  
1087 [2019.](#)

1088 [Ghan, S. J.: Technical Note: Estimating aerosol effects on cloud radiative forcing, Atmos. Chem. Phys.,](#)  
1089 [13, 9971-9974, 10.5194/acp-13-9971-2013, 2013.](#)

1090 [Hansen, J., Sato, M., Ruedy, R., Nazarenko, L., Lacis, A., Schmidt, G. A., Russell, G., Aleinov, I.,](#)  
1091 [Bauer, M., Bauer, S., Bell, N., Cairns, B., Canuto, V., Chandler, M., Cheng, Y., Del Genio, A., Faluvegi,](#)  
1092 [G., Fleming, E., Friend, A., Hall, T., Jackman, C., Kelley, M., Kiang, N., Koch, D., Lean, J., Lerner, J.,](#)  
1093 [Lo, K., Menon, S., Miller, R., Minnis, P., Novakov, T., Oinas, V., Perlwitz, J., Perlwitz, J., Rind, D.,](#)  
1094 [Romanou, A., Shindell, D., Stone, P., Sun, S., Tausnev, N., Thresher, D., Wielicki, B., Wong, T., Yao,](#)  
1095 [M., and Zhang, S.: Efficacy of climate forcings, Journal of Geophysical Research: Atmospheres, 110,](#)  
1096 [10.1029/2005jd005776, 2005.](#)

1097 [Hoesly, R. M., Smith, S. J., Feng, L., Klimont, Z., Janssens-Maenhout, G., Pitkanen, T., Seibert, J. J.,](#)  
1098 [Vu, L., Andres, R. J., Bolt, R. M., Bond, T. C., Dawidowski, L., Kholod, N., Kurokawa, J.-i., Li, M.,](#)  
1099 [Liu, L., Lu, Z., Moura, M. C. P., O'Rourke, P. R., and Zhang, Q.: Historical \(1750–2014\) anthropogenic](#)  
1100 [emissions of reactive gases and aerosols from the Community Emissions Data System \(CEDS\),](#)  
1101 [Geoscientific Model Development \(Online\), Medium: ED; Size: p. 369-408, 2018.](#)

1102 [Horowitz, L. W., Naik, V., Paulot, F., Ginoux, P. A., Dunne, J. P., Mao, J., Schnell, J., Chen, X., He,](#)  
1103 [J., John, J. G., Lin, M., Lin, P., Malyshev, S., Paynter, D., Shevliakova, E., and Zhao, M.: The GFDL](#)  
1104 [Global Atmospheric Chemistry-Climate Model AM4.1: Model Description and Simulation](#)

1105 [Characteristics, Journal of Advances in Modeling Earth Systems, n/a, e2019MS002032,](#)  
1106 [10.1029/2019ms002032, 2020.](#)

1107 [Johnson, B. T., Haywood, J. M., and Hawcroft, M. K.: Are Changes in Atmospheric Circulation](#)  
1108 [Important for Black Carbon Aerosol Impacts on Clouds, Precipitation, and Radiation?, Journal of](#)  
1109 [Geophysical Research: Atmospheres, 124, 7930-7950, 10.1029/2019jd030568, 2019.](#)

1110 [Kawai, H., Yukimoto, S., Koshiro, T., Oshima, N., Tanaka, T., Yoshimura, H., and Nagasawa, R.:](#)  
1111 [Significant improvement of cloud representation in the global climate model MRI-ESM2, Geosci.](#)  
1112 [Model Dev., 12, 2875-2897, 10.5194/gmd-12-2875-2019, 2019.](#)

1113 [Keeble, J., Hassler, B., Banerjee, A., Checa-Garcia, R., Chiodo, G., Davis, S., Eyring, V., Griffiths, P.](#)  
1114 [T., Morgenstern, O., Nowack, P., Zeng, G., Zhang, J., Bodeker, G., Cugnet, D., Danabasoglu, G.,](#)  
1115 [Deushi, M., Horowitz, L. W., Li, L., Michou, M., Mills, M. J., Nabat, P., Park, S., and Wu, T.:](#)  
1116 [Evaluating stratospheric ozone and water vapor changes in CMIP6 models from 1850-2100, Atmos.](#)  
1117 [Chem. Phys. Discuss., 2020, 1-68, 10.5194/acp-2019-1202, 2020.](#)

1118 [Lurton, T., Balkanski, Y., Bastrikov, V., Bekki, S., Bopp, L., Braconnot, P., Brockmann, P., Cadule,](#)  
1119 [P., Contoux, C., Cozic, A., Cugnet, D., Dufresne, J.-L., Éthé, C., Foujols, M.-A., Ghattas, J.,](#)  
1120 [Hauglustaine, D., Hu, R.-M., Kageyama, M., Khodri, M., Lebas, N., Levvasseur, G., Marchand, M.,](#)  
1121 [Ottlé, C., Peylin, P., Sima, A., Szopa, S., Thiéblemont, R., Vuichard, N., and Boucher, O.:](#)  
1122 [Implementation of the CMIP6 Forcing Data in the IPSL-CM6A-LR Model, Journal of Advances in](#)  
1123 [Modeling Earth Systems, 12, e2019MS001940, 10.1029/2019ms001940, 2020.](#)

1124 [Matthes, K., Funke, B., Andersson, M. E., Barnard, L., Beer, J., Charbonneau, P., Clilverd, M. A.,](#)  
1125 [Dudok de Wit, T., Haberreiter, M., Hendry, A., Jackman, C. H., Kretzschmar, M., Kruschke, T., Kunze,](#)  
1126 [M., Langematz, U., Marsh, D. R., Maycock, A. C., Misios, S., Rodger, C. J., Scaife, A. A., Seppälä, A.,](#)  
1127 [Shangguan, M., Sinnhuber, M., Tourpali, K., Usoskin, I., van de Kamp, M., Verronen, P. T., and](#)  
1128 [Versick, S.: Solar forcing for CMIP6 \(v3.2\), Geosci. Model Dev., 10, 2247-2302, 10.5194/gmd-10-](#)  
1129 [2247-2017, 2017.](#)

1130 [Meinshausen, M., Vogel, E., Nauels, A., Lorbacher, K., Meinshausen, N., Etheridge, D. M., Fraser, P.](#)  
1131 [J., Montzka, S. A., Rayner, P. J., Trudinger, C. M., Krummel, P. B., Beyerle, U., Canadell, J. G., Daniel,](#)  
1132 [J. S., Enting, I. G., Law, R. M., Lunder, C. R., O'Doherty, S., Prinn, R. G., Reimann, S., Rubino, M.,](#)  
1133 [Velders, G. J. M., Vollmer, M. K., Wang, R. H. J., and Weiss, R.: Historical greenhouse gas](#)  
1134 [concentrations for climate modelling \(CMIP6\), Geosci. Model Dev., 10, 2057-2116, 10.5194/gmd-10-](#)  
1135 [2057-2017, 2017.](#)

1136 [Michou, M., Nabat, P., Saint-Martin, D., Bock, J., Decharme, B., Mallet, M., Roehrig, R., Séférian, R.,](#)  
1137 [Sénési, S., and Voltaire, A.: Present-Day and Historical Aerosol and Ozone Characteristics in CNRM](#)  
1138 [CMIP6 Simulations, Journal of Advances in Modeling Earth Systems, 12, e2019MS001816,](#)  
1139 [10.1029/2019ms001816, 2020.](#)

1140 [Morgenstern, O., Braesicke, P., O'Connor, F. M., Bushell, A. C., Johnson, C. E., Osprey, S. M., and](#)  
1141 [Pyle, J. A.: Evaluation of the new UKCA climate-composition model – Part 1: The stratosphere, Geosci.](#)  
1142 [Model Dev., 2, 43-57, 10.5194/gmd-2-43-2009, 2009.](#)

1143 [Morgenstern, O., O'Connor, F. M., Johnson, B. T., Zeng, G., Mulcahy, J. P., Williams, J., Teixeira, J.,](#)  
1144 [Michou, M., Nabat, P., Horowitz, L. W., Naik, V., Sentman, L. T., Deushi, M., Bauer, S. E., Tsigaridis,](#)  
1145 [K., Shindell, D. T., and Kinnison, D. E.: Reappraisal of the climate impacts of ozone-depleting](#)  
1146 [substances., Gephys. Res. Lett., 2020.](#)

1147 [Mulcahy, J. P., Johnson, C., Jones, C. G., Povey, A. C., Scott, C. E., Sellar, A., Turnock, S. T.,](#)  
1148 [Woodhouse, M. T., Abraham, N. L., Andrews, M. B., Bellouin, N., Browse, J., Carslaw, K. S., Dalvi,](#)  
1149 [M., Folberth, G. A., Glover, M., Grosvenor, D., Hardacre, C., Hill, R., Johnson, B., Jones, A., Kipling,](#)

1150 [Z., Mann, G., Mollard, J., O'Connor, F. M., Palmieri, J., Reddington, C., Rumbold, S. T., Richardson,](#)  
1151 [M., Schutgens, N. A. J., Stier, P., Stringer, M., Tang, Y., Walton, J., Woodward, S., and Yool, A.:](#)  
1152 [Description and evaluation of aerosol in UKESM1 and HadGEM3-GC3.1 CMIP6 historical](#)  
1153 [simulations, Geosci. Model Dev. Discuss., 2020, 1-59, 10.5194/gmd-2019-357, 2020.](#)

1154 [Myhre, G., D. Shindell, F.-M. Bréon, W. Collins, J. Fuglestedt, J. Huang, D. Koch, J.-F. Lamarque,](#)  
1155 [D. Lee, B. Mendoza, T. Nakajima, A. Robock, G. Stephens, Takemura, T., and Zhang, H.:](#)  
1156 [Anthropogenic and Natural Radiative Forcing. In: Climate Change 2013: The Physical Science Basis.](#)  
1157 [Contribution of Working Group I to the Fifth Assessment Report of the Intergovernmental Panel on](#)  
1158 [Climate Change, 2013a.](#)

1159 [Myhre, G., Samset, B. H., Schulz, M., Balkanski, Y., Bauer, S., Bernsten, T. K., Bian, H., Bellouin, N.,](#)  
1160 [Chin, M., Diehl, T., Easter, R. C., Feichter, J., Ghan, S. J., Hauglustaine, D., Iversen, T., Kinne, S.,](#)  
1161 [Kirkevåg, A., Lamarque, J. F., Lin, G., Liu, X., Lund, M. T., Luo, G., Ma, X., van Noije, T., Penner, J.](#)  
1162 [E., Rasch, P. J., Ruiz, A., Seland, Ø., Skeie, R. B., Stier, P., Takemura, T., Tsigaridis, K., Wang, P.,](#)  
1163 [Wang, Z., Xu, L., Yu, H., Yu, F., Yoon, J. H., Zhang, K., Zhang, H., and Zhou, C.: Radiative forcing](#)  
1164 [of the direct aerosol effect from AeroCom Phase II simulations, Atmos. Chem. Phys., 13, 1853-1877,](#)  
1165 [10.5194/acp-13-1853-2013, 2013b.](#)

1166 [O'Connor, F. M., Johnson, C. E., Morgenstern, O., Abraham, N. L., Braesicke, P., Dalvi, M., Folberth,](#)  
1167 [G. A., Sanderson, M. G., Telford, P. J., Voulgarakis, A., Young, P. J., Zeng, G., Collins, W. J., and](#)  
1168 [Pyle, J. A.: Evaluation of the new UKCA climate-composition model – Part 2: The Troposphere,](#)  
1169 [Geosci. Model Dev., 7, 41-91, 10.5194/gmd-7-41-2014, 2014.](#)

1170 [O'Connor, F. M., Abraham, N. L., Dalvi, M., Folberth, G., Griffiths, P., Hardacre, C., Johnson, B. T.,](#)  
1171 [Kahana, R., Keeble, J., Kim, B., Morgenstern, O., Mulcahy, J. P., Richardson, M. G., Robertson, E.,](#)  
1172 [Seo, J., Shim, S., Teixeira, J. C., Turnock, S., Williams, J., Wiltshire, A., and Zeng, G.: Assessment of](#)  
1173 [pre-industrial to present-day anthropogenic climate forcing in UKESM1, Atmos. Chem. Phys. Discuss.,](#)  
1174 [2020, 1-49, 10.5194/acp-2019-1152, 2020.](#)

1175 [O'Connor, F. M., Abraham, N. L., Dalvi, M., Folberth, G., Griffiths, P., Hardacre, C., Johnson, B. T.,](#)  
1176 [Kahana, R., Keeble, J., Kim, B., Morgenstern, O., Mulcahy, J. P., Richardson, M. G., Robertson, E.,](#)  
1177 [Seo, J., Shim, S., Teixeira, J. C., Turnock, S., Williams, J., Wiltshire, A., and Zeng, G.: Assessment of](#)  
1178 [pre-industrial to present-day anthropogenic climate forcing in UKESM1, Atmospheric Chemistry and](#)  
1179 [Physics, Submitted, 2020a.](#)

1180 [O'Connor, F. M., Jamil, O., Andrews, T., Johnson, B. T., Mulcahy, J. P., and Manners, J.:](#)  
1181 [Apportionment of the Pre-Industrial to Present-Day Climate Forcing by Methane using UKESM1,](#)  
1182 [JAMES, submitted, 2020b.](#)

1183 [Oshima, N., Yukimoto, S., Deushi, M., Koshiro, T., Kawai, H., Tanaka, T. Y., and Yoshida, K.: Global](#)  
1184 [and Arctic effective radiative forcing of anthropogenic gases and aerosols in MRI-ESM2.0, Prog. Earth.](#)  
1185 [Planet. Sci, 2020.](#)

1186 [Pendergrass, A. G., Conley, A., and Vitt, F. M.: Surface and top-of-atmosphere radiative feedback](#)  
1187 [kernels for CESM-CAM5, Earth Syst. Sci. Data, 10, 317-324, 10.5194/essd-10-317-2018, 2018.](#)

1188 [Pincus, R., and Baker, M. B.: Effect of precipitation on the albedo susceptibility of clouds in the marine](#)  
1189 [boundary layer, Nature, 372, 250-252, 10.1038/372250a0, 1994.](#)

1190 [Pincus, R., Forster, P. M., and Stevens, B.: The Radiative Forcing Model Intercomparison Project](#)  
1191 [\(RFMIP\): experimental protocol for CMIP6, Geosci. Model Dev., 9, 3447-3460, 10.5194/gmd-9-3447-](#)  
1192 [2016, 2016.](#)



1193 [Samset, B. H., and Myhre, G.: Climate response to externally mixed black carbon as a function of](#)  
1194 [altitude, \*Journal of Geophysical Research: Atmospheres\*, 120, 2913-2927, 10.1002/2014jd022849,](#)  
1195 [2015.](#)

1196 [Samset, B. H., Myhre, G., Forster, P. M., Hodnebrog, Ø., Andrews, T., Faluvegi, G., Fläschner, D.,](#)  
1197 [Kasoar, M., Kharin, V., Kirkevåg, A., Lamarque, J.-F., Olivie, D., Richardson, T., Shindell, D., Shine,](#)  
1198 [K. P., Takemura, T., and Voulgarakis, A.: Fast and slow precipitation responses to individual climate](#)  
1199 [forcers: A PDRMIP multimodel study, \*Geophysical Research Letters\*, 43, 2782-2791,](#)  
1200 [10.1002/2016gl068064, 2016.](#)

1201 [Saunio, M., Stavert, A. R., Poulter, B., Bousquet, P., Canadell, J. G., Jackson, R. B., Raymond, P. A.,](#)  
1202 [Dlugokencky, E. J., Houweling, S., Patra, P. K., Ciais, P., Arora, V. K., Bastviken, D., Bergamaschi,](#)  
1203 [P., Blake, D. R., Brailsford, G., Bruhwiler, L., Carlson, K. M., Carrol, M., Castaldi, S., Chandra, N.,](#)  
1204 [Crevoisier, C., Crill, P. M., Covey, K., Curry, C. L., Etiope, G., Frankenberg, C., Gedney, N., Hegglin,](#)  
1205 [M. I., Höglund-Isaksson, L., Hugelius, G., Ishizawa, M., Ito, A., Janssens-Maenhout, G., Jensen, K. M.,](#)  
1206 [Joos, F., Kleinen, T., Krummel, P. B., Langenfelds, R. L., Laruelle, G. G., Liu, L., Machida, T.,](#)  
1207 [Maksyutov, S., McDonald, K. C., McNorton, J., Miller, P. A., Melton, J. R., Morino, I., Müller, J.,](#)  
1208 [Murguía-Flores, F., Naik, V., Niwa, Y., Noce, S., O'Doherty, S., Parker, R. J., Peng, C., Peng, S., Peters,](#)  
1209 [G. P., Prigent, C., Prinn, R., Ramonet, M., Regnier, P., Riley, W. J., Rosentretter, J. A., Segers, A.,](#)  
1210 [Simpson, I. J., Shi, H., Smith, S. J., Steele, L. P., Thornton, B. F., Tian, H., Tohjima, Y., Tubiello, F.](#)  
1211 [N., Tsuruta, A., Viovy, N., Voulgarakis, A., Weber, T. S., van Weele, M., van der Werf, G. R., Weiss,](#)  
1212 [R. F., Worthy, D., Wunch, D., Yin, Y., Yoshida, Y., Zhang, W., Zhang, Z., Zhao, Y., Zheng, B., Zhu,](#)  
1213 [Q., Zhu, Q., and Zhuang, Q.: The Global Methane Budget 2000–2017, \*Earth Syst. Sci. Data\*, 12, 1561-](#)  
1214 [1623, 10.5194/essd-12-1561-2020, 2020.](#)

1215 [Séférian, R., Nabat, P., Michou, M., Saint-Martin, D., Voldoire, A., Colin, J., Decharme, B., Delire, C.,](#)  
1216 [Berthet, S., Chevallier, M., Sénési, S., Franchisteguy, L., Vial, J., Mallet, M., Joetzjer, E., Geoffroy, O.,](#)  
1217 [Guérémy, J.-F., Moine, M.-P., Msadek, R., Ribes, A., Rocher, M., Roehrig, R., Salas-y-Méllia, D.,](#)  
1218 [Sanchez, E., Terray, L., Valcke, S., Waldman, R., Aumont, O., Bopp, L., Deshayes, J., Éthé, C., and](#)  
1219 [Madec, G.: Evaluation of CNRM Earth-System model, CNRM-ESM 2-1: role of Earth system](#)  
1220 [processes in present-day and future climate, \*Journal of Advances in Modeling Earth Systems\*, n/a,](#)  
1221 [10.1029/2019ms001791, 2019.](#)

1222 [Seland, Ø., Bentsen, M., Seland Graff, L., Olivie, D., Toniazzo, T., Gjermundsen, A., Debernard, J. B.,](#)  
1223 [Gupta, A. K., He, Y., Kirkevåg, A., Schwinger, J., Tjiputra, J., Schancke Aas, K., Bethke, I., Fan, Y.,](#)  
1224 [Griesfeller, J., Grini, A., Guo, C., Ilicak, M., Hafsahl Karset, I. H., Landgren, O., Liakka, J., Onsum](#)  
1225 [Moseid, K., Nummelin, A., Spensberger, C., Tang, H., Zhang, Z., Heinze, C., Iverson, T., and Schulz,](#)  
1226 [M.: The Norwegian Earth System Model, NorESM2 - Evaluation of theCMIP6 DECK and historical](#)  
1227 [simulations, \*Geosci. Model Dev. Discuss.\*, 2020, 1-68, 10.5194/gmd-2019-378, 2020.](#)

1228 [Sellar, A. A., Jones, C. G., Mulcahy, J., Tang, Y., Yool, A., Wiltshire, A., O'Connor, F. M., Stringer,](#)  
1229 [M., Hill, R., Palmieri, J., Woodward, S., de Mora, L., Kuhlbrodt, T., Rumbold, S., Kelley, D. I., Ellis,](#)  
1230 [R., Johnson, C. E., Walton, J., Abraham, N. L., Andrews, M. B., Andrews, T., Archibald, A. T., Berthou,](#)  
1231 [S., Burke, E., Blockley, E., Carslaw, K., Dalvi, M., Edwards, J., Folberth, G. A., Gedney, N., Griffiths,](#)  
1232 [P. T., Harper, A. B., Hendry, M. A., Hewitt, A. J., Johnson, B., Jones, A., Jones, C. D., Keeble, J.,](#)  
1233 [Liddicoat, S., Morgenstern, O., Parker, R. J., Predoi, V., Robertson, E., Siahann, A., Smith, R. S.,](#)  
1234 [Swaminathan, R., Woodhouse, M. T., Zeng, G., and Zerroukat, M.: UKESM1: Description and](#)  
1235 [evaluation of the UK Earth System Model, \*Journal of Advances in Modeling Earth Systems\*, n/a,](#)  
1236 [10.1029/2019ms001739, 2020.](#)

1237 [Sherwood, S. C., Bony, S., Boucher, O., Bretherton, C., Forster, P. M., Gregory, J. M., and Stevens, B.:](#)  
1238 [Adjustments in the Forcing-Feedback Framework for Understanding Climate Change, \*Bulletin of the\*](#)  
1239 [American Meteorological Society](#), 96, 217-228, 10.1175/bams-d-13-00167.1, 2015.

1240 [Shine, K. P., Cook, J., Highwood, E. J., and Joshi, M. M.: An alternative to radiative forcing for](#)  
1241 [estimating the relative importance of climate change mechanisms, \*Geophysical Research Letters\*, 30,](#)  
1242 [10.1029/2003gl018141, 2003.](#)

1243 [Skeie, R. B., Myhre, G., Hodnebrog, Ø., Cameron-Smith, P. J., Deushi, M., Hegglin, M. I., Horowitz,](#)  
1244 [L. W., Kramer, R. J., Michou, M., Mills, M. J., Olivie, D. J. L., O'Connor, F. M., Paynter, D., Samset,](#)  
1245 [B. H., Sellar, A., Shindell, D., Takemura, T., Tilmes, S., and Wu, T.: Historical total ozone radiative](#)  
1246 [forcing derived from CMIP6 simulations, \*npj Climate and Atmospheric Science\* 2020.](#)

1247 [Smith, C. J., Kramer, R. J., Myhre, G., Forster, P. M., Soden, B. J., Andrews, T., Boucher, O., Faluvegi,](#)  
1248 [G., Fläschner, D., Hodnebrog, Ø., Kasoar, M., Kharin, V., Kirkevåg, A., Lamarque, J.-F., Mülmenstädt,](#)  
1249 [J., Olivie, D., Richardson, T., Samset, B. H., Shindell, D., Stier, P., Takemura, T., Voulgarakis, A., and](#)  
1250 [Watson-Parris, D.: Understanding Rapid Adjustments to Diverse Forcing Agents, \*Geophysical\*](#)  
1251 [Research Letters](#), 45, 12.023-012.031, doi:10.1029/2018GL079826, 2018.

1252 [Smith, C. J., Kramer, R. J., Myhre, G., Alterskjær, K., Collins, W., Sima, A., Boucher, O., Dufresne, J.](#)  
1253 [L., Nabat, P., Michou, M., Yukimoto, S., Cole, J., Paynter, D., Shiogama, H., O'Connor, F. M.,](#)  
1254 [Robertson, E., Wiltshire, A., Andrews, T., Hannay, C., Miller, R., Nazarenko, L., Kirkevåg, A., Olivie,](#)  
1255 [D., Fiedler, S., Pincus, R., and Forster, P. M.: Effective radiative forcing and adjustments in CMIP6](#)  
1256 [models, \*Atmos. Chem. Phys.\*, 20, 9591-9618, 10.5194/acp-20-9591-2020, 2020a.](#)

1257 [Smith, C. J., Kramer, R. J., and Sima, A.: The HadGEM3-GA7.1 radiative kernel: the importance of a](#)  
1258 [well-resolved stratosphere, \*Earth Syst. Sci. Data Discuss.\*, 2020, 1-16, 10.5194/essd-2019-254, 2020b.](#)

1259 [Soden, B. J., Held, I. M., Colman, R., Shell, K. M., Kiehl, J. T., and Shields, C. A.: Quantifying Climate](#)  
1260 [Feedbacks Using Radiative Kernels, \*Journal of Climate\*, 21, 3504-3520, 10.1175/2007jcli2110.1, 2008.](#)

1261 [Stevenson, D. S., Young, P. J., Naik, V., Lamarque, J. F., Shindell, D. T., Voulgarakis, A., Skeie, R.](#)  
1262 [B., Dalsoren, S. B., Myhre, G., Berntsen, T. K., Folberth, G. A., Rumbold, S. T., Collins, W. J.,](#)  
1263 [MacKenzie, I. A., Doherty, R. M., Zeng, G., van Noije, T. P. C., Strunk, A., Bergmann, D., Cameron-](#)  
1264 [Smith, P., Plummer, D. A., Strode, S. A., Horowitz, L., Lee, Y. H., Szopa, S., Sudo, K., Nagashima, T.,](#)  
1265 [Josse, B., Cionni, I., Righi, M., Eyring, V., Conley, A., Bowman, K. W., Wild, O., and Archibald, A.:](#)  
1266 [Tropospheric ozone changes, radiative forcing and attribution to emissions in the Atmospheric](#)  
1267 [Chemistry and Climate Model Intercomparison Project \(ACCMIP\), \*Atmos. Chem. Phys.\*, 13, 3063-](#)  
1268 [3085, 10.5194/acp-13-3063-2013, 2013.](#)

1269 [Stevenson, D. S., Zhao, A., Naik, V., O'Connor, F. M., Tilmes, S., Zeng, G., Murray, L. T., Collins, W.](#)  
1270 [J., Griffiths, P., Shim, S., Horowitz, L. W., Sentman, L., and Emmons, L.: Trends in global tropospheric](#)  
1271 [hydroxyl radical and methane lifetime since 1850 from AerChemMIP, \*Atmos. Chem. Phys. Discuss.\*,](#)  
1272 [2020, 1-25, 10.5194/acp-2019-1219, 2020.](#)

1273 [Stjern, C. W., Samset, B. H., Myhre, G., Forster, P. M., Hodnebrog, Ø., Andrews, T., Boucher, O.,](#)  
1274 [Faluvegi, G., Iversen, T., Kasoar, M., Kharin, V., Kirkevåg, A., Lamarque, J.-F., Olivie, D., Richardson,](#)  
1275 [T., Shawki, D., Shindell, D., Smith, C. J., Takemura, T., and Voulgarakis, A.: Rapid Adjustments Cause](#)  
1276 [Weak Surface Temperature Response to Increased Black Carbon Concentrations, \*Journal of\*](#)  
1277 [Geophysical Research: Atmospheres](#), 122, 11,462-411,481, 10.1002/2017jd027326, 2017.

1278 [Suzuki, K., and Takemura, T.: Perturbations to Global Energy Budget Due to Absorbing and Scattering](#)  
1279 [Aerosols, \*Journal of Geophysical Research: Atmospheres\*, 124, 2194-2209, 10.1029/2018jd029808,](#)  
1280 [2019.](#)

1281 [Takemura, T., Nozawa, T., Emori, S., Nakajima, T. Y., and Nakajima, T.: Simulation of climate](#)  
1282 [response to aerosol direct and indirect effects with aerosol transport-radiation model, \*Journal of\*](#)  
1283 [Geophysical Research: Atmospheres](#), 110, 10.1029/2004jd005029, 2005.

1284 [Takemura, T., and Suzuki, K.: Weak global warming mitigation by reducing black carbon emissions, Scientific Reports, 9, 4419, 10.1038/s41598-019-41181-6, 2019.](#)  
1285

1286 [Takemura, T., et al: Development of a global aerosol climate model SPRINTARS, CGER's Supercomputer Monograph Report, 24, 2018.](#)  
1287

1288 [Tang, T., Shindell, D., Faluvegi, G., Myhre, G., Olivié, D., Voulgarakis, A., Kasoar, M., Andrews, T., Boucher, O., Forster, P. M., Hodnebrog, Ø., Iversen, T., Kirkevåg, A., Lamarque, J.-F., Richardson, T., Samset, B. H., Stjern, C. W., Takemura, T., and Smith, C.: Comparison of Effective Radiative Forcing Calculations Using Multiple Methods, Drivers, and Models, Journal of Geophysical Research: Atmospheres, 124, 4382-4394, 10.1029/2018jd030188, 2019.](#)  
1289  
1290  
1291  
1292

1293 [Tatebe, H., Ogura, T., Nitta, T., Komuro, Y., Ogochi, K., Takemura, T., Sudo, K., Sekiguchi, M., Abe, M., Saito, F., Chikira, M., Watanabe, S., Mori, M., Hirota, N., Kawatani, Y., Mochizuki, T., Yoshimura, K., Takata, K., O'Ishi, R., Yamazaki, D., Suzuki, T., Kurogi, M., Kataoka, T., Watanabe, M., and Kimoto, M.: Description and basic evaluation of simulated mean state, internal variability, and climate sensitivity in MIROC6, Geoscientific Model Development, 12, 2727-2765, <http://dx.doi.org/10.5194/gmd-12-2727-2019>, 2019.](#)  
1294  
1295  
1296  
1297  
1298

1299 [Thornhill, G., Collins, W., Olivié, D., Archibald, A., Bauer, S., Checa-Garcia, R., Fiedler, S., Folberth, G., Gjernmunsen, A., Horowitz, L., Lamarque, J. F., Michou, M., Mulcahy, J., Nabat, P., Naik, V., O'Connor, F. M., Paulot, F., Schulz, M., Scott, C. E., Seferian, R., Smith, C., Takemura, T., Tilmes, S., and Weber, J.: Climate-driven chemistry and aerosol feedbacks in CMIP6 Earth system models, Atmos. Chem. Phys. Discuss., 2020, 1-36, 10.5194/acp-2019-1207, 2020.](#)  
1300  
1301  
1302  
1303

1304 [Tilmes, S., Hodzic, A., Emmons, L. K., Mills, M. J., Gettelman, A., Kinnison, D. E., Park, M., Lamarque, J. F., Vitt, F., Shrivastava, M., Campuzano-Jost, P., Jimenez, J. L., and Liu, X.: Climate Forcing and Trends of Organic Aerosols in the Community Earth System Model \(CESM2\), Journal of Advances in Modeling Earth Systems, n/a, 10.1029/2019MS001827, 2019.](#)  
1305  
1306  
1307

1308 [Twomey, S.: Pollution and the planetary albedo, Atmospheric Environment \(1967\), 8, 1251-1256, \[https://doi.org/10.1016/0004-6981\\(74\\)90004-3\]\(https://doi.org/10.1016/0004-6981\(74\)90004-3\), 1974.](#)  
1309

1310 [van Marle, M. J. E., Kloster, S., Magi, B. I., Marlon, J. R., Daniau, A. L., Field, R. D., Arneeth, A., Forrest, M., Hantson, S., Kehrwald, N. M., Knorr, W., Lasslop, G., Li, F., Mangeon, S., Yue, C., Kaiser, J. W., and van der Werf, G. R.: Historic global biomass burning emissions for CMIP6 \(BB4CMIP\) based on merging satellite observations with proxies and fire models \(1750–2015\), Geosci. Model Dev., 10, 3329-3357, 10.5194/gmd-10-3329-2017, 2017.](#)  
1311  
1312  
1313  
1314

1315 [Vial, J., Dufresne, J.-l., and Bony, S.: On the interpretation of inter-model spread in CMIP5 climate sensitivity estimates, Climate Dynamics, 41, 3339-3362, <http://dx.doi.org/10.1007/s00382-013-1725-9>, 2013.](#)  
1316  
1317

1318 [Watanabe, M., Suzuki, T., O'ishi, R., Komuro, Y., Watanabe, S., Emori, S., Takemura, T., Chikira, M., Ogura, T., Sekiguchi, M., Takata, K., Yamazaki, D., Yokohata, T., Nozawa, T., Hasumi, H., Tatebe, H., and Kimoto, M.: Improved Climate Simulation by MIROC5: Mean States, Variability, and Climate Sensitivity, Journal of Climate, 23, 6312-6335, 10.1175/2010jcli3679.1, 2010.](#)  
1319  
1320  
1321

1322 [Woodward, S.: Modeling the atmospheric life cycle and radiative impact of mineral dust in the Hadley Centre climate model, Journal of Geophysical Research: Atmospheres, 106, 18155-18166, 10.1029/2000jd900795, 2001.](#)  
1323  
1324

1325 [Wu, T., Lu, Y., Fang, Y., Xin, X., Li, L., Li, W., Jie, W., Zhang, J., Liu, Y., Zhang, L., Zhang, F., Zhang, Y., Wu, F., Li, J., Chu, M., Wang, Z., Shi, X., Liu, X., Wei, M., Huang, A., Zhang, Y., and Liu,](#)  
1326



1327 [X.: The Beijing Climate Center Climate System Model \(BCC-CSM\): the main progress from CMIP5](#)  
1328 [to CMIP6, Geosci. Model Dev., 12, 1573-1600, 10.5194/gmd-12-1573-2019, 2019.](#)

1329 [Wu, T., Zhang, F., Zhang, J., Jie, W., Zhang, Y., Wu, F., Li, L., Liu, X., Lu, X., Zhang, L., Wang, J.,](#)  
1330 [and Hu, A.: Beijing Climate Center Earth System Model version 1 \(BCC-ESM1\): Model Description](#)  
1331 [and Evaluation, Geosci. Model Dev. , 13, 977-1005, 10.5194/gmd-2019-172, 2020.](#)

1332 [Yukimoto, S., Kawai, H., Koshiro, T., Oshima, N., Yoshida, K., Urakawa, S., Tsujino, H., Deushi, M.,](#)  
1333 [Tanaka, T., Hosaka, M., Yabu, S., Yoshimura, H., Shindo, E., Mizuta, R., Obata, A., Adachi, Y., and](#)  
1334 [Ishii, M.: The Meteorological Research Institute Earth System Model Version 2.0, MRI-ESM2.0:](#)  
1335 [Description and Basic Evaluation of the Physical Component, J. Meteor. Soc. Japan, 97, 931-965,](#)  
1336 [10.2151/jmsj.2019-051, 2019.](#)

1337 [Zelinka, M. D., Andrews, T., Forster, P. M., and Taylor, K. E.: Quantifying components of aerosol-](#)  
1338 [cloud-radiation interactions in climate models, Journal of Geophysical Research: Atmospheres, 119,](#)  
1339 [7599-7615, 10.1002/2014jd021710, 2014.](#)

1340

## 1341 Supplementary Material for

## 1342 Effective radiative forcing from emissions of reactive gases and 1343 aerosols – a multi-model comparison

### 1344 S1 Table of model characteristics

1345 The table of models used in the paper with information on resolution and aerosol and chemistry modules.

1346 Table S 1 Table of model properties, aerosol schemes, and chemistry (SU = sulphate; OA = organic aerosol; BC = black  
1347 carbon; DU = dust; SS = sea salt; NO3 =nitrate)

<u>Earth System</u>	<u>Resolution</u>	<u>Description of aerosol module</u>	<u>References</u>
<u>Model</u> <u>(component models)</u>			

<p><u>IPSL-CM6A-LR</u> <u>(LMDz, INCA)</u></p>	<p><u>1.25°(lat) x</u> <u>2.5°(lon)</u> <u>79 vertical</u> <u>levels</u> <u>LMDzORIN</u> <u>CA</u> <u>Two</u></p>	<p><u>LMDzORINCA</u> <u>Two-moment (mass and number) aerosol scheme</u> <u>with 5 lognormal modes.</u>  <u>The IPSLCM6A-LR-INCA model used for this</u> <u>analysis has interactive aerosols but a limited gas-</u> <u>phase model. Aerosol scheme is based a sectional</u> <u>approach with to represent the size distributionof</u> <u>dust, Sea- salt (which has an additional super-coarse</u> <u>mode to model largest emission of spray-salt</u> <u>aerosols), BC, NH4, NO3, SO4, SO2 and OA with a</u> <u>combination of accumulation and coarse log-normal</u> <u>modes with both, soluble and insoluble, treated as</u> <u>independent modes. DMS emissions are prescribed</u> <u>and not interactively calculated. BC is modelled as</u> <u>internally mixed with sulphate (Wang et al., 2016),</u> <u>where the refractive index is relies on Garnet-</u> <u>Maxwell method. Its emissions are derived from</u> <u>inventories. A new dust refractive index is</u> <u>implemented (Di Biagio et al., 2019). Well mixed</u> <u>trace gases concentrations/emissions are forced with</u> <u>AMIP/CMIP6 datasets (Lurton et al., 2020) ozone</u> <u>by (Checa-Garcia et al., 2018) and solar forcing by</u> <u>(Matthes et al., 2017)</u>  <u>Components included: SU, BC, OA, SS, DU, NO3</u></p>	<p><u>(Balkanski et al., 2010)</u> <u>(Hauglustaine et al.,</u> <u>2014)</u></p>
--	---	--	--

<p><u>UKESM11</u> <u>(HadGEM3,</u> <u>UKCA, JULES)</u></p>	<p><u>1.25°(lat) x</u> <u>1.88°(lon)</u> <u>85 vertical</u> <u>levels</u></p>	<p><u>UKCA contains the GLOMAP-mode aerosol microphysics scheme</u></p> <p><u>Two-moment (mass and number) aerosol scheme with 5 lognormal modes (nucleation soluble, Aitken soluble, Aitken insoluble, accumulation soluble, coarse soluble)</u></p> <p><u>Components included: SU, BC, OA, SS, DU*</u></p> <p><u>*Dust component tracked independently in six size bins</u></p> <p><u>UKCA contains a stratosphere-troposphere chemistry scheme, consisting of 84 tracers, 81 species, 199 bimolecular reactions, 25 uni- or termolecular reactions, 5 heterogeneous, 3 aqueous phase reactions, and 59 photolytic reactions. Secondary aerosol formation of sulphate and secondary organic aerosol is determined by the interactive oxidants.</u></p> <p><u>The UKCA aerosol scheme, called GLOMAP-mode, is a two-moment scheme for the simulation of tropospheric black carbon (BC), organic carbon (OC), SO<sub>4</sub>, and sea salt. Dust is modelled independently using the bin scheme of Woodward (2001). The UKCA chemistry and aerosol schemes are coupled such that the secondary aerosol (SO<sub>4</sub>, OA) formation rates depend on oxidants from the stratosphere-troposphere chemistry scheme. Aerosol particles are activated into cloud droplets using the activation scheme of Abdul-Razzak and Ghan (2000) which is dependent on aerosol size distribution, aerosol composition, and meteorological conditions. Changes in CDNC affect cloud droplet effective radius ((Jones et al., 2001) and the autoconversion of cloud liquid water in to rain water (Khairoutdinov and Kogan, 2000), which both influence cloud albedo. Stratospheric aerosols (aerosol optical depth and surface area density) are prescribed in the model (Sellar et al., 2019b).</u></p>	<p><u>(Sellar et al.)</u> <u>(Williams et al., 2018)</u> <u>(Walters et al., 2019)</u> <u>(Kuhlbrodt et al., 2018)</u> <u>GLOMAP-mode by (Mann et al., 2010)</u> <u>(Mulcahy et al., 2018)</u> <u>(Morgenstern et al., 2009)</u> <u>(O'Connor et al., 2014)</u> <u>(Archibald et al., 2020;Sellar et al., 2020;Mulcahy et al., 2020)</u></p>
--	---	---	--

<p><u>CNRM-ESM2-1</u> (<u>ARPEGE</u>climatv6.3, <u>ISBA-CTRIP</u>, <u>TACTIC</u>, <u>REPROBUS</u>, <u>PISCES</u>)</p>	<p><u>1.4°(lat) x</u> <u>1.4°(lon)</u> <u>91 vertical</u> <u>levels</u></p>	<p><u>Aerosols: TACTIC v2 tropospheric aerosol bin scheme. 12 bins in total for SU, BC, OA, SS, DU, with 3 bins for SS, and 3 bins for DD.</u> <u>REPROBUS v2 stratospheric chemistry scheme with 63 variables, 44 transported by the model large-scale transport scheme, and 168 chemical reactions, among which 39 photolysis and 9 heterogeneous reactions</u></p>	<p>(<u>Séférian et al., 2016</u>;<u>Michou et al., 2015</u>) (<u>Séférian et al.</u>) 2019 <u>Michou et al 2019</u> <u>Model description website:</u> <u><a href="http://www.umrcnrm.fr/cmip6/spip.php?article10">http://www.umrcnrm.fr/cmip6/spip.php?article10</a></u></p>
<p><u>NorESM2</u> <u>CAM6-Nor, CLM5)</u></p>	<p><u>1.9°(lat) x</u> <u>2.5°(lon)</u> <u>32 vertical</u> <u>levels</u></p>	<p><u>OsloAero6</u> <u>Production-tagged aerosol module with background lognormal modes (Aitken, accumulation, coarse). Process tracers can alter the shape and composition of the initially lognormal background modes to generate mixtures.</u> <u>OsloAero6 aerosol module which contains some slight updates since (Kirkevåg et al., 2018) describes the formation and evolution of BC, OC, SO<sub>4</sub>, dust, sea-salt and SOA. There is a limited gas-phase chemistry describing the oxidation of the aerosol precursors DMS, SO<sub>2</sub>, isoprene, and monoterpenes. Oxidant fields of OH, HO<sub>2</sub>, NO<sub>3</sub> and O<sub>3</sub> are prescribed climatological fields. As there is no ozone chemistry in the model, prescribed monthly-varying ozone fields are used for the radiation.</u>  <u>Components included: SU, BC, OA, SS, DU</u></p>	<p>(<u>Kirkevåg et al., 2018</u>)</p>

<p><u>MRI-ESM2</u></p>	<p><u>MRI-AGCM3.5:</u>  <u>TL159; 320 x 160 lon/lat,</u></p> <p><u>MASINGAR mk-2r4c:</u>  <u>TL95; 192 x 96 lon/lat,</u></p> <p><u>MRI-CCM2.1:</u>  <u>T42; 128 x 64 lon/lat, with 80 vertical levels</u></p>	<p><u>MASINGAR mk-2r4c is an aerosol model that is a component of MRI-ESM2.0. MASINGAR mk-2r4c treats atmospheric aerosol physical and chemical processes (e.g., emission, transport, diffusion, chemical reactions, and dry and wet depositions). The size distributions of sea salt and mineral dust are divided into 10 discrete bins and those of other aerosols are represented by lognormal size distributions.</u></p> <p><u>Components included: SU, BC, OA, SS, DU</u></p>	<p><u>(Yukimoto et al., 2019)</u></p> <p><u>(Oshima et al., 2020)</u></p>
<p><u>MIROC6</u></p>	<p><u>1.4° (lat) x 1.4° (lon)</u></p>	<p><u>Spectral Radiation-Transport Model for Aerosol Species (SPRINTARS) predicts mass mixing ratios of the main tropospheric aerosols, and models aerosol-cloud interactions in which aerosols alter cloud microphysical properties and affect the radiation budget by acting as cloud condensation and ice nuclei. The SO<sub>4</sub>, BC and OC aerosols are treated as externally mixed in this model. The CDNC and ice crystal number are used to calculate the aerosol indirect effect and cloud nucleation process</u></p> <p><u>Components included: SU, BC, OA, SS, DU</u></p>	<p><u>(Takemura et al., 2005;Watanabe et al., 2010;Takemura and Suzuki, 2019;Takemura, 2018;Tatebe et al., 2019)</u></p>

<p><u>BCC-ESM1</u> (<u>BCC-AGCM3-Chem,</u> <u>BCC-AVIM2,</u> <u>MOM4-L40,</u> <u>SIS</u>)</p>	<p><u>2.8125° (lat) x</u> <u>2.8125° (lon)</u> <u>26 vertical</u> <u>levels with top</u> <u>level at 2.914</u> <u>hPa</u></p>	<p><u>The model prognoses mass distribution of five</u> <u>aerosol types including sulfate, dust, black carbon,</u> <u>organic carbon, and sea salt based on their emissions</u> <u>(and precursor emissions), chemical production for</u> <u>sulfate and secondary organics, dry and wet (rainout</u> <u>and washout) deposition, transport by advection, and</u> <u>dry and wet convection.</u></p> <p><u>It uses the BCC-AGCM3-Chem atmospheric</u> <u>chemistry model based on MOZART2 (Horowitz et</u> <u>al., 2003) It uses the BCC-AGCM3-Chem</u> <u>atmospheric chemistry model based on MOZART2</u> <u>(Horowitz et al., 2003) which does not include</u> <u>stratospheric chemistry, so concentrations of O<sub>3</sub>,</u> <u>CH<sub>4</sub>, and N<sub>2</sub>O at the top two model levels are the</u> <u>zonally and monthly values derived from the CMIP6</u> <u>data package.</u></p> <p><u>Components included: SU, BC, OA, SS, DU</u></p> <p><u>Effects of aerosols on radiation, cloud, and</u> <u>precipitation are treated.</u></p>	<p><u>(Wu et al., 2020)</u></p>
---	---	---	---------------------------------

<p><u>GFDL-ESM4</u></p>	<p><u>(C96 96x96 cells)</u> <u>49 vertical levels</u></p>	<p><u>The model includes 56 prognostic (transported) tracers and 36 diagnostic (non-transported) chemical tracers, with 43 photolysis reactions, 190 gas-phase kinetic reactions, and 15 heterogeneous reactions. The tropospheric chemistry includes reactions for the NO<sub>x</sub>-HO<sub>x</sub>-O<sub>3</sub>-CO-CH<sub>4</sub> system and oxidation schemes for other non-methane volatile organic compounds. The stratospheric chemistry accounts for the major ozone loss cycles (O<sub>x</sub>, HO<sub>x</sub>, NO<sub>x</sub>, ClO<sub>x</sub>, and BrO<sub>x</sub>) and heterogeneous reactions on liquid and solid stratospheric aerosols as in Austin et al. (2013). The bulk aerosol scheme, including 18 transported aerosol tracers, is similar to that in AM4.0 (Zhao et al., 2018), with the following updates: (1) ammonium and nitrate aerosols are treated explicitly, with ISORROPIA (Fountoukis and Nenes, 2007) used to simulate the sulfate–nitrate–ammonia thermodynamic equilibrium; (2) oxidation of sulfur dioxide and dimethyl sulfide to produce sulfate aerosol is driven by the gas-phase oxidant concentrations (OH, H<sub>2</sub>O<sub>2</sub>, and O<sub>3</sub>) and cloud pH simulated by the online chemistry scheme, and (3) the rate of aging of black and organic carbon aerosols from hydrophobic to hydrophilic forms varies with calculated concentrations of hydroxyl radical (OH). Aerosol species, including sulfate, BC, organic aerosols, sea-salt, dust and nitrate are treated explicitly.</u></p>	<p><u>(Horowitz et al., 2020)(Dunne et al., 2020)</u></p>
<p><u>GISS-E2-1 (p3 variant)</u></p>	<p><u>2° latitude by 2.5° in longitude 40 vertical layers surface to 0.1 hPa in</u></p>	<p><u>Aerosols and ozone are calculated prognostically using the One-Moment Aerosol (OMA). Aerosol scheme is coupled to the tropospheric chemistry scheme which includes inorganic chemistry of O<sub>x</sub>, NO<sub>x</sub>, HO<sub>x</sub>, CO, and organic chemistry of CH<sub>4</sub> and higher hydrocarbons using the CBM4 scheme and the stratospheric chemistry scheme which includes chlorine and bromine chemistry together with polar stratospheric clouds.</u></p>	<p><u>(Bauer et al., 2020;Shindell et al., 2001;Shindell et al., 2003;Gery et al., 1989;Shindell et al., 2006)</u></p>



CESM2-WACCM	0.9 (lat) x 1.25 (lon), 70 levels	Chemistry and aerosols for the troposphere, stratosphere, mesosphere and lower thermosphere are calculated interactively. It simulates 228 compounds, including the 4-mode Modal Aerosol Model (MAM4). This version of MAM4 is modified to allow for the simulation of stratospheric aerosols from volcanic eruptions (from their SO <sub>2</sub> emissions) and oxidation of OCS. The representation of secondary organic aerosols follows the Volatility Basis Set approach.	(Emmons et al., 2020; Danabasoglu, 2019; Danabasoglu, 2019; Gettelman et al., 2019; Tilmes et al., 2019) Mills et al., 2016)
-------------	---	--	--

1348

1349 (Table for European models updated from:

1350 Crescendo Report Horizon 2020

1351 H2020-SC5-2014 Advanced Earth-system models

1352 (Grant Agreement 641816)

1353 Coordinated Research in Earth Systems and Climate: Experiments, kNowledge, Dissemination and

1354 Outreach Deliverable D\_6.2

1355

1356 **S2 Tables of ERF and ERF<sub>ts</sub> for all models analysed**

1357 By removing the adjustment due to the changes in the land surface temperature (as calculated from radiative

1358 kernels) we show the ERF<sub>ts</sub> for those models where the adjustment was available in the following table.

1359 The tables below give the 1850-2014 ERF and the ERF<sub>ts</sub> calculated from the TOA flux differences for each

1360 model for each experiment.

1361

1362 **Table S 2 ERFs and ERF<sub>ts</sub> for the aerosols, including multi-model means with standard errors.**

ERF	aer		BC		OC		SO <sub>2</sub>		NH <sub>3</sub>	
	ERF	ERF <sub>ts</sub>	ERF	ERF <sub>ts</sub>	ERF	ERF <sub>ts</sub>	ERF	ERF <sub>ts</sub>	ERF	ERF <sub>ts</sub>
CNRM-ESM2	-0.74	-0.79	0.11	0.11	-0.17	-0.18	-0.75	-0.78	-	-
UKESM1	-1.10	-1.15	0.37	0.36	-0.21	-0.23	-1.36	-1.41	-	-
MRI-ESM2	-1.21	-1.24	0.25	0.27	-0.32	-0.32	-1.37	-1.42	-	-
BCC-ESM1	-1.47	-1.54	0.21	0.21	-	-	-1.54	-1.62	-	-



	<u>0.0212</u>	<u>-0.0094</u>	<u>-0.0147</u>	<u>-0.0013</u>	<u>0.0010</u>	<u>0.0007</u>	<u>0.1200</u>	<u>0.0048</u>
--	---------------	----------------	----------------	----------------	---------------	---------------	---------------	---------------

1370

1371

### 1372 **S3 Kernel Breakdown of atmospheric adjustments for each experiment**

1373 The full breakdowns of the rapid adjustments as calculated from the kernels is shown for each of the models and  
 1374 experiments where the relevant data was available and shows the differences in models for how the rapid  
 1375 adjustments from different processes contributed to the overall rapid adjustment.

### 1376 **Table S5a Adjustments for piClim-aer experiment**

<u>piClim-aer</u>	<u>CNRM-ESM2</u>	<u>UKESM1</u>	<u>MRI-ESM2</u>	<u>BCC-ESM1</u>	<u>MIROC6</u>	<u>NorESM2</u>	<u>GFDL-ESM4</u>	<u>GISS-E2-1</u>
<u>albedo</u>	<u>-0.017</u>	<u>-0.049</u>	<u>-0.009</u>	<u>-0.095</u>	<u>-0.026</u>	<u>-0.015</u>	<u>-0.044</u>	<u>0.003</u>
<u>cloud</u>	<u>-0.661</u>	<u>-0.915</u>	<u>-0.842</u>	<u>-0.900</u>	<u>-0.945</u>	<u>-1.093</u>	<u>-0.452</u>	<u>-0.581</u>
<u>W.V.</u>	<u>-0.055</u>	<u>0.017</u>	<u>0.169</u>	<u>-0.008</u>	<u>-0.085</u>	<u>0.029</u>	<u>0.094</u>	<u>-0.046</u>
<u>T_trop</u>	<u>0.107</u>	<u>0.023</u>	<u>-0.243</u>	<u>0.092</u>	<u>0.183</u>	<u>0.038</u>	<u>-0.138</u>	<u>0.137</u>
<u>T_strat</u>	<u>-0.015</u>	<u>-0.006</u>	<u>-0.014</u>	<u>-0.038</u>	<u>0.010</u>	<u>-0.054</u>	<u>-0.027</u>	<u>-0.038</u>
<u>T_surface</u>	<u>0.054</u>	<u>0.049</u>	<u>0.032</u>	<u>0.075</u>	<u>0.059</u>	<u>0.001</u>	<u>0.035</u>	<u>0.052</u>

1377

### 1378 **Table S5b Adjustments for piClim-BC experiment**

<u>piClim-BC</u>	<u>CNRM-ESM2</u>	<u>UKESM1</u>	<u>MRI-ESM2</u>	<u>BCC-ESM1</u>	<u>MIROC6</u>	<u>NorESM2</u>	<u>GISS-E2-1</u>
<u>albedo</u>	<u>0.003</u>	<u>-0.013</u>	<u>0.067</u>	<u>0.015</u>	<u>-0.002</u>	<u>0.076</u>	<u>0.046</u>
<u>cloud</u>	<u>-0.010</u>	<u>-0.013</u>	<u>0.163</u>	<u>0.053</u>	<u>-0.282</u>	<u>-0.067</u>	<u>-0.184</u>
<u>W.V.</u>	<u>0.060</u>	<u>0.057</u>	<u>0.329</u>	<u>0.076</u>	<u>-0.042</u>	<u>0.097</u>	<u>0.038</u>
<u>T_trop</u>	<u>-0.088</u>	<u>-0.137</u>	<u>-0.509</u>	<u>-0.131</u>	<u>0.033</u>	<u>-0.137</u>	<u>-0.051</u>
<u>T_strat</u>	<u>-0.003</u>	<u>0.043</u>	<u>0.021</u>	<u>-0.004</u>	<u>-0.008</u>	<u>-0.025</u>	<u>-0.003</u>
<u>T_surface</u>	<u>0.001</u>	<u>0.005</u>	<u>-0.022</u>	<u>-0.002</u>	<u>0.021</u>	<u>-0.003</u>	<u>0.003</u>

1379

### 1380 **Table S5c Adjustments for piClim-OC experiment**

<u>piClim-OC</u>	<u>CNRM-ESM2</u>	<u>UKESM</u>	<u>MRI</u>	<u>MIROC6</u>	<u>NorESM2</u>	<u>GISS-E2-1</u>
<u>albedo</u>	<u>0.008</u>	<u>-0.015</u>	<u>-0.006</u>	<u>-0.017</u>	<u>0.002</u>	<u>0.001</u>
<u>cloud</u>	<u>-0.083</u>	<u>0.052</u>	<u>-0.129</u>	<u>-0.087</u>	<u>-0.100</u>	<u>-0.290</u>
<u>W.V.</u>	<u>0.000</u>	<u>-0.018</u>	<u>-0.009</u>	<u>-0.004</u>	<u>-0.008</u>	<u>-0.054</u>
<u>T_trop</u>	<u>0.025</u>	<u>0.023</u>	<u>-0.016</u>	<u>0.029</u>	<u>0.066</u>	<u>0.057</u>
<u>T_strat</u>	<u>-0.019</u>	<u>-0.003</u>	<u>-0.010</u>	<u>-0.008</u>	<u>-0.016</u>	<u>-0.015</u>
<u>T_surface</u>	<u>0.011</u>	<u>0.015</u>	<u>0.009</u>	<u>0.035</u>	<u>0.010</u>	<u>0.012</u>

1381

1382

1383

1384

1385 **Table S5d Adjustments for piClim-SO2 experiment**

<u>piClim-SO2</u>	<u>CNRM-ESM2</u>	<u>UKESM1</u>	<u>MRI-ESM2</u>	<u>BCC-ESM1</u>	<u>MIROC6</u>	<u>NorESM2</u>	<u>GISS-E2-1</u>
<u>albedo</u>	<u>0.01</u>	<u>-0.03</u>	<u>-0.04</u>	<u>-0.10</u>	<u>-0.02</u>	<u>-0.09</u>	<u>-0.04</u>
<u>cloud</u>	<u>-0.49</u>	<u>-0.79</u>	<u>-0.73</u>	<u>-0.43</u>	<u>-0.40</u>	<u>-0.96</u>	<u>-0.02</u>
<u>W.V.</u>	<u>-0.04</u>	<u>-0.10</u>	<u>-0.05</u>	<u>-0.07</u>	<u>-0.06</u>	<u>-0.05</u>	<u>-0.06</u>
<u>T trop</u>	<u>0.10</u>	<u>0.20</u>	<u>0.08</u>	<u>0.22</u>	<u>0.11</u>	<u>0.16</u>	<u>0.14</u>
<u>T strat</u>	<u>-0.01</u>	<u>-0.02</u>	<u>-0.02</u>	<u>-0.03</u>	<u>0.00</u>	<u>-0.03</u>	<u>-0.01</u>
<u>T surface</u>	<u>0.03</u>	<u>0.04</u>	<u>0.06</u>	<u>0.07</u>	<u>0.04</u>	<u>0.01</u>	<u>0.03</u>

1386

1387 **Table S5e Adjustments for piClim-CH4 experiment**

<u>piClim-CH4</u>	<u>CNRM-ESM2</u>	<u>UKESM1</u>	<u>MRI-ESM2</u>	<u>BCC-ESM1</u>	<u>NorESM2</u>	<u>GFDL-ESM4</u>	<u>GISS-E2-1</u>	<u>CESM2-WACCM</u>
<u>albedo</u>	<u>0.019</u>	<u>0.019</u>	<u>0.013</u>	<u>0.031</u>	<u>0.010</u>	<u>0.014</u>	<u>0.007</u>	<u>0.023</u>
<u>cloud</u>	<u>-0.038</u>	<u>0.242</u>	<u>-0.056</u>	<u>0.008</u>	<u>-0.041</u>	<u>-0.054</u>	<u>0.035</u>	<u>0.045</u>
<u>W.V.</u>	<u>0.071</u>	<u>0.109</u>	<u>0.070</u>	<u>0.055</u>	<u>0.018</u>	<u>0.117</u>	<u>0.021</u>	<u>0.068</u>
<u>T trop</u>	<u>-0.084</u>	<u>-0.162</u>	<u>-0.138</u>	<u>-0.127</u>	<u>-0.080</u>	<u>-0.147</u>	<u>-0.056</u>	<u>-0.082</u>
<u>T strat</u>	<u>0.114</u>	<u>0.115</u>	<u>0.124</u>	<u>0.039</u>	<u>0.057</u>	<u>0.109</u>	<u>0.053</u>	<u>0.103</u>
<u>T surface</u>	<u>-0.017</u>	<u>-0.031</u>	<u>-0.028</u>	<u>-0.046</u>	<u>-0.018</u>	<u>-0.023</u>	<u>-0.019</u>	<u>-0.031</u>

1388

1389 **Table S5f Adjustments for piClim-HC experiment**

<u>piClim-HC</u>	<u>CNRM-ESM2</u>	<u>UKESM1</u>	<u>MRI-ESM2</u>	<u>GFDL-ESM4</u>	<u>GISS-E2-1</u>	<u>CESM2-WACCM</u>
<u>albedo</u>	<u>0.01</u>	<u>-0.02</u>	<u>0.00</u>	<u>0.00</u>	<u>-0.01</u>	<u>0.01</u>
<u>cloud</u>	<u>-0.05</u>	<u>-0.09</u>	<u>-0.02</u>	<u>-0.03</u>	<u>0.03</u>	<u>0.06</u>
<u>W.V.</u>	<u>-0.02</u>	<u>-0.09</u>	<u>0.02</u>	<u>-0.01</u>	<u>-0.01</u>	<u>0.01</u>
<u>T trop</u>	<u>0.03</u>	<u>0.10</u>	<u>-0.03</u>	<u>-0.03</u>	<u>-0.01</u>	<u>0.00</u>
<u>T strat</u>	<u>0.21</u>	<u>0.47</u>	<u>0.16</u>	<u>0.26</u>	<u>0.30</u>	<u>0.16</u>
<u>T surface</u>	<u>0.00</u>	<u>0.01</u>	<u>0.00</u>	<u>-0.02</u>	<u>-0.01</u>	<u>-0.03</u>

1390

1391 **Table S5g Adjustments for piClim-N2O experiment**

<u>piClim-NO2</u>	<u>CNRM-ESM2</u>	<u>UKESM1</u>	<u>MRI-ESM2</u>	<u>NorESM2</u>	<u>GISS-E2-1</u>	<u>CESM2-WACCM</u>
<u>albedo</u>	<u>0.021</u>	<u>0.001</u>	<u>0.005</u>	<u>0.003</u>	<u>0.000</u>	<u>0.008</u>
<u>cloud</u>	<u>-0.010</u>	<u>0.047</u>	<u>0.004</u>	<u>0.059</u>	<u>0.026</u>	<u>0.119</u>
<u>W.V.</u>	<u>0.038</u>	<u>-0.002</u>	<u>-0.015</u>	<u>-0.012</u>	<u>-0.006</u>	<u>0.016</u>
<u>T trop</u>	<u>-0.035</u>	<u>-0.006</u>	<u>-0.022</u>	<u>-0.037</u>	<u>-0.002</u>	<u>-0.014</u>

<u>T_strat</u>	<u>0.094</u>	<u>0.074</u>	<u>0.108</u>	<u>0.003</u>	<u>0.130</u>	<u>0.089</u>
<u>T_surface</u>	<u>-0.016</u>	<u>-0.011</u>	<u>-0.005</u>	<u>-0.014</u>	<u>0.005</u>	<u>-0.016</u>

1392

1393 **Table S5h Adjustments for piClim-NOx experiment**

<u>piClim-NOx</u>	<u>UKESM1</u>	<u>MRI-ESM2</u>	<u>BCC-ESM1</u>	<u>GFDL-ESM4</u>	<u>GISS-E2-1</u>	<u>CESM2-WACCM</u>
<u>albedo</u>	<u>-0.005</u>	<u>0.018</u>	<u>0.023</u>	<u>0.010</u>	<u>0.003</u>	<u>0.041</u>
<u>cloud</u>	<u>-0.036</u>	<u>-0.041</u>	<u>0.007</u>	<u>-0.065</u>	<u>-0.052</u>	<u>0.104</u>
<u>Spec. Hum.</u>	<u>-0.003</u>	<u>-0.040</u>	<u>0.031</u>	<u>0.029</u>	<u>0.005</u>	<u>0.062</u>
<u>T_trop</u>	<u>0.002</u>	<u>-0.014</u>	<u>-0.063</u>	<u>-0.057</u>	<u>-0.001</u>	<u>-0.056</u>
<u>T_strat</u>	<u>-0.024</u>	<u>-0.161</u>	<u>0.029</u>	<u>0.038</u>	<u>0.056</u>	<u>0.095</u>
<u>T_surface</u>	<u>-0.012</u>	<u>-0.012</u>	<u>-0.026</u>	<u>-0.025</u>	<u>-0.001</u>	<u>-0.030</u>

1394

1395 **Table S5i Adjustments for piClim-O3 experiment**

<u>piClim-O3</u>	<u>UKESM1</u>	<u>MRI-ESM2</u>	<u>BCC-ESM1</u>	<u>GFDL-ESM4</u>	<u>GISS-E2-1</u>
<u>albedo</u>	<u>0.001</u>	<u>0.002</u>	<u>0.026</u>	<u>0.009</u>	<u>-0.003</u>
<u>cloud</u>	<u>0.091</u>	<u>-0.126</u>	<u>0.096</u>	<u>-0.079</u>	<u>-0.021</u>
<u>W.V.</u>	<u>0.006</u>	<u>0.010</u>	<u>0.054</u>	<u>0.082</u>	<u>-0.004</u>
<u>T_trop</u>	<u>-0.034</u>	<u>-0.062</u>	<u>-0.115</u>	<u>-0.083</u>	<u>-0.021</u>
<u>T_strat</u>	<u>0.009</u>	<u>-0.036</u>	<u>0.047</u>	<u>0.094</u>	<u>0.113</u>
<u>T_surface</u>	<u>-0.016</u>	<u>-0.010</u>	<u>-0.037</u>	<u>-0.015</u>	<u>0.002</u>

1396

1397 **Table S5j Adjustments for piClim-VOC experiment**

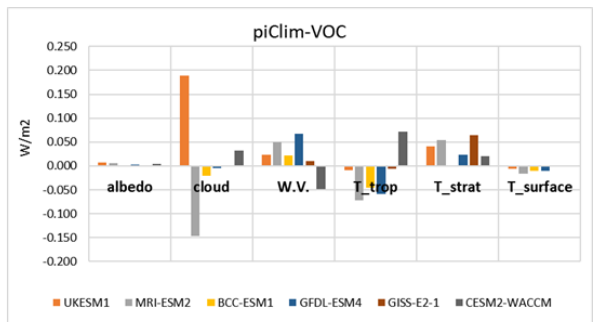
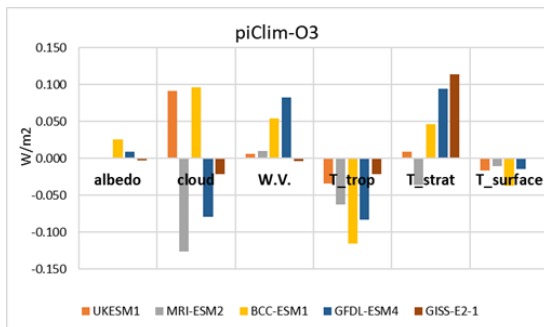
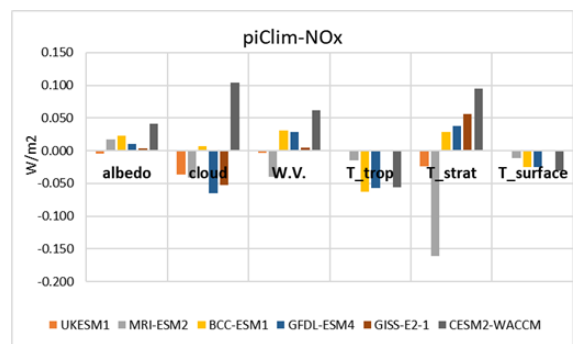
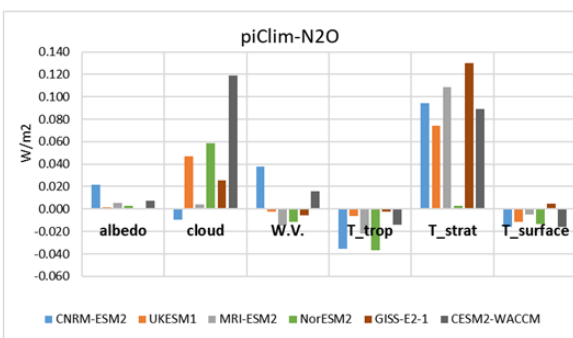
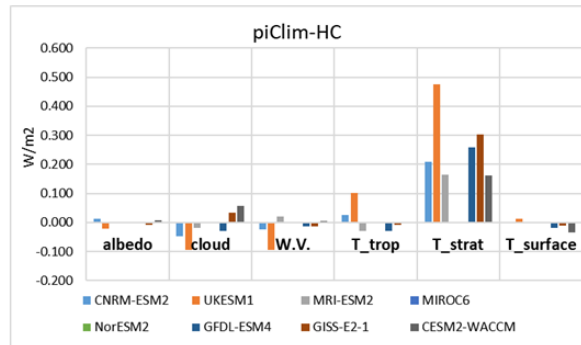
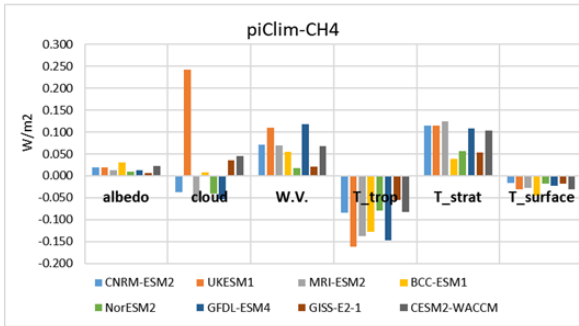
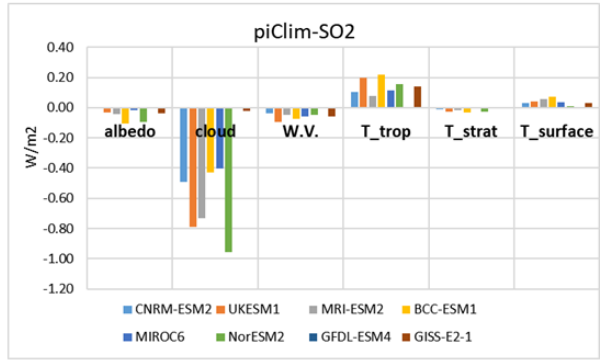
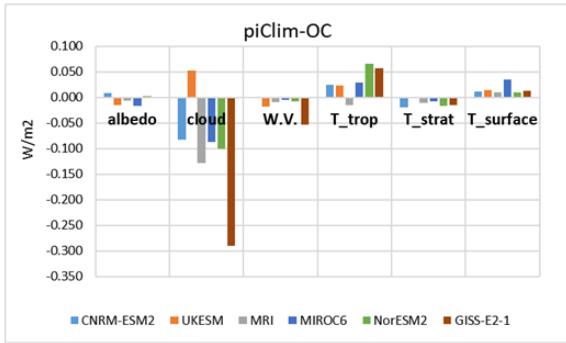
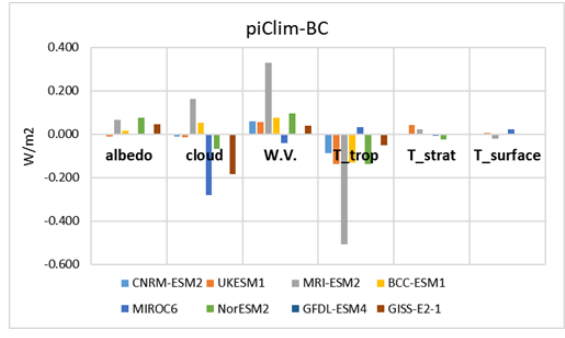
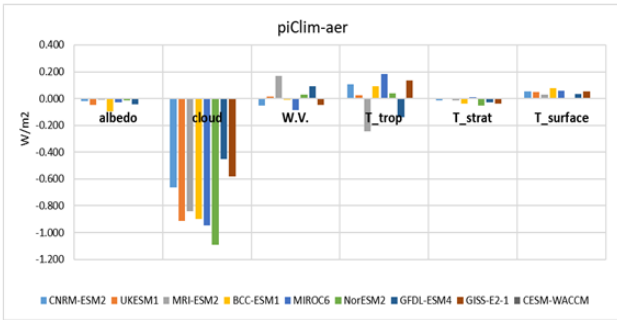
<u>piClim-VOC</u>	<u>UKESM1</u>	<u>MRI-ESM2</u>	<u>BCC-ESM1</u>	<u>GFDL-ESM4</u>	<u>GISS-E2-1</u>	<u>CESM2-WACCM</u>
<u>albedo</u>	<u>0.008</u>	<u>0.006</u>	<u>0.000</u>	<u>0.002</u>	<u>-0.001</u>	<u>0.004</u>
<u>cloud</u>	<u>0.190</u>	<u>-0.147</u>	<u>-0.020</u>	<u>-0.004</u>	<u>-0.001</u>	<u>0.033</u>
<u>W.V.</u>	<u>0.023</u>	<u>0.050</u>	<u>0.022</u>	<u>0.067</u>	<u>0.010</u>	<u>-0.049</u>
<u>T_trop</u>	<u>-0.009</u>	<u>-0.072</u>	<u>-0.046</u>	<u>-0.059</u>	<u>-0.006</u>	<u>0.072</u>
<u>T_strat</u>	<u>0.042</u>	<u>0.054</u>	<u>-0.001</u>	<u>0.024</u>	<u>0.064</u>	<u>0.021</u>
<u>T_surface</u>	<u>-0.006</u>	<u>-0.016</u>	<u>-0.011</u>	<u>-0.011</u>	<u>0.002</u>	<u>0.000</u>

1398

1399

1400

1401 Bar charts showing the atmospheric adjustments calculated from the kernel analysis are included below,  
 1402 showing adjustments for surface albedo, cloud, water vapour, tropospheric temperature, stratospheric  
 1403 temperature, and surface temperature.



1405

1406 [Figure S 1](#) Plots showing the breakdown of rapid adjustments for all experiments and models with the appropriate  
 1407 [diagnostics](#)

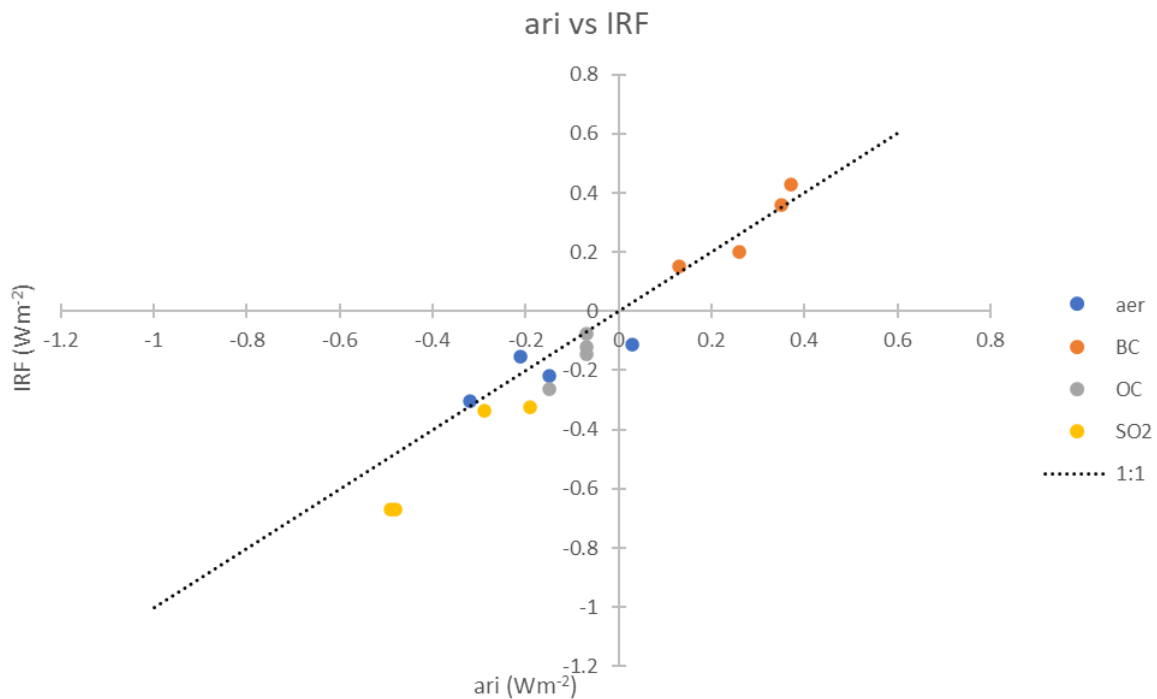
1408

1409 [Table S 5](#) Comparison of IRF and cloud adjustment with Smith et al. (2020) for piClim-aer experiment.

<b>piClim-aer</b> (Wm <sup>-2</sup> )	<u>IRF</u> (This work)	<u>IRF</u> (Smith et al., 2020))	<u>IRF</u> <u>Diff</u>	<u>Cloud</u> <u>adj.</u> (This work)	<u>Cloud</u> <u>adj.</u> (Smith et al., 2020)	<u>Cloud</u> <u>adj.</u> <u>Diff</u>	<u>IRF+Cl</u> <u>Adj</u> (this work)	<u>IRF+Cloud</u> <u>Adj.</u> (Smith et al., 2020)	<u>Total</u> <u>Diff</u>	<u>% Diff</u>
CNRM-ESM2-1	<u>-0.15</u>	<u>-0.75</u>	<u>0.60</u>	<u>-0.66</u>	<u>-0.06</u>	<u>-0.60</u>	<u>-0.82</u>	<u>-0.81</u>	<u>-0.01</u>	<u>0.63</u>
GFDL-ESM4	<u>-0.16</u>	<u>-0.37</u>	<u>0.21</u>	<u>-0.45</u>	<u>-0.26</u>	<u>-0.19</u>	<u>-0.61</u>	<u>-0.63</u>	<u>0.02</u>	<u>-2.77</u>
GISS-E2-1-G (p3)	<u>-0.42</u>	<u>-1.00</u>	<u>0.58</u>	<u>-0.60</u>	<u>-0.01</u>	<u>-0.59</u>	<u>-1.02</u>	<u>-1.01</u>	<u>-0.01</u>	<u>1.33</u>
MIROC6	<u>-0.21</u>	<u>-1.13</u>	<u>0.92</u>	<u>-0.95</u>	<u>-0.02</u>	<u>-0.93</u>	<u>-1.16</u>	<u>-1.15</u>	<u>-0.01</u>	<u>0.80</u>
MRI-ESM2-0	<u>-0.30</u>	<u>-0.46</u>	<u>0.16</u>	<u>-0.85</u>	<u>-0.68</u>	<u>-0.17</u>	<u>-1.15</u>	<u>-1.14</u>	<u>-0.01</u>	<u>0.79</u>
NorESM2-LM	<u>-0.11</u>	<u>-1.09</u>	<u>0.98</u>	<u>-1.11</u>	<u>-0.08</u>	<u>-1.03</u>	<u>-1.22</u>	<u>-1.17</u>	<u>-0.05</u>	<u>4.28</u>
UKESM1-0-LL	<u>-0.22</u>	<u>-0.97</u>	<u>0.75</u>	<u>-0.93</u>	<u>-0.18</u>	<u>-0.75</u>	<u>-1.15</u>	<u>-1.15</u>	<u>0.00</u>	<u>0.17</u>
<b>Mean</b>	<b><u>-0.23</u></b>	<b><u>-0.82</u></b>	<b><u>0.60</u></b>	<b><u>-0.79</u></b>	<b><u>-0.18</u></b>	<b><u>-0.61</u></b>	<b><u>-1.02</u></b>	<b><u>-1.01</u></b>	<b><u>-0.01</u></b>	<b><u>1.01</u></b>

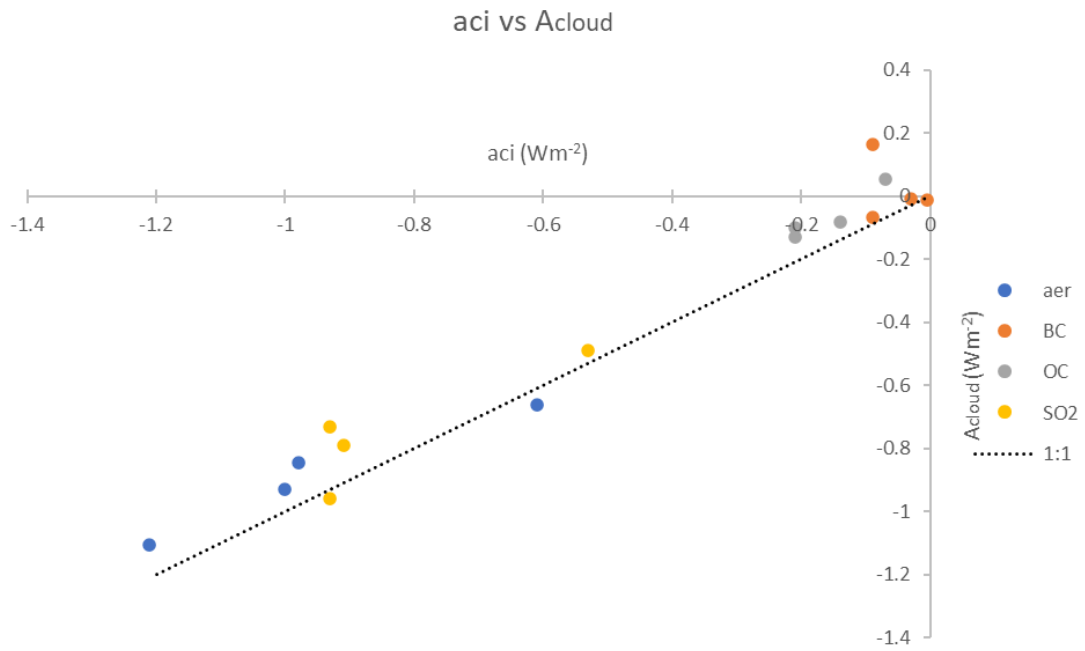
1410

1411 (a)



1412





1413 (b)

1414

1415 **Figure S 2 Scatter plots comparing direct and indirect aerosol effects from Ghan diagnostics (x-axes) with**  
 1416 **kernel-derived breakdown (y-axes). Points are from 4 models that included Ghan diagnostics (CNRM-**  
 1417 **ESM1, UKESM1, MRI-ESM2, NorESM2) (a) Comparison of IRFari with kernel IRF. (b) Comparison of**  
 1418 **ERFaci with kernel cloud adjustment (Acloud).**

1419

1420 **S4 AOD scaling**

1421  
1422

In Fig (S2) we compare the ERF originally calculated from the radiative fluxes for the (piClim-xx –piClim-control) experiments – referred to as Calc ERF to the ERF contributions obtained from using the AOD scaling.



**Figure S 3 Comparison of the ERF calculated from radiative fluxes with that from the ERF from AOD-scaled values.**

1423  
1424  
1425  
1426  
1427  
1428  
1429  
1430  
1431  
1432  
1433  
1434

e.g. the BC AOD in the piClim-BC experiment. In general, the change in the single species is responsible for most of the change in the ERF in these experiments, however in the MIROC6 piClim-OC experiment there is a significant contribution from the organic carbon, indicating this is not as clean a method for obtaining the scaling in this case as for the other models and experiments. In the case of NorESM2 for the SO<sub>2</sub> experiment we also have some contribution from the OA, which may be attributable to the way the nucleation scheme works in NorESM2. Their nucleation scheme looks at the combination of H<sub>2</sub>SO<sub>4</sub> and low-volatile organic vapours (precursors of SOA), so changing the SO<sub>2</sub> emissions might therefore indirectly change the pathway for the SOA precursors, leading to a shift in how much nucleates and how much condensates. This might lead to a difference in lifetime of SOA (which is part of OM), leading to differences in the OM burden or AOD. (Dirk Olive, pers. Communication).

In Table S6 the ERF per Tg burden is shown for the piClim-BC, piClim-SO<sub>2</sub> and piClim-OC experiments.

1435 **Table S 6 Table of ERF/burden for individual aerosol experiments**

<u>ERF/burden</u> <u>(Wm<sup>-2</sup>Tg<sup>-1</sup>)</u>	<u>CNRM-</u> <u>ESM2</u>	<u>MIROC6</u>	<u>NorESM2</u>	<u>UKESM1</u>	<u>GISS-</u> <u>E2-1</u>	<u>MRI-</u> <u>ESM2</u>	<u>BCC-</u> <u>ESM1</u>	<u>IPSL-</u> <u>INCA</u>
<u>piClim-BC</u>	<u>1.43</u>	<u>-2.49</u>	<u>2.38</u>	<u>4.07</u>	<u>0.92</u>	<u>1.74</u>	<u>1.63</u>	<u>0.90</u>
<u>piClim-OC</u>	<u>-0.68</u>	<u>-0.67</u>	<u>-0.55</u>	<u>-0.45</u>	<u>-1.42</u>	<u>-1.02</u>		<u>-0.35</u>
<u>piClim-SO2</u>	<u>-1.12</u>	<u>-0.93</u>	<u>-1.17</u>	<u>-1.34</u>	<u>-1.01</u>	<u>-1.47</u>	<u>-1.33</u>	<u>-0.64</u>

1436

1437

1438 **S5 Detailed plot of the atmospheric adjustments for the piClim-CH4 model results**

1439 The rapid adjustments for the CH4 experiment are broken down to show the model differences and the  
 1440 contributions of the individual rapid adjustments to the overall rapid adjustment contribution to the ERF.

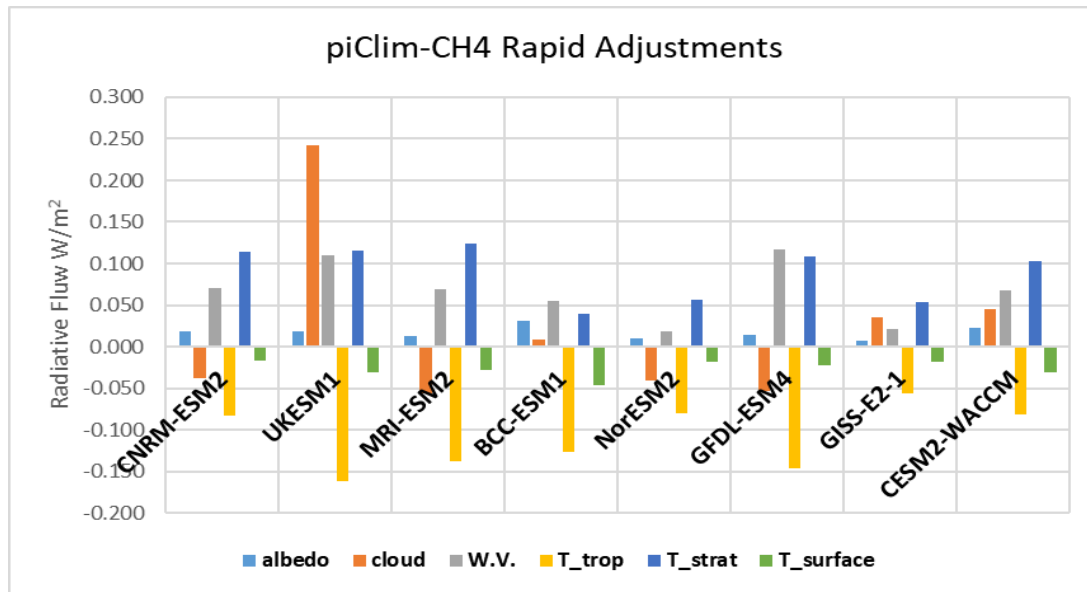


Figure S 4 Plots showing the rapid adjustments for the piClim-CH4 experiments

1441

1442 **S5 Plots of the Ghan Calculations**

We also plotted the breakdown of the ERF into the ERF<sub>Fari</sub>, ERF<sub>cloud</sub> and the ERF<sub>cs,af</sub> (clear sky, no aerosol) for models with the appropriate diagnostics, shown in Fig. S4 below.

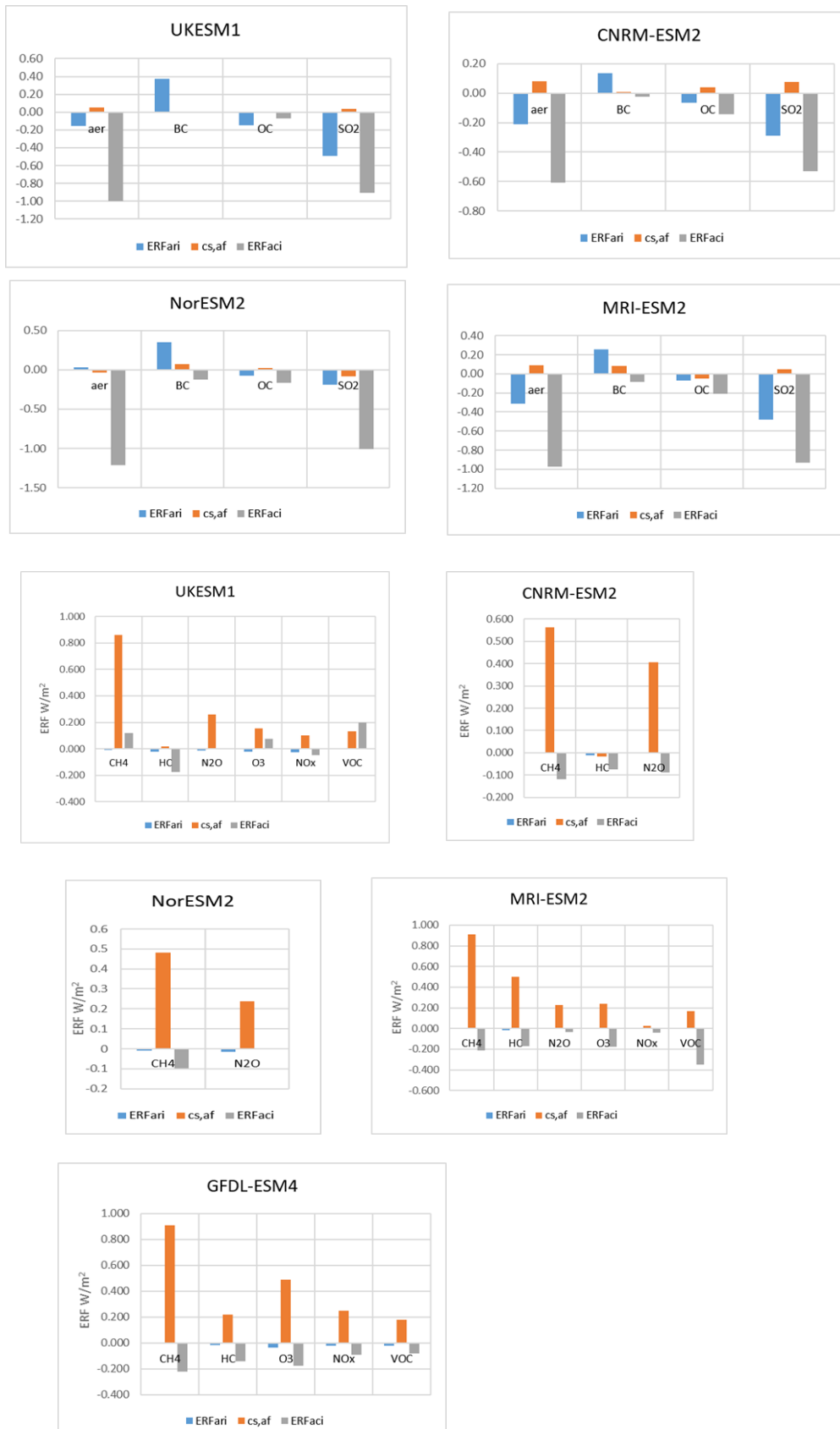


Figure S 5 Breakdown of the ERFs using the double-call method, showing IRFari, ERF<sub>cs,af</sub> and ERF<sub>aci</sub>

1445  
1446  
1447  
1448  
1449  
1450  
1451  
1452  
1453  
1454  
1455  
1456  
1457  
1458  
1459  
1460  
1461  
1462  
1463  
1464  
1465  
1466  
1467  
1468  
1469  
1470  
1471  
1472  
1473  
1474  
1475  
1476  
1477  
1478  
1479  
1480  
1481

**S6 Experiments using NorESM2 to examine adding 2014 aerosols to an atmosphere with 2014 oxidants.**

The following sensitivity experiments were done with the NorESM aerosol scheme. To study the effect of SO<sub>2</sub> emissions, we have done a few extra simulations in addition to piClim-control and piClim-SO<sub>2</sub> : two additional experiments which we called piClim-oxid and piClim-oxidSO<sub>2</sub>.

These experiments are :

- (1) piClim-control : SO<sub>2</sub> emissions are 1850, oxidants are 1850
- (2) piClim-SO<sub>2</sub> : SO<sub>2</sub> emissions are 2014, oxidants are 1850
- (3) piClim-oxid : SO<sub>2</sub> emissions are 1850, oxidants are 2014
- (4) piClim-oxid+SO<sub>2</sub> : SO<sub>2</sub> emissions are 2014, oxidants are 2014

The standard results in this paper compare (2) with (1) : this gives ERF = -1.303 W/m<sup>2</sup> (N.B the calculations here were done over 25 years, not 30 years as in the rest of the paper). It reflects the impact of adding SO<sub>2</sub> emissions in a clean pre-industrial atmosphere (both (1) and (2) have the oxidants on 1850 levels, as if NO<sub>x</sub>, CO, VOC, ... emissions are all 1850).

However, if we compare (4) with (3) : this gives -1.479 W/m<sup>2</sup>. It is the impact of adding SO<sub>2</sub> emissions, already in a polluted atmosphere where NO<sub>x</sub>, CO, VOC, ... emissions are at 2014 levels, and therefore high oxidant values.

It shows that we have differences of the order of 13% : ERF = -1.303 W/m<sup>2</sup> compared to -1.479 W/m<sup>2</sup>.

Similar experiments for all aerosols together result in the following :

- (1) piClim-control : aerosol emissions are 1850, oxidants are 1850
- (2) piClim-aer : aerosol emissions are 2014, oxidants are 1850
- (3) piClim-oxid : aerosol emissions are 1850, oxidants are 2014
- (4) piClim-oxid+aer : aerosol emissions are 2014, oxidants are 2014

Comparing here (2) with (1) gives ERF = -1.214 W/m<sup>2</sup> and comparing (4) with (3) gives ERF = -1.458 W/m<sup>2</sup>. This gives a difference of around 20%.

This result is only obtained in a simplified setup (prescribed oxidants), but it might give an indication of how the "chemical climate" affects the result.

The climate conditions (different temperature and deposition rates in 1850 and 2014) are of course not covered by the above experiment. It remains in an 1850 climate.

Finally, the impact of large emission reductions (like 100% for SO<sub>2</sub>) can show a different sensitivity than smaller mitigation-type reduction sizes due to non-linearity.

(D. Olivie, pers. Comm).

1482

1483

1484 **S7 Breakdown of Ozone changes**

1485 Table S 7 Column ozone, and ozone changes resulting from changes concentrations (CH<sub>4</sub>, N<sub>2</sub>O, HC) or emissions (NO<sub>x</sub>, VOC, O<sub>3</sub>, NTCF) of reactive gases. The multi  
 1486 model mean does not include the results for CNRM-ESM2 for tropospheric ozone.

<u>Experiment</u>	<u>CNRM-ESM2</u>		<u>UKSM1</u>		<u>MRI-ESM2</u>		<u>BCC-ESM1</u>		<u>GFDL-ESM4</u>		<u>GISS-E2</u>		<u>CESM2-WACCM</u>		<u>Multi-model</u>	
	<u>trop</u>	<u>strat</u>	<u>trop</u>	<u>strat</u>	<u>trop</u>	<u>Strat</u>	<u>trop</u>	<u>strat</u>	<u>trop</u>	<u>strat</u>	<u>trop</u>	<u>strat</u>	<u>trop</u>	<u>strat</u>	<u>trop</u>	<u>strat</u>
<u>Control</u> <u>DU</u>		<u>303.0</u> <u>±0.2</u>	<u>25.71</u> <u>±0.06</u>	<u>313.2</u> <u>±0.6</u>	<u>19.88</u> <u>±0.04</u>	<u>294.8</u> <u>±0.4</u>	<u>23.20</u> <u>±0.03</u>		<u>20.15</u> <u>±0.02</u>	<u>267.0</u> <u>±0.2</u>	<u>20.45</u> <u>±0.04</u>	<u>258.5</u> <u>±0.1</u>	<u>20.33</u> <u>±0.04</u>	<u>260.3</u> <u>±0.2</u>	<u>22.3</u> <u>±2.60</u>	<u>283</u> <u>±20</u>
<u>CH<sub>4</sub></u> <u>DU</u>		<u>+6.1±0.3</u>	<u>3.02</u> <u>±0.08</u>	<u>+2.0</u> <u>±0.6</u>	<u>+2.48</u> <u>±0.04</u>	<u>+2.9</u> <u>±0.5</u>	<u>+2.42</u> <u>±0.03</u>		<u>2.50</u> <u>±0.04</u>	<u>+2.1</u> <u>±0.2</u>	<u>2.17</u> <u>±0.05</u>	<u>+5.3</u> <u>±0.2</u>	<u>+3.15</u> <u>±0.04</u>	<u>+2.9±0.2</u>	<u>+2.6</u> <u>±0.3</u>	<u>+4</u> <u>±2</u>
<u>NO<sub>x</sub></u> <u>DU</u>			<u>5.20</u> <u>±0.08</u>	<u>+4.6</u> <u>±0.6</u>	<u>+4.09</u> <u>±0.05</u>	<u>+10.5</u> <u>±0.5</u>	<u>7.23</u> <u>±0.03</u>		<u>6.61</u> <u>±0.03</u>	<u>+1.1</u> <u>±0.2</u>	<u>9.19</u> <u>±0.05</u>	<u>+1.0</u> <u>±0.2</u>	<u>+6.97</u> <u>±0.04</u>	<u>+0.1</u> <u>±0.2</u>	<u>+6.5</u> <u>±1.6</u>	<u>+3</u> <u>±3</u>
<u>VOC</u> <u>DU</u>			<u>1.47</u> <u>±0.08</u>	<u>+1.6</u> <u>±0.6</u>	<u>+1.99</u> <u>±0.05</u>	<u>+2.0</u> <u>±0.5</u>	<u>0.79</u> <u>±0.03</u>		<u>1.94</u> <u>±0.03</u>	<u>+2.5</u> <u>±0.2</u>	<u>1.90</u> <u>±0.05</u>	<u>-1.9</u> <u>±0.3</u>	<u>+1.57</u> <u>±0.05</u>	<u>+2.0</u> <u>±0.2</u>	<u>+1.6</u> <u>±0.4</u>	<u>+1</u> <u>±1</u>
<u>O<sub>3</sub></u> <u>DU</u>			<u>6.86</u> <u>±0.08</u>	<u>+5.1</u> <u>±0.6</u>	<u>+7.51</u> <u>±0.04</u>	<u>7.2</u> <u>±0.5</u>	<u>8.52</u> <u>±0.03</u>		<u>9.46</u> <u>±0.03</u>	<u>+2.8</u> <u>±0.2</u>	<u>11.38</u> <u>±0.06</u>	<u>-0.6</u> <u>±0.3</u>			<u>+8.7</u> <u>±1.6</u>	<u>+4</u> <u>±3</u>
<u>N<sub>2</sub>O</u> <u>DU</u>		<u>-6.7 ±0.3</u>	<u>0.16 ±</u> <u>0.08</u>	<u>-3.1</u> <u>±0.6</u>	<u>--0.05</u> <u>±0.04</u>	<u>-4.7</u> <u>±0.5</u>					<u>0.23</u> <u>±0.05</u>	<u>-7.6</u> <u>±0.2</u>	<u>+0.41</u> <u>±0.04</u>	<u>-4.5 ±0.2</u>	<u>+0.2</u> <u>±0.2</u>	<u>-5 ±1</u>
<u>HC</u> <u>DU</u>		<u>-23.4</u> <u>±0.8</u>	<u>-2.12±</u> <u>0.08</u>	<u>-38.2</u> <u>±0.6</u>	<u>-0.41</u> <u>±0.05</u>	<u>-13.4</u> <u>±0.5</u>			<u>-1.51</u> <u>±0.0</u>	<u>-23.3</u> <u>±0.2</u>	<u>-2.54</u> <u>±0.05</u>	<u>-24.2</u> <u>±0.2</u>	<u>-0.61</u> <u>±0.06</u>	<u>-22.7</u> <u>±0.4</u>	<u>-1.4</u> <u>±0.8</u>	<u>-23</u> <u>±8</u>

1487

1488

1489

**Table S 8 Percentage change in total aerosol mass (sulphate, nitrate and secondary organic) from the reactive gas experiments.**

Experiment	UKESM	MRI-ESM2	BCC-ESM2	GFDL-ESM4			GISS-E2			CESM2-WACCM	
				SO4	NO3	SOA	SO4	NO3	SOA	SO4	SOA
CH4	-2	+2	+1	+6	0	0	-1	-11	+1	-1	-1
NOx	-2	0	+9	-8	+200	+1	-19	+120	+19	+2	-10
VOC	-3	+1	0	+4	-5	+8	-2	0	+1	-2	+34
O3	-4	+1	+10	-3	+190	+7	-21	+130	+21		
N2O	+1	+1					+1	+7	+1	+1	+1
HC	+2	+1		+1	0	+1	+1	-11	+1	-1	+1

1490

1491

1492

1493

1494

1495

1496

1497

1498

1499

1500

1501



## S8 Methane Lifetime

**Table S 9 Methane lifetime (years), and change due to each experiment (%). Multi-model mean and standard deviation. Lifetimes assume a soil loss of 120 years. Stratospheric loss is included in the model calculations.**

<u>Experiment</u>	<u>UKESM1</u>	<u>CESM2- WACCM</u>	<u>GFDL- ESM4</u>	<u>BCC</u>	<u>GISS- E2</u>	<u>MRI- ESM2</u>	<u>Multi- model</u>
<u>Control</u> <u>years</u>	<u>8.0</u>	<u>8.7</u>	<u>9.6</u>	<u>6.3</u>	<u>13.4</u>	<u>10.1</u>	<u>10.0 ±1.9</u>
<u>CH4</u> <u>%</u>	<u>+22</u>	<u>+22</u>	<u>+21</u>	<u>+26</u>	<u>+18</u>	<u>+22</u>	<u>22±3</u>
<u>NOx</u> <u>%</u>	<u>-25</u>	<u>-35</u>	<u>-33</u>		<u>-46</u>	<u>-26</u>	<u>-33±8</u>
<u>VOC</u> <u>%</u>	<u>+11</u>		<u>+15</u>		<u>+27</u>	<u>+21</u>	<u>+19±6</u>
<u>O3</u> <u>%</u>	<u>-19</u>		<u>-24</u>		<u>-40</u>	<u>-20</u>	<u>-16±9</u>
<u>HC</u> <u>%</u>	<u>-4.9</u>		<u>-7.5</u>		<u>-0.6</u>	<u>-2.4</u>	<u>-3.7 ±2.4</u>
<u>N2O</u>	<u>-1.2</u>	<u>-2.8</u>			<u>-3.9</u>	<u>-1.3</u>	<u>-2.0 ±1.1</u>

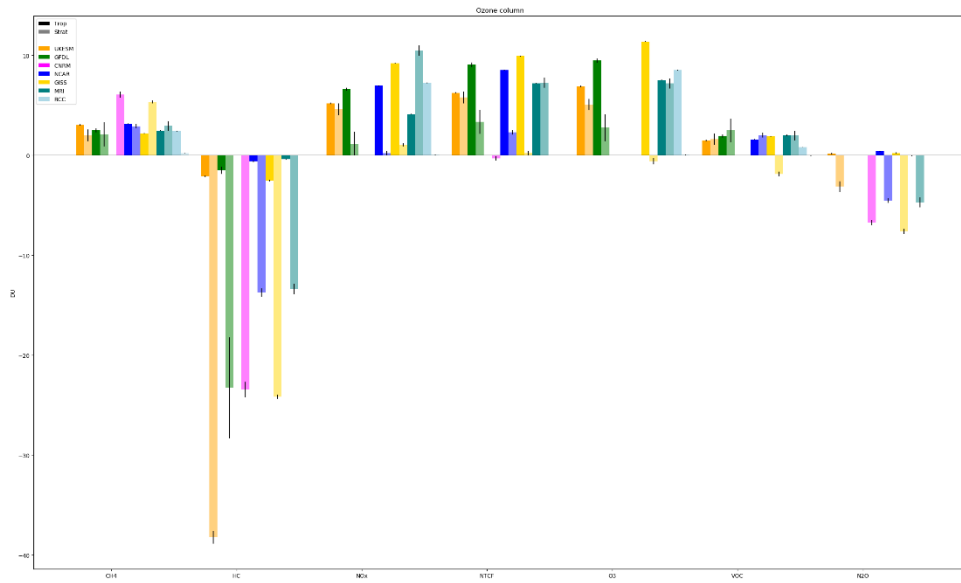


Figure S 6 Ozone column values for the troposphere and stratosphere for the reactive greenhouse gas experiments

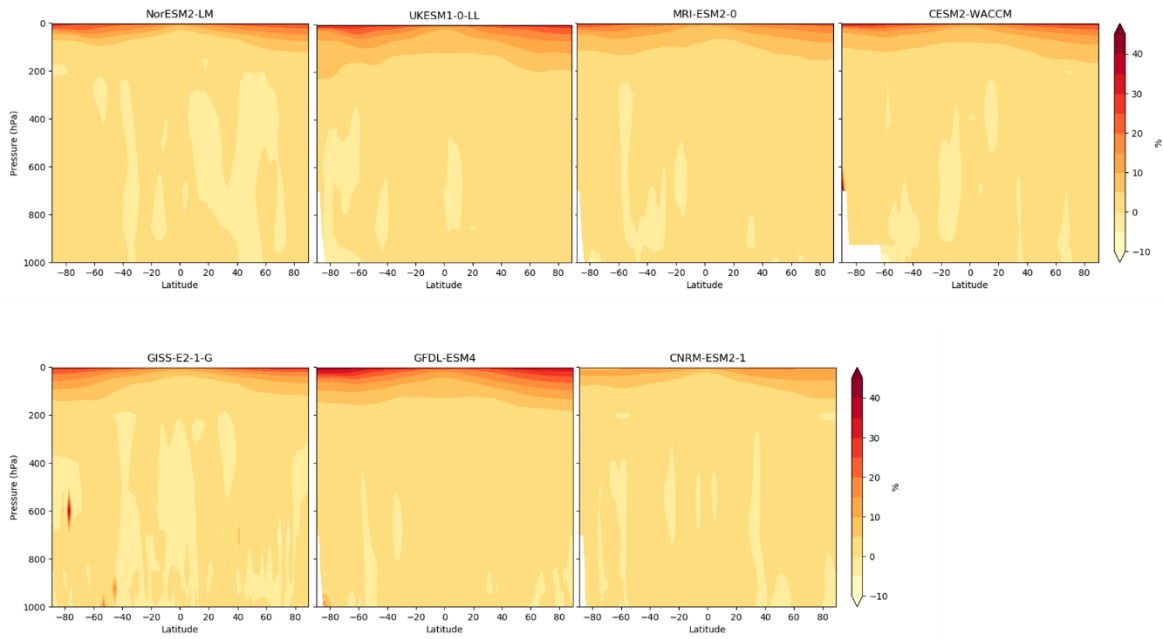


Figure S 7 Percentage changes in water vapour from the piClim-CH4 experiments.

[Abdul-Razzak, H., and Ghan, S. J.: A parameterization of aerosol activation: 2. Multiple aerosol types, Journal of Geophysical Research: Atmospheres, 105, 6837-6844, 10.1029/1999jd901161, 2000.](#)

[Archibald, A. T., O'Connor, F. M., Abraham, N. L., Archer-Nicholls, S., Chipperfield, M. P., Dalvi, M., Folberth, G. A., Dennison, F., Dhomse, S. S., Griffiths, P. T., Hardacre, C., Hewitt, A. J., Hill, R.,](#)

Johnson, C. E., Keeble, J., Köhler, M. O., Morgenstern, O., Mulchay, J. P., Ordóñez, C., Pope, R. J., Rumbold, S., Russo, M. R., Savage, N., Sellar, A., Stringer, M., Turnock, S., Wild, O., and Zeng, G.: Description and evaluation of the UKCA stratosphere-troposphere chemistry scheme (StratTrop v1.0) implemented in UKESM1, *Geosci. Model Dev. Discuss.*, 2019, 1-82, 10.5194/gmd-2019-246, 2020.

Balkanski, Y., Myhre, G., Gauss, M., Rädcl, G., Highwood, E. J., and Shine, K. P.: Direct radiative effect of aerosols emitted by transport: from road, shipping and aviation, *Atmos. Chem. Phys.*, 10, 4477-4489, 10.5194/acp-10-4477-2010, 2010.

Bauer, S. E., Tsigaridis, K., Faluvegi, G., Kelley, M., Lo, K. K., Miller, R. L., Nazarenko, L., Schmidt, G. A., and Wu, J.: Historical (1850–2014) Aerosol Evolution and Role on Climate Forcing Using the GISS ModelE2.1 Contribution to CMIP6, *Journal of Advances in Modeling Earth Systems*, 12, e2019MS001978, 10.1029/2019ms001978, 2020.

Checa-Garcia, R., Hegglin, M. I., Kinnison, D., Plummer, D. A., and Shine, K. P.: Historical Tropospheric and Stratospheric Ozone Radiative Forcing Using the CMIP6 Database, *Geophysical Research Letters*, 45, 3264-3273, 10.1002/2017gl076770, 2018.

Danabasoglu, G.: NCAR CESM2-WACCM model output prepared for CMIP6 CMIP historical, <https://doi.org/10.22033/ESGF/CMIP6.10071>, <https://doi.org/10.22033/ESGF/CMIP6.10071>, 2019.

Danabasoglu, G.: NCAR CESM2-WACCM model output prepared for CMIP6 ScenarioMIP, <https://doi.org/10.22033/ESGF/CMIP6.10026>, <http://cera-www.dkrz.de/WDCC/meta/CMIP6/CMIP6.ScenarioMIP.NCAR.CESM2-WACCM>, 2019.

Di Biagio, C., Formenti, P., Balkanski, Y., Caponi, L., Cazaunau, M., Pangui, E., Journet, E., Nowak, S., Andreae, M., Kandler, K., Saeed, T., Piketh, S., Seibert, D., Williams, E., and Doussin, J.-F.: Complex refractive indices and single scattering albedo of global dust aerosols in the shortwave spectrum and relationship to iron content and size, *Atmospheric Chemistry and Physics Discussions*, 1-42, 10.5194/acp-2019-145, 2019.

Dunne, J. P., Horowitz, L. W., Adcroft, A. J., Ginoux, P., Held, I. M., John, J. G., Krasting, J. P., Malyshev, S., Naik, V., Paulot, F., Shevliakova, E., Stock, C. A., Zadeh, N., Balaji, V., Blanton, C., Dunne, K. A., Dupuis, C., Durachta, J., Dussin, R., Gauthier, P. P. G., Griffies, S. M., Guo, H., Hallberg, R. W., Harrison, M., He, J., Hurlin, W., McHugh, C., Menzel, R., Milly, P. C. D., Nikonov, S., Paynter, D. J., Ploshay, J., Radhakrishnan, A., Rand, K., Reichl, B. G., Robinson, T., Schwarzkopf, D. M., Sentman, L. T., Underwood, S., Vahlenkamp, H., Winton, M., Wittenberg, A. T., Wyman, B., Zeng, Y., and Zhao, M.: The GFDL Earth System Model version 4.1 (GFDL-ESM 4.1): Overall coupled model description and simulation characteristics, *Journal of Advances in Modeling Earth Systems*, n/a, e2019MS002015, 10.1029/2019ms002015, 2020.

Emmons, L. K., Schwantes, R. H., Orlando, J. J., Tyndall, G., Kinnison, D., -F., L. J., Marsh, D., Mills, M., Tilmes, S., Bardeen, C., Buchholz, R. R., Conley, A., Gettelman, A., Garcia, R., Simpson, I., Blake, D. R., Meinardi, S., and Pétron, G.: The Chemistry Mechanism in the Community Earth System Model version 2 (CESM2), *J. Advances in Modeling Earth Systems*, 12, <https://doi.org/10.1029/2019MS001882>, 2020.

Gery, M. W., Whitten, G. Z., Killus, J. P., and Dodge, M. C.: A photochemical kinetics mechanism for urban and regional scale computer modeling., *Journal of Geophysical Research*, 94, 925-956, 1989.

Gettelman, A., Mills, M. J., Kinnison, D. E., Garcia, R. R., Smith, A. K., Marsh, D. R., Tilmes, S., Vitt, F., Bardeen, C. G., McInerny, J., Liu, H. L., Solomon, S. C., Polvani, L. M., Emmons, L. K., Lamarque, J. F., Richter, J. H., Glanville, A. S., Bacmeister, J. T., Phillips, A. S., Neale, R. B.,

Simpson, I. R., DuVivier, A. K., Hodzic, A., and Randel, W. J.: The Whole Atmosphere Community Climate Model Version 6 (WACCM6), Journal of Geophysical Research: Atmospheres, n/a, 10.1029/2019JD030943, 2019.

Hauglustaine, D. A., Balkanski, Y., and Schulz, M.: A global model simulation of present and future nitrate aerosols and their direct radiative forcing of climate, Atmos. Chem. Phys., 14, 11031-11063, 10.5194/acp-14-11031-2014, 2014.

Horowitz, L. W., Walters, S., Mauzerall, D. L., Emmons, L. K., Rasch, P. J., Granier, C., Tie, X., Lamarque, J.-F., Schultz, M. G., Tyndall, G. S., Orlando, J. J., and Brasseur, G. P.: A global simulation of tropospheric ozone and related tracers: Description and evaluation of MOZART, version 2, Journal of Geophysical Research: Atmospheres, 108, 10.1029/2002jd002853, 2003.

Horowitz, L. W., Naik, V., Paulot, F., Ginoux, P. A., Dunne, J. P., Mao, J., Schnell, J., Chen, X., He, J., John, J. G., Lin, M., Lin, P., Malyshev, S., Paynter, D., Shevliakova, E., and Zhao, M.: The GFDL Global Atmospheric Chemistry-Climate Model AM4.1: Model Description and Simulation Characteristics, Journal of Advances in Modeling Earth Systems, n/a, e2019MS002032, 10.1029/2019ms002032, 2020.

Jones, A., Roberts, D. L., Woodage, M. J., and Johnson, C. E.: Indirect sulphate aerosol forcing in a climate model with an interactive sulphur cycle, Journal of Geophysical Research: Atmospheres, 106, 20293-20310, 10.1029/2000jd000089, 2001.

Khairoutdinov, M., and Kogan, Y.: A New Cloud Physics Parameterization in a Large-Eddy Simulation Model of Marine Stratocumulus, Monthly Weather Review, 128, 229-243, 10.1175/1520-0493(2000)128<0229:ancppi>2.0.co;2, 2000.

Kirkevåg, A., Grini, A., Olivie, D., Seland, Ø., Alterskjær, K., Hummel, M., Karset, I. H. H., Lewinschal, A., Liu, X., Makkonen, R., Bethke, I., Griesfeller, J., Schulz, M., and Iversen, T.: A production-tagged aerosol module for Earth system models, OsloAero5.3 – extensions and updates for CAM5.3-Oslo, Geosci. Model Dev., 11, 3945-3982, 10.5194/gmd-11-3945-2018, 2018.

Kuhlbrodt, T., Jones, C. G., Sellar, A., Storkey, D., Blockley, E., Stringer, M., Hill, R., Graham, T., Ridley, J., Blaker, A., Calvert, D., Copley, D., Ellis, R., Hewitt, H., Hyder, P., Ineson, S., Mulcahy, J., Sahaan, A., and Walton, J.: The Low-Resolution Version of HadGEM3 GC3.1: Development and Evaluation for Global Climate, Journal of Advances in Modeling Earth Systems, 10, 2865-2888, 10.1029/2018ms001370, 2018.

Lurton, T., Balkanski, Y., Bastrikov, V., Bekki, S., Bopp, L., Braconnot, P., Brockmann, P., Cadule, P., Contoux, C., Cozic, A., Cugnet, D., Dufresne, J.-L., Éthé, C., Foujols, M.-A., Ghattas, J., Hauglustaine, D., Hu, R.-M., Kageyama, M., Khodri, M., Lebas, N., Levvasseur, G., Marchand, M., Ottlé, C., Peylin, P., Sima, A., Szopa, S., Thiéblemont, R., Vuichard, N., and Boucher, O.: Implementation of the CMIP6 Forcing Data in the IPSL-CM6A-LR Model, Journal of Advances in Modeling Earth Systems, 12, e2019MS001940, 10.1029/2019ms001940, 2020.

Mann, G. W., Carslaw, K. S., Spracklen, D. V., Ridley, D. A., Manktelow, P. T., Chipperfield, M. P., Pickering, S. J., and Johnson, C. E.: Description and evaluation of GLOMAP-mode: a modal global aerosol microphysics model for the UKCA composition-climate model, Geosci. Model Dev., 3, 519-551, 10.5194/gmd-3-519-2010, 2010.

Matthes, K., Funke, B., Andersson, M. E., Barnard, L., Beer, J., Charbonneau, P., Clilverd, M. A., Dudok de Wit, T., Haberreiter, M., Hendry, A., Jackman, C. H., Kretzschmar, M., Kruschke, T., Kunze, M., Langematz, U., Marsh, D. R., Maycock, A. C., Misios, S., Rodger, C. J., Scaife, A. A., Seppälä, A., Shangguan, M., Sinnhuber, M., Tourpali, K., Usoskin, I., van de Kamp, M., Verronen, P.

T., and Versick, S.: Solar forcing for CMIP6 (v3.2), Geosci. Model Dev., 10, 2247-2302, 10.5194/gmd-10-2247-2017, 2017.

Michou, M., Nabat, P., and Saint-Martin, D.: Development and basic evaluation of a prognostic aerosol scheme (v1) in the CNRM Climate Model CNRM-CM6, Geosci. Model Dev., 8, 501-531, 10.5194/gmd-8-501-2015, 2015.

Morgenstern, O., Braesicke, P., O'Connor, F. M., Bushell, A. C., Johnson, C. E., Osprey, S. M., and Pyle, J. A.: Evaluation of the new UKCA climate-composition model – Part 1: The stratosphere, Geosci. Model Dev., 2, 43-57, 10.5194/gmd-2-43-2009, 2009.

Mulcahy, J. P., Jones, C., Sellar, A., Johnson, B., Boutle, I. A., Jones, A., Andrews, T., Rumbold, S. T., Mollard, J., Bellouin, N., Johnson, C. E., Williams, K. D., Grosvenor, D. P., and McCoy, D. T.: Improved Aerosol Processes and Effective Radiative Forcing in HadGEM3 and UKESM1, Journal of Advances in Modeling Earth Systems, 10, 2786-2805, 10.1029/2018ms001464, 2018.

Mulcahy, J. P., Johnson, C., Jones, C. G., Povey, A. C., Scott, C. E., Sellar, A., Turnock, S. T., Woodhouse, M. T., Abraham, N. L., Andrews, M. B., Bellouin, N., Browse, J., Carslaw, K. S., Dalvi, M., Folberth, G. A., Glover, M., Grosvenor, D., Hardacre, C., Hill, R., Johnson, B., Jones, A., Kipling, Z., Mann, G., Mollard, J., O'Connor, F. M., Palmieri, J., Reddington, C., Rumbold, S. T., Richardson, M., Schutgens, N. A. J., Stier, P., Stringer, M., Tang, Y., Walton, J., Woodward, S., and Yool, A.: Description and evaluation of aerosol in UKESM1 and HadGEM3-GC3.1 CMIP6 historical simulations, Geosci. Model Dev. Discuss., 2020, 1-59, 10.5194/gmd-2019-357, 2020.

O'Connor, F. M., Johnson, C. E., Morgenstern, O., Abraham, N. L., Braesicke, P., Dalvi, M., Folberth, G. A., Sanderson, M. G., Telford, P. J., Voulgarakis, A., Young, P. J., Zeng, G., Collins, W. J., and Pyle, J. A.: Evaluation of the new UKCA climate-composition model – Part 2: The Troposphere, Geosci. Model Dev., 7, 41-91, 10.5194/gmd-7-41-2014, 2014.

Oshima, N., Yukimoto, S., Deushi, M., Koshiro, T., Kawai, H., Tanaka, T. Y., and Yoshida, K.: Global and Arctic effective radiative forcing of anthropogenic gases and aerosols in MRI-ESM2.0, Prog. Earth. Planet. Sci., 2020.

Séférian, R., Nabat, P., Michou, M., Saint-Martin, D., Voldoire, A., Colin, J., Decharme, B., Delire, C., Berthet, S., Chevallier, M., Sénési, S., Franchistéguy, L., Vial, J., Mallet, M., Joetzjer, E., Geoffroy, O., Guérémy, J.-F., Moine, M.-P., Msadek, R., Ribes, A., Rocher, M., Roehrig, R., Salas-y-Méllia, D., Sanchez, E., Terray, L., Valcke, S., Waldman, R., Aumont, O., Bopp, L., Deshayes, J., Éthé, C., and Madec, G.: Evaluation of CNRM Earth-System model, CNRM-ESM 2-1: role of Earth system processes in present-day and future climate, Journal of Advances in Modeling Earth Systems, n/a, 10.1029/2019ms001791.

Séférian, R., Delire, C., Decharme, B., Voldoire, A., Salas Y Melia, D., Chevallier, M., Saint-Martin, D., Aumont, O., Calvet, J.-C., Carrer, D., Douville, H., Franchistéguy, L., Joetzjer, E., and Sénési, S.: Development and evaluation of CNRM Earth system model – CNRM-ESM1, Geoscientific Model Development, 9, 1423-1453, 10.5194/gmd-9-1423-2016, 2016.

Sellar, A. A., Jones, C. G., Mulcahy, J., Tang, Y., Yool, A., Wiltshire, A., O'Connor, F. M., Stringer, M., Hill, R., Palmieri, J., Woodward, S., de Mora, L., Kuhlbrodt, T., Rumbold, S., Kelley, D. I., Ellis, R., Johnson, C. E., Walton, J., Abraham, N. L., Andrews, M. B., Andrews, T., Archibald, A. T., Berthou, S., Burke, E., Blockley, E., Carslaw, K., Dalvi, M., Edwards, J., Folberth, G. A., Gedney, N., Griffiths, P. T., Harper, A. B., Hendry, M. A., Hewitt, A. J., Johnson, B., Jones, A., Jones, C. D., Keeble, J., Liddicoat, S., Morgenstern, O., Parker, R. J., Predoi, V., Robertson, E., Siahann, A., Smith, R. S., Swaminathan, R., Woodhouse, M. T., Zeng, G., and Zerroukat, M.: UKESM1: Description and evaluation of the UK Earth System Model, Journal of Advances in Modeling Earth Systems, n/a, 10.1029/2019ms001739.

Sellar, A. A., Jones, C. G., Mulcahy, J., Tang, Y., Yool, A., Wiltshire, A., O'Connor, F. M., Stringer, M., Hill, R., Palmieri, J., Woodward, S., de Mora, L., Kuhlbrodt, T., Rumbold, S., Kelley, D. I., Ellis, R., Johnson, C. E., Walton, J., Abraham, N. L., Andrews, M. B., Andrews, T., Archibald, A. T., Berthou, S., Burke, E., Blockley, E., Carslaw, K., Dalvi, M., Edwards, J., Folberth, G. A., Gedney, N., Griffiths, P. T., Harper, A. B., Hendry, M. A., Hewitt, A. J., Johnson, B., Jones, A., Jones, C. D., Keeble, J., Liddicoat, S., Morgenstern, O., Parker, R. J., Predoi, V., Robertson, E., Siahann, A., Smith, R. S., Swaminathan, R., Woodhouse, M. T., Zeng, G., and Zerroukat, M.: UKESM1: Description and evaluation of the UK Earth System Model, *Journal of Advances in Modeling Earth Systems*, n/a, [10.1029/2019ms001739](https://doi.org/10.1029/2019ms001739), 2020.

Shindell, D. T., Grenfell, J. L., Rind, D., Grewe, V., and Price, C.: Chemistry-climate interactions in the Goddard Institute for Space Studies general circulation model: 1. Tropospheric chemistry model description and evaluation, *Journal of Geophysical Research: Atmospheres*, 106, 8047-8075, [10.1029/2000jd900704](https://doi.org/10.1029/2000jd900704), 2001.

Shindell, D. T., Faluvegi, G., and Bell, N.: Preindustrial-to-present-day radiative forcing by tropospheric ozone from improved simulations with the GISS chemistry-climate GCM, *Atmos. Chem. Phys.*, 3, 1675-1702, [10.5194/acp-3-1675-2003](https://doi.org/10.5194/acp-3-1675-2003), 2003.

Shindell, D. T., Faluvegi, G., Unger, N., Aguilar, E., Schmidt, G. A., Koch, D. M., Bauer, S. E., and Miller, R. L.: Simulations of preindustrial, present-day, and 2100 conditions in the NASA GISS composition and climate model G-PUCCINI, *Atmos. Chem. Phys.*, 6, 4427-4459, [10.5194/acp-6-4427-2006](https://doi.org/10.5194/acp-6-4427-2006), 2006.

Smith, C. J., Kramer, R. J., Myhre, G., Alterskjær, K., Collins, W., Sima, A., Boucher, O., Dufresne, J. L., Nabat, P., Michou, M., Yukimoto, S., Cole, J., Paynter, D., Shiogama, H., O'Connor, F. M., Robertson, E., Wiltshire, A., Andrews, T., Hannay, C., Miller, R., Nazarenko, L., Kirkevåg, A., Olivié, D., Fiedler, S., Pincus, R., and Forster, P. M.: Effective radiative forcing and adjustments in CMIP6 models, *Atmos. Chem. Phys.*, 20, 9591-9618, [10.5194/acp-20-9591-2020](https://doi.org/10.5194/acp-20-9591-2020), 2020.

Takemura, T., Nozawa, T., Emori, S., Nakajima, T. Y., and Nakajima, T.: Simulation of climate response to aerosol direct and indirect effects with aerosol transport-radiation model, *Journal of Geophysical Research: Atmospheres*, 110, [10.1029/2004jd005029](https://doi.org/10.1029/2004jd005029), 2005.

Takemura, T., and Suzuki, K.: Weak global warming mitigation by reducing black carbon emissions, *Scientific Reports*, 9, 4419, [10.1038/s41598-019-41181-6](https://doi.org/10.1038/s41598-019-41181-6), 2019.

Takemura, T., et al: Development of a global aerosol climate model SPRINTARS, CGER's Supercomputer Monograph Report, 24, 2018.

Tatebe, H., Ogura, T., Nitta, T., Komuro, Y., Ogochi, K., Takemura, T., Sudo, K., Sekiguchi, M., Abe, M., Saito, F., Chikira, M., Watanabe, S., Mori, M., Hirota, N., Kawatani, Y., Mochizuki, T., Yoshimura, K., Takata, K., O'Ishi, R., Yamazaki, D., Suzuki, T., Kurogi, M., Kataoka, T., Watanabe, M., and Kimoto, M.: Description and basic evaluation of simulated mean state, internal variability, and climate sensitivity in MIROC6, *Geoscientific Model Development*, 12, 2727-2765, <http://dx.doi.org/10.5194/gmd-12-2727-2019>, 2019.

Tilmes, S., Hodzic, A., Emmons, L. K., Mills, M. J., Gettelman, A., Kinnison, D. E., Park, M., Lamarque, J. F., Vitt, F., Shrivastava, M., Campuzano-Jost, P., Jimenez, J. L., and Liu, X.: Climate Forcing and Trends of Organic Aerosols in the Community Earth System Model (CESM2), *Journal of Advances in Modeling Earth Systems*, n/a, [10.1029/2019MS001827](https://doi.org/10.1029/2019MS001827), 2019.

Walters, D., Baran, A. J., Boutle, I., Brooks, M., Earnshaw, P., Edwards, J., Furtado, K., Hill, P., Lock, A., Manners, J., Morcrette, C., Mulcahy, J., Sanchez, C., Smith, C., Stratton, R., Tennant, W., Tomassini, L., Van Weverberg, K., Vosper, S., Willett, M., Browse, J., Bushell, A., Carslaw, K.,



Dalvi, M., Essery, R., Gedney, N., Hardiman, S., Johnson, B., Johnson, C., Jones, A., Jones, C., Mann, G., Milton, S., Rumbold, H., Sellar, A., Ujiie, M., Whittall, M., Williams, K., and Zerroukat, M.: The Met Office Unified Model Global Atmosphere 7.0/7.1 and JULES Global Land 7.0 configurations, *Geosci. Model Dev.*, 12, 1909-1963, 10.5194/gmd-12-1909-2019, 2019.

Wang, R., Balkanski, Y., Boucher, O., Ciais, P., Schuster, G. L., Chevallier, F., Samset, B. H., Liu, J., Piao, S., Valari, M., and Tao, S.: Estimation of global black carbon direct radiative forcing and its uncertainty constrained by observations, *Journal of Geophysical Research: Atmospheres*, 121, 5948-5971, 10.1002/2015jd024326, 2016.

Watanabe, M., Suzuki, T., O'ishi, R., Komuro, Y., Watanabe, S., Emori, S., Takemura, T., Chikira, M., Ogura, T., Sekiguchi, M., Takata, K., Yamazaki, D., Yokohata, T., Nozawa, T., Hasumi, H., Tatebe, H., and Kimoto, M.: Improved Climate Simulation by MIROC5: Mean States, Variability, and Climate Sensitivity, *Journal of Climate*, 23, 6312-6335, 10.1175/2010jcli3679.1, 2010.

Williams, K. D., Copsey, D., Blockley, E. W., Bodas-Salcedo, A., Calvert, D., Comer, R., Davis, P., Graham, T., Hewitt, H. T., Hill, R., Hyder, P., Ineson, S., Johns, T. C., Keen, A. B., Lee, R. W., Megann, A., Milton, S. F., Rae, J. G. L., Roberts, M. J., Scaife, A. A., Schiemann, R., Storkey, D., Thorpe, L., Watterson, I. G., Walters, D. N., West, A., Wood, R. A., Woollings, T., and Xavier, P. K.: The Met Office Global Coupled Model 3.0 and 3.1 (GC3.0 and GC3.1) Configurations, *Journal of Advances in Modeling Earth Systems*, 10, 357-380, 10.1002/2017ms001115, 2018.

Woodward, S.: Modeling the atmospheric life cycle and radiative impact of mineral dust in the Hadley Centre climate model, *Journal of Geophysical Research: Atmospheres*, 106, 18155-18166, 10.1029/2000jd900795, 2001.

Wu, T., Zhang, F., Zhang, J., Jie, W., Zhang, Y., Wu, F., Li, L., Liu, X., Lu, X., Zhang, L., Wang, J., and Hu, A.: Beijing Climate Center Earth System Model version 1 (BCC-ESM1): Model Description and Evaluation, *Geosci. Model Dev.*, 13, 977-1005, 10.5194/gmd-2019-172, 2020.

Yukimoto, S., Kawai, H., Koshiro, T., Oshima, N., Yoshida, K., Urakawa, S., Tsujino, H., Deushi, M., Tanaka, T., Hosaka, M., Yabu, S., Yoshimura, H., Shindo, E., Mizuta, R., Obata, A., Adachi, Y., and Ishii, M.: The Meteorological Research Institute Earth System Model Version 2.0, MRI-ESM2.0: Description and Basic Evaluation of the Physical Component, *J. Meteor. Soc. Japan*, 97, 931-965, 10.2151/jmsj.2019-051, 2019.